OPERATIONAL CHALLENGES IN GAS-TO-LIQUID (GTL) TRANSPORTATION THROUGH TRANS ALASKA PIPELINE SYSTEM (TAPS)

FINAL REPORT
(Reporting period: 10/1/2001 to 6/30/2006)

Principal Author: Godwin A. Chukwu, Ph.D., P.E.

Co-P.I.s: Santanu Khataniar, Ph.D.
Shirish Patil, Associate Professor
Abhijit Dandekar, Associate Professor

Revised March 2007

Work Performed under Cooperative Agreement No. DE-FC26-01NT41228

Submitted by:

Petroleum Development Laboratory
Institute of Northern Engineering
University of Alaska Fairbanks
P.O. Box 755880
Fairbanks, AK 99775-5880

Prepared for:

The US Department of Energy
National Energy Technology Laboratory
P.O. Box 880
Morgantown, WV 26507-08

DISCLAIMER

ABSTRACT

Oil production from Alaskan North Slope oil fields has steadily declined. In the near future, ANS crude oil production will decline to such a level (200,000 to 400,000 bbl/day) that maintaining economic operation of the Trans-Alaska Pipeline System (TAPS) will require pumping alternative products through the system. Heavy oil deposits in the West Sak and Ugnu formations are a potential resource, although transporting these products involves addressing important sedimentation issues. One possibility is the use of Gas-to-Liquid (GTL) technology. Estimated recoverable gas reserves of 38 trillion cubic feet (TCF) on the North Slope of Alaska can be converted to liquid with GTL technology and combined with the heavy oils for a product suitable for pipeline transport.

Issues that could affect transport of this such products through TAPS include pumpability of GTL and crude oil blends, cold restart of the pipeline following a prolonged winter shutdown, and solids deposition inside the pipeline.

This study examined several key fluid properties of GTL, crude oil and four selected blends under TAPS operating conditions. Key measurements included Reid Vapor Pressure, density and viscosity, PVT properties, and solids deposition.

Results showed that gel strength is not a significant factor for the ratios of GTL-crude oil blend mixtures (1:1; 1:2; 1:3; 1:4) tested under TAPS cold re-start conditions at temperatures above -20°F, although Bingham fluid flow characteristics exhibited by the blends at low temperatures indicate high pumping power requirements following prolonged shutdown.

Solids deposition is a major concern for all studied blends. For the commingled flow profile studied, decreased throughput can result in increased and more rapid solid deposition along the pipe wall, resulting in more frequent pigging of the pipeline or, if left unchecked, pipeline corrosion.

TABLE OF CONTENTS

LIST OF FIGURES

LIST OF TABLES

OPERATIONAL CHALLENGES IN GAS-TO-LIQUID (GTL) TRANSPORTATION THROUGH TRANS-ALASKA PIPELINE SYSTEMS (TAPS)

EXECUTIVE SUMMARY

The Alaskan North Slope (ANS) has extensive natural gas reserves, which have excellent economic potential for the state of Alaska. Estimated ANS proven and recoverable natural gas reserves in known reservoirs is about 38 trillion standard cubic feet (TCF) [Thomas et al. 1996]. Currently ANS natural gas is primarily used for pressure maintenance, miscible injection, running gas turbines in pump stations 1 to 4, power oil production facilities, and Enhanced Oil Recovery (EOR) projects. Some strategies for economic use of ANS oil reserves could result in most of the gas remaining unrecovered, or stranded, unless a means of transportation is developed to make recovery more marketable.

Conversion of gas to gas-to-liquid products (GTL), blending it with ANS crude oil and transporting the resulting liquid through the Trans-Alaska Pipeline System (TAPS) is one option under discussion. A study by Thomas et al. (1996) concluded that "state-of-the-art GTL conversion technology appears to be feasible and could be deployed within a meaningful time frame to sustain ANS and TAPS oil operations for 20 or more years beyond what might be anticipated without GTL." GTL technology might also prove successful for enhancing the economic potential of other stranded natural gas reserves worldwide.

With ANS oil production dwindling, oil throughput for the Trans-Alaska Pipeline System (TAPS) is declining steadily. Khataniar et al. (2004) reported that in the near future (5 to 10 years), ANS crude oil production will decline to levels insufficient to maintain economic TAPS operation. GTL production from ANS natural gas could extend the pipeline's economic life.

The primary goal of this study was to study the flow of GTL/ANS crude blend mixtures through TAPS and to examine the likelihood and impact of the above operational challenges. Work included experimental and simulation study of GTL product properties and their blends under a range of TAPS operating conditions, including a cold weather shutdown.

Schematic commercialization of stranded natural gas resources using GTL technology has received much attention from both the government and private industry. As new GTL technologies have matured, energy companies are investing in moving from small pilot GTL facilities to commercial developments. British Petroleum Exploration Alaska (BPXA) has completed and tested a 300 bbl/day pilot GTL facility in Nikiski, Alaska. This facility was designed to demonstrate a new synthesis gas generation technology and to assess challenges of GTL production in a cold climate. The results could benefit design of a commercial GTL facility for the ANS.

An earlier DOE-sponsored study (Chukwu et al. 2002) evaluated two modes of GTL product transportation through the TAPS, batching and commingling. Given the economic parameters and assumptions made in their study, the batching mode was favored based on higher rate of return on the capital investment. The major concern with batching, the study concluded, "is the length of mixing zone or interface and the purity of GTL products as they arrive the marine terminal in Valdez".

The expected loss of purity in the blended product and a trade-off between loss in product value (due to contamination) and the capital costs involved in delivering a pure product to the terminal are major factors of consideration for further study on commingled transportation of a blended mixture of ANS crude and GTL products. Using existing infrastructure allows for only minimal additions to capital costs for transportation. This includes using present holding tanks at the ANS and storage tanks at the Valdez

Marine Terminal (VMT). In the pump stations, pressure relief tanks are required for emergency operations, and these could serve as temporary storage in case of unforeseen valve or process malfunctions to reduce any pressure build up in the pipeline.

The TAPS was specifically designed for transporting Prudhoe Bay crude oil. While it is possible that introducing GTL products might lead to some operational problems, this strategy may avoid other problems. GTL products are less viscous than crude oil. ANS oil viscosity has been increasing with increased oil production. Although the TAPS was originally designed for less viscous fluids, large amounts of viscous oil from West Sak, Schrader Bluff and Ugnu fields will most likely be transported through the pipeline. While blending the light GTL products with crude oil could help in retaining the fluid API that TAPS was originally designed for, the increasing viscosity of the crude oil might adversely affect the TAPS operational life. Anticipated problems with transporting GTL products include altered pumping power requirements, possibility of vapor formation, solids precipitation and deposition, and gel formation.

Briefly, report findings include:

- Fluid gel strengths generally do not pose a problem during normal pipeline operations at high ambient temperatures. Gel strengths are reduced as the percentage of GTL in the crude oil-GTL mixture increases, even at a low temperature of -20°F. This therefore is favorable to pipeline re-start conditions after an extended shut down at temperatures reaching -20°F (cold re-start conditions). High gel strengths significantly reduce the amount of time available to make repairs and return the pipeline to a flowing condition. Altering the final boiling point of the GTL product introduced into the pipeline reduces the gel strength of the commingled GTL and crude oil mixture. Additionally, the resulting mixture has gel strength lower than that of the crude with which the GTL is mixed.
- All the blends (1:1; 1:2; 1:3; 1:4) tested show Pseudo-plastic behavior at higher temperatures (above room temperature), Newtonian at intermediate (around room temperature), and Bingham plastic behavior at lower temperatures (near 0°Celsius and below). This Bingham Plastic flow characteristic indicates that high pumping power requirements are necessary to re-start the pipeline after extended shut down at low temperatures.
- The vapor pressure increased with the addition of GTL but the values are below the minimum TAPS operating pressure, ensuring a single phase only liquid flow of the blends. Also, the bubble point pressure results showed that the blends would flow through the TAPS as compressed liquids from inception to discharge. Therefore, vapor formation in the pipeline as the blends are transported is not possible. Under current TAPS operating conditions and for all blend ratios considered in this study, the fluid will always exist as a single phase liquid.
- Asphaltene flocculation and deposition is a potential major problem in transporting blends through the TAPS. Although ANS crude retains asphaltene in solution during transport, addition of GTL disrupts this stability, and significant amounts of asphaltenes precipitate out. Asphaltene flocculation occurred in a blend containing as little as 5.7% by volume of a GTL product.
- Further investigation of solid deposition in GTL/ANS crude oil mixtures under dynamic conditions is necessary. Studying the solid deposition rate in the fluid main stream and along the walls of the pipeline will reveal how such mixtures behave under practical operating conditions.
- GTL technology may serve as a way to recover and transport Alaska's heavy oil resources. A feasibility study and flow characterization for blends of GTL and ANS heavy oil through the TAPS is necessary.

CHAPTER 1
INTRODUCTION

Background

The Alaskan North Slope is one of the largest hydrocarbon reserves in the United States where Gas-to-Liquids (GTL) technology might be successfully exploited and implemented. Conventional natural gas proven and recoverable reserves in the developed and undeveloped fields of the Alaskan North Slope (ANS) are estimated at 38 trillion standard cubic feet (TCF). In addition, estimates of undiscovered gas reserves in the Arctic fields range from 64 TCF upwards to 142 TCF [1, 2]. Currently, a portion of the natural gas produced on the ANS is used in the oil-field operations such as gas lift and power generation, and in local sales. The unused portion is injected back into the reservoir for pressure maintenance and oil production. As crude oil production on the North Slope declines, approximately 26 TCF of ANS natural gas could become available for sale, transportation, or conversion to liquid. Any significant commercial sale of ANS natural gas is hindered by a need for a costly gas pipeline that can transport this gas from the remote fields to the markets, located in the continental United States, thousands of miles from the ANS. These severe logistical as well as geopolitical problems complicate effective use of this valuable and abundant resource.

Of the several existing options for transporting ANS gas resources, the two most promising are: (i) transportation via a new gas pipeline, called the Trans-Alaska-Gas-System (TAGS), followed by Liquefaction to LNG, then transportation to Pacific-Rim markets via LNG tankers, or the North American Gas Pipeline Transportation System (NAGPTS), which might be routed through Canada to the Midwestern United States; or (ii) conversion of the gas to GTL products on the ANS followed by transportation via the existing Trans-Alaska Pipeline System (TAPS). Robertson et al., [3] concluded that the TAGS/LNG and the GTL options appear economically promising and warrant consideration in the decision-making process. The main drawback of the NAGPTS and TAGS-LNG option is that it requires large capital investment and faces strong competition from worldwide LNG projects. The GTL-TAPS option will use existing infrastructure. Currently, 4 of 12 pump stations have been shut down due to decline in TAPS throughput. It is projected that by the year 2020, ANS crude oil production will decline to such a level (200,000 to 400,000 bbl/day) that, without the addition of supplementary liquids, the

pipeline will be far less economical to operate. Pumping GTL products through TAPS will significantly increase the pipeline's economic life. Reasons for considering transporting GTL products through TAPS include: 1) enhancing the value of ANS gas resources; 2) using existing oil pipeline and other infrastructure for GTL transport; and 3) using GTL products to increase pipeline throughput. Demand for efficient use of natural gas resources will only increase in near future.

1.1 Alaska North Slope (ANS) Gas Utilization Options

In the past, ANS natural gas has been used as a tertiary oil recovery injectant, for converting methane to methanol as a vehicle fuel, and as a local source of power in remote Alaskan villages. Gas-to-liquids (GTL) conversion technology, where natural gas is chemically converted to transportable hydrocarbon liquid products, is an emerging technology that will undoubtedly reach commercialization within the next decade. Some current research is developing a novel ceramic membrane technology suitable for converting natural gas to transportation-grade liquid fuels and premium chemicals.

New GTL technology may provide a means of effectively using the vast natural gas resources of Alaska's North Slope. This study measured various fluid properties of GTL and GTL-Crude Oil blends; its primary goal was to address possible problems involved in GTL product transport through the existing Trans-Alaska Pipeline System (TAPS). Previous studies [4,5] identified technical and economic factors affecting the feasibility of moving GTL-liquid products through the TAPS. This work formed this basis for modeling studies and solids deposition studies

The types and composition of various GTL materials were determined and a program for testing GTL materials and GTL/crude blends was designed. Experimental and simulation studies were conducted to determine properties of various blends of GTL product and ANS crude and to study flow behavior of GTL transport through the TAPS.

1.2 GTL Transportation issues through Trans Alaska pipeline System (TAPS)

GTL technology is gaining world-wide approval among oil- and gas-producing countries as a means to effectively capitalize on remote (stranded) reserves of natural gas. It has been termed

the 'fuel for the 21st century' because it is a clean fuel with zero-sulfur. In Alaska, this technology is one of the options under consideration for monetizing ANS gas, because of the existing TAPS. Using this existing infrastructure could minimize the initial investment costs of GTL technology.

1.2.1 Pipeline Specifications

Understanding the hydraulics of fluid transport through TAPS is the first step to optimizing the structure for GTL use. The Trans-Alaska Pipeline System is 800.32 miles long, with an inner diameter of 46.98 inches, and average pipeline thickness of 0.512 inches. Starting at Prudhoe Bay and ending at the Valdez terminal with a total line fill of 9.06 million barrels, the TAPS maximum design and operating pressure is 1180 psi. Of the original 12 pump stations with 4 pumps each, Pump Station 5 is now a relief station with no pumping capacity, and stations 2, 6, 8, 10 and 12 are currently shut down. The pipeline's control system provides instantaneous monitoring and control of significant aspects of operation and pipeline leak detection. Table 1.1 shows the locations and elevations of the various pump stations. Figure 1.1 shows a map of Alaska, the path of the TAPS, and the pump stations. The TAPS maximum daily throughput is 2.136 million barrels, with 11 pump stations operating.

Table 1.1. Locations and Elevation of Pump Stations (TAPS FACTS, 2004).

Pump Station	Location	Distance (miles)	Elevation (feet)
1	Prudhoe Bay	0	39
2	Happy Valley	57.76	602
3	Happy Valley	104.27	1383
4	Galbraith Lake	144.05	2763
5	Prospect Creek	274.74	1066
6	Five Mile	354.94	881
7	Fairbanks	414.12	905
8	Eielson AFB	489.22	1029
9	Big Delta	548.69	1509
10	Gulkana	585.77	2392
12	Gulkana	735.04	1821
Terminal	Valdez	800.27	142

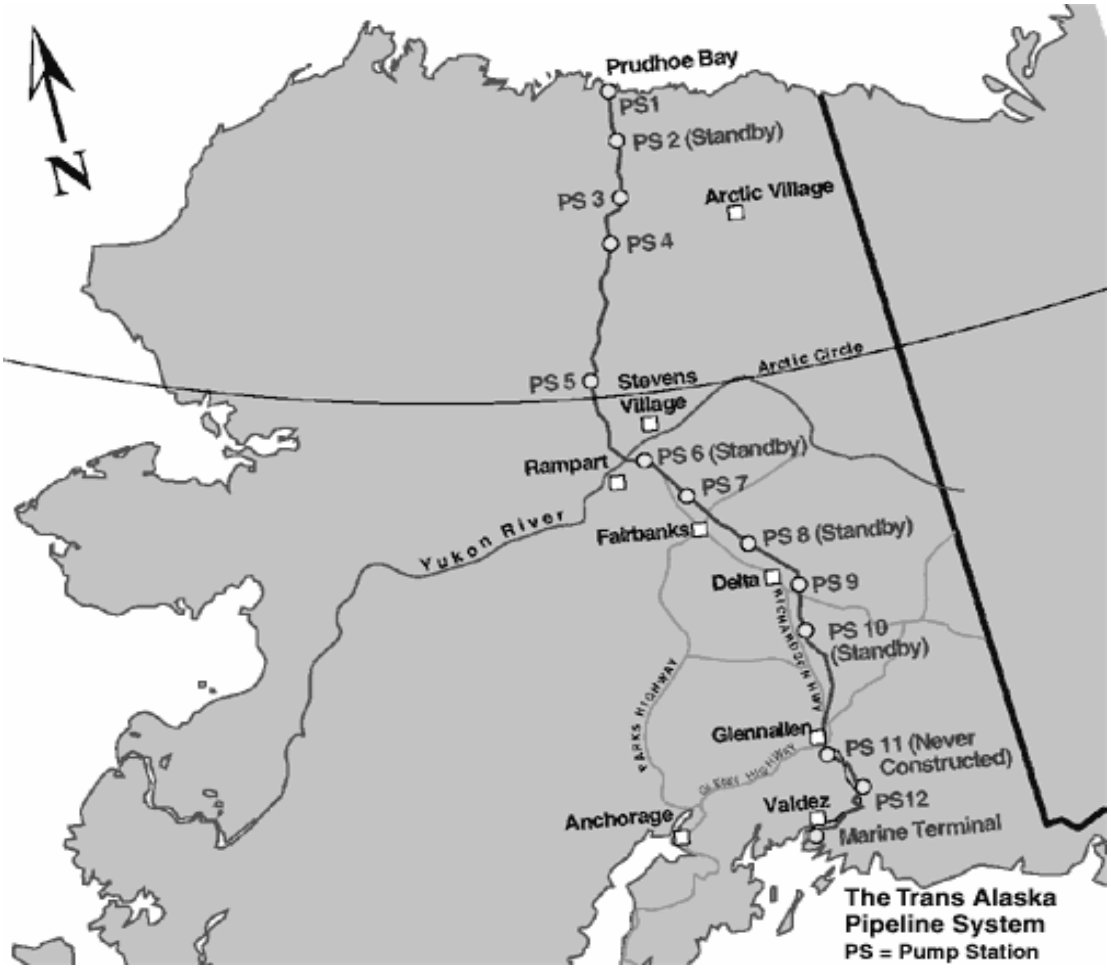

Figure 1.1. Map of Alaska showing the Trans Alaska Pipeline and the pump stations.

1.2.2 Travel Time and Temperatures of Crude Oil

Crude oil travels at an average velocity of 3.7 miles per hour through TAPS, and the total time to travel from Pump Station 1 to Valdez is 9 days. Table 1.2 shows travel time for each pump station. Table 1.3 shows inlet and exit temperatures of the crude oil at working pump stations at a flow rate of 1.02 MMbpd for the month of February, 2004. TAPS operating pressure was 1180 psi.

Table 1.2. Travel Miles and Line Fill Between Stations (Pipeline Facts, 2004).

Travel time at 1.02 million bbl./day and miles and line fill between stations			
From	**Hours**	**Miles**	**Line fill (bbl.)**
PS 1-2	15.71	57.76	653,862
PS 2-3	12.65	46.51	526,508
PS 3-4	10.82	39.78	450,322
PS 4-5	35.56	130.77	1,480,358
PS 5-6	21.81	80.18	907,663
PS 6-7	16.09	59.18	669,937
PS 7-8	20.42	75.10	850,156
PS 8-9	16.17	59.46	673,106
PS 9-10	10.09	37.09	419,871
PS 10-11	27.24	100.16	1,133,843
PS 11-12	13.36	49.11	555,941
PS 12- Valdez	17.74	65.22	738,311
	217.65	**Approx. 800.32**	**9,059,879**

Table 1.3. Crude Oil Temperatures at Various Pump Stations

Pump Station	Inlet Temperature (°C)	Exit Temperature (°C)
1		45.9
3	26.3	28.6
4	26.2	26.9
5	Relief Station	
7	14.3	16.0
9	16.9	18.5
Valdez	14.9	

1.2.3 Transportation Issues

Operational issues to be addressed when considering transporting blends of crude oil-GTL product mixtures through TAPS include:

i. Cold temperature effects on the gel strength of the crude oil-GTL blends with respect to cold restart of the pipeline during prolonged shut downs.
ii. Phase behavior of the GTL products and any vapor pressure concerns
iii. Effect of solids precipitation and deposition of the blends (wax and or asphaltenes) within the pipeline.

1.3 Project Objectives

This study, working in collaboration with Alyeska Pipeline Service Company (APSC), the TAPS operator, determined that the main operational issues in transportation of GTL products via TAPS are: (i) cold restart of the pipeline and (ii) solids deposition in the pipeline. Due to extreme arctic conditions, fluids transported via TAPS must be such that the pipeline can be restarted from an extended shutdown with cold GTL or GTL-crude oil blends in the pipeline. Additionally, GTL presence in the pipeline may enhance precipitation of solids (asphaltenes and wax), which causes problems with metering, solids buildup inside the pipeline, and pressure losses. This project investigated the flow of GTL products through TAPS in view of these operational challenges. The scope of this work included experimental and simulation study of the properties of GTL products and their blends at a wide range of possible TAPS operating conditions, including a cold weather shutdown.

1.4 Project Tasks

The following tasks were designed to determine the operational constraints of a GTL/Crude blend.

Task 1: Sample preparation and characterization. Fluid samples for the project experiments were prepared to represent a wide range of possible GTL output from a BPX GTL Pilot plant on the ANS. Fischer-Tropsch synthesis for GTL production results in a highly variable liquid composition depending on the exact process used. Additionally, blends of GTL and crude oil were prepared for testing. Because GTL throughput rate is expected to be lower than the crude

oil throughput rate, the proportion of GTL in the GTL-crude oil blends did not exceed 50%. Compositional analysis was performed using High Temperature Gas Chromatograph (HTGC) in order to characterize the samples in terms of carbon numbers. Based on data from these tests, GTL composition acceptable for transportation through TAPS can be established. The pipeline owners can use this information to assess risk-versus-reward scenarios for producing GTL products of given compositions and building additional facilities such as distillation and hydrocracking plants on the ANS.

Task 2: Gel strength measurement. Feasibility of moving any GTL product or its blend through TAPS must be determined by cold restart of fluid flow in the pipeline. Cold restart depends on gel strength. During shut down at low temperatures (below 40°F), liquid movement in pipes is impeded by the liquid's gel structure. With decreasing temperature, the gel strength increases, resulting in increased viscosity. Under the cold weather conditions common to Alaska, it is important to determine the amount of pressure, known as the cold restart pressure, at which the liquid in the pipeline will yield. Thus, cold restart pressure is a function of gel strength.

A cold restart depends on the gel strength of the chilled pipeline fluid, pipeline geometry, and pump station capabilities. Since geometry and pumping capability are fixed, the gel strength of various GTL and GTL-crude oil blends were measured using a custom-designed Vane Viscometer. The gel strength of various GTL products and North Slope crude oil blends were determined by the rotating vane method. This method determines the minimum amount of torque necessary to initiate oil movement at low shear, and subsequent gel breakdown after flow initiation. The data obtained can be directly used in modeling both crude oil and GTL behavior in pipes during start-up conditions.

Alyeska Pipeline Service Company (TAPS operator) currently uses services of the Westport Technology Center, Houston, TX, to perform standardized gel strength tests using vane viscometry. Although duplicating such tests at the University of Alaska Fairbanks was prohibitively expensive, the principles of vane viscometry were used to custom-design vane spindles for UAF's existing Brookfield viscometers with small sample adapters. These custom-

built vane spindles were used to estimate gel strengths of GTL products and their blends with crude oil.

A slow cooling process (cold ramp) in sample preparation is often used to simulate an extended cold weather pipeline shutdown. However, using the slow cold ramp process requires an inordinate amount of time to obtain a single data point. Therefore, researchers used a fast cold ramp procedure along with the custom-built vane spindles to estimate gel strength in a relatively short time period. Results from these tests can be used to quickly identify GTL and GTL-crude oil mixtures that are unsuitable for transportation through TAPS, and those mixtures that merit further study.

Task 3: RVP measurement. Reid Vapor Pressure (RVP) measurements provided vapor pressure data, which, in conjunction with gel strength, helped determine the range of GTL and crude oil blends that can be transported via TAPS. Reid Vapor Pressure, a technique (ASTM method D-323) used to measure vapor pressure, is converted to True Vapor Pressure (TVP) by using the API nomograph or an equivalent mathematical equation given in API publication 2517. RVP measurements are taken at 100°F. True Vapor Pressure is an industry standard, mandated by regulatory agencies such as EPA, and can be determined with commonly available technology. The API conversion to TVP corrects for temperature effect on vapor pressure and for partial vaporization of the sample in the Reid's apparatus. The practice provides the basis for correlation of hydrocarbon content of tank vapors and vapor emissions.

Task 4: Density and viscosity measurement. Density and viscosity affect the pressure requirements for operating TAPS, and these measurements are necessary to characterize flow conditions in the pipeline for a given fluid. A Brookfield LV viscometer with a small sample adapter and a Brookfield cone-plate viscometer were used to measure fluid viscosity as a function of temperature at atmospheric pressure. A digital density-meter was used to measure fluid density as a function of temperature at TAPS operating pressure. The density-meter was calibrated at the test temperature and pressure conditions using nitrogen and double distilled degassed water. The density and viscosity data of GTL and crude oil and their blends were used in the pipeline flow model for batching and blending modes of GTL transportation. Also, the

measured fluid densities and viscosities were used for matching the equation of state phase behavior simulations. Prior to carrying out measurements on GTL and crude oil blends, the accuracy and reliability of the density-meter and the viscometer were assessed by measuring data on normal alkane systems and comparing them with standardized data from literature.

Task 5: GTL and crude oil phase behavior study. The phase behavior studies were based on current TAPS operating conditions. This task included generating phase envelopes for GTL, crude oil and their blends; bubble point measurements; flash vaporization; and constant composition expansion (CCE) experiments using a windowed DBR JEFFRI PVT cell. These tests provided reliable data for safe and efficient operation of TAPS under various GTL flow conditions and helped evaluate the risks of solids precipitation. Measurements were conducted at five different isotherms. The visual information obtained from the windowed DBR JEFFRI PVT cell indicated solid formation at the various isotherms. A separator type test, conducted on the different blends and pure GTL and crude oil by flashing to a gasometer, provided valuable separator data for the downstream end of TAPS.

Task 6: Phase behavior modeling. GTL and crude oil properties are likely to alter after a certain period. Therefore a numerical reference model for accurate and reliable prediction of physical properties and phase behavior of GTL and crude oil and their blends was constructed. This numerical reference model allowed comparison of predicted and measured physical properties and phase behavior of GTL, crude oil and their blends. Phase behavior was predicted by using the Soave-Redlich-Kwong (SRK) equations of state (EOS). Prediction models were tuned by changing the properties of the pseudo-plus (C_{30+}) fractions, depending on the comparative study. The numerical reference model will be a useful tool for future applications.

Task 7: Solids deposition study. Solid deposits of wax and/or asphaltene can pose major problems in reservoirs, pipelines and separators. These unwanted deposits can hamper the TAPS efficiency and GTL transportation economics. The risk, nature and severity of solids deposition in TAPS under GTL flow conditions was studied in this project. High Temperature Gas Chromatograph (HTGC) and ASTM distillation apparatus were used for compositional analysis of pipeline wax. Asphaltene particles are known to provide sites for wax crystal buildup, which

leads to increased wax deposition. Co-precipitation of asphaltenes and associated resins with wax could result in excessive solids buildup with significantly different properties (hardness); these could in turn adversely affect pipeline operation. Static asphaltene precipitation tests and total wax precipitation tests at varying temperatures were conducted to study the effect of asphaltene on wax deposition. Total precipitated solids (wax and asphaltene) were determined by low temperature centrifuge. Additionally, GTL presence was expected to alter the wax deposition characteristics of the crude oil in TAPS. Wax appearance temperatures for GTL and GTL-crude oil blends at atmospheric and typical TAPS operating pressures were determined under static conditions. The instability of the crude oil for asphaltene deposition was determined using flocculation onset titration on crude oil and its blends using n-heptane as a precipitant. However, some flocculation onset titration tests were conducted on crude oil using GTL as a precipitant.

Standard asphaltenes were determined by using the IP 143 method on crude oil and its blends with GTL. Also, standard asphaltenes were determined using the IP 143 method, but using GTL as a precipitant on 100% crude oil samples. The IP 143 tests indicated the presence of asphaltenes in crude oil and its blends with GTL. The flocculation onset titration yielded information on the stability/instability of the crude oil and its blends with GTL, as regards asphaltene deposition. Static Wax Appearance Temperature measurements, at TAPS operating conditions, in conjunction with the phase behavior study, aided in constructing the Solid-Liquid-Vapor (SLV) diagram/envelope of the GTL, crude oil and their blend system. Changes from Newtonian to non-Newtonian behavior of the tested liquids were indicated by the WAT measurements. The data collected under this task served as input parameters for wax deposition modeling for pipeline control.

References:

1. 1995 Assessment of United States Oil and Gas Resources," US Geological Survey, Circular No. 1118, (1995).
2. "Natural Gas 1994, Issues and Trends," DOE/EIA Report No. 8520, (July 1994).
3. Robertson, E.P., Thomas, C.P., and Avellanet, R.A. "Economics of Alaska North Slope Gas Utilization Options," A paper presented at the SPE Western regional Meeting, Anchorage AK, (May 1996).
4. Akwukwaegbu, C.F. "Evaluation of the Modes of Transporting GTL Products Through the Trans Alaska Pipeline System (TAPS)", M.S. Thesis, University of Alaska Fairbanks, May 2001.
5. Ramakrishnan, H. "Experimental and Economic Evaluation of GTL Fluid Flow Properties and Effect on TAPS", M.S. Thesis, University of Alaska Fairbanks, December 2000.

CHAPTER 2
SAMPLE PREPARATION AND EXPERIMENTAL EQUIPMENT

The goal of our sample preparation methodology was to produce samples that represented a wide range of possible GTL output. Samples of GTL products were available from the BPX GTL Pilot plant operating on the Alaska North Slope (ANS). Additionally, blends of GTL and crude oil were prepared for testing. The sections below correspond to the project tasks outlined in Section 1.4 (last chapter).

2.1 Sample Preparation

The ANS crude oil sample was taken at TAPS pipeline conditions directly into a Welker Constant Pressure Sample Cylinder in order to preserve its composition. GTL samples from the BPX GTL Pilot plant in Alaska (referred to here as "AKGTL" or "BPGTL") were received from BP Exploration Alaska Inc. in sealed 1-US gallon cans. The AKGTL in each can was used as soon as the can was opened, ensuring no change in the composition. The samples were used to evaluate for density, viscosity and solids precipitation.

2.2 Sample Blending Procedure

The AKGTL and the crude oil samples were blended gravimetrically at room temperature (21°C). The procedure is described below:

Let

V = Required volume of sample (blend)

ρ_{BPGTL} = Density of AKGTL at room temperature

ρ_{CO} = Density of crude oil at room temperature

α = Fraction of AKGTL in the required sample

Then,

Total mass of required sample, $M = \dfrac{\rho_{GTL}\rho_{CO}V}{\alpha\rho_{CO} + (1-\alpha)\rho_{GTL}}$ 2.1

Mass of AKGTL in the sample, $M_{BPGTL} = \alpha M$ 2.2

Mass of crude oil in the sample, $M_{CO} = (1-\alpha)M$ 2.3

Using a mass balance, the masses of AKGTL and ANS crude oil calculated above were obtained and poured into a sample bottle. The sample bottle was closed and shaken to obtain the required homogeneous blend of the two fluids.

For the stability test, the test fluids were prepared to contain a certain volume of toluene per gram of crude oil. A total of 5 cc of toluene was added to 10 gm of crude oil to produce a test fluid of 0.5 cc toluene per gm of crude oil.

Because the density of the crude oil was not measured under high pressure conditions, a separate volumetric blending procedure was employed for the phase behavior (bubble point pressure) studies. A predetermined amount of AKGTL was initially charged into the sample cylinder. The correct volume of pre-reconditioned crude oil was allowed to flow directly from the Welker cylinder into the sample cylinder to produce the required blend ratio. Charging the crude oil directly from the Welker cylinder into the sample cylinder ensured that light crude oil ends did not escape. Thus, the original composition of the crude oil was preserved.

2.3 Welker Constant Pressure Sample Cylinder

The Welker Constant Pressure Sample Cylinder, shown in Figure 2.1 on a retort stand, is designed to maintain samples at pipeline conditions. It also provides for adequate mixing, laboratory repeatability and safe handling of the sample. The cylinder has two ends – the "Product Inlet" end and the "Pre-charge" end. An internal floating piston separates the two ends. The Product Inlet end accommodates the sample while the pressurizing fluid (usually nitrogen gas) occupies the Pre-charge end. Sharma [1] has provided a more detailed description of the cylinder.

In order to obtain samples from the cylinder, the sample is re-conditioned to pipeline temperature (90°F) using the heating drum shown in Figure 2.1. The crude oil is allowed to equilibrate at this temperature for about two hours. During this period, the sample is mixed at least three times. Sharma [1] has described the crude oil aliquoting procedure in greater detail.

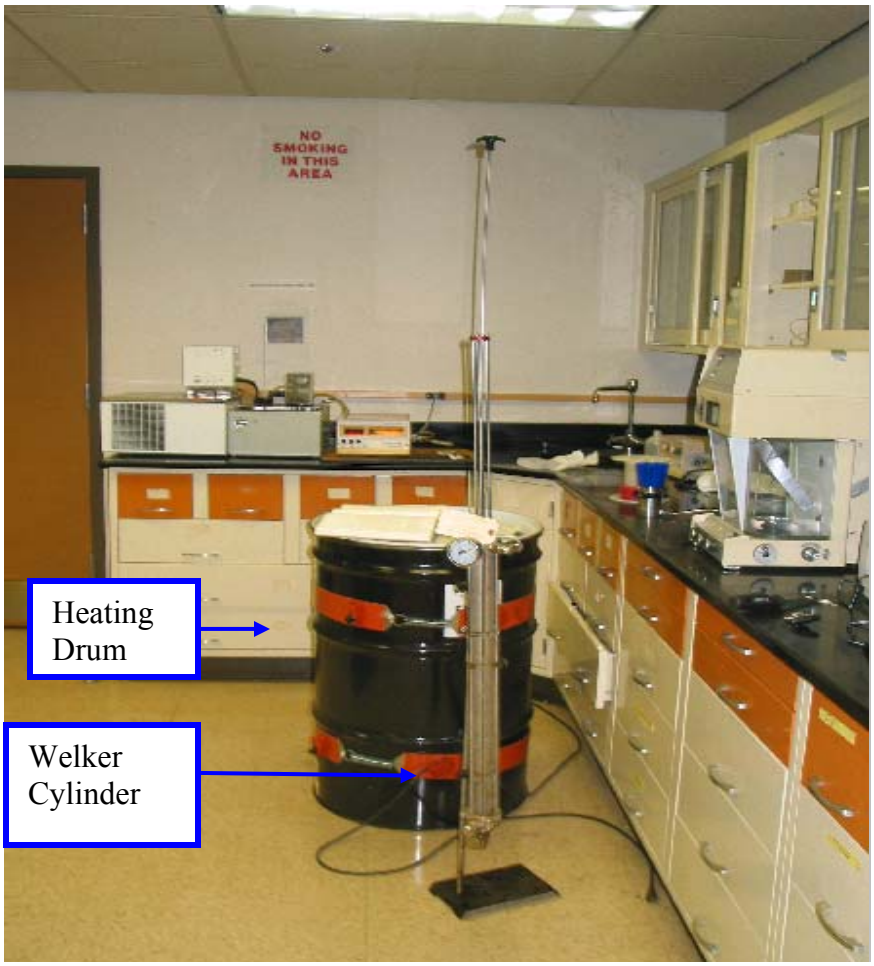

Figure 2.1. A Welker Cylinder in front of the Heating Drum.

2.4 Density Measurement Apparatus

The apparatus shown in Figure 2.2 consists of a Mettler/Paar DMA-45 digital density meter, a Brookfield TC-500 temperature bath and plastic syringes with a capacity of 2cc.

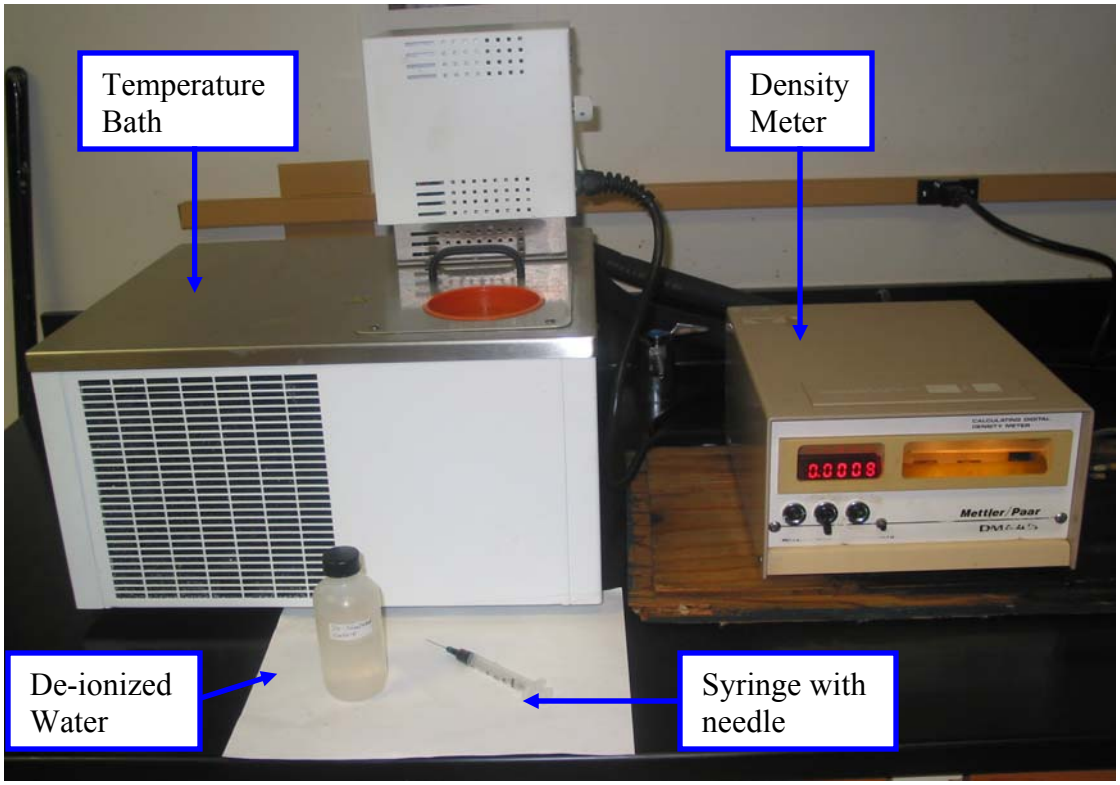

Figure 2.2. Density measurement apparatus.

The Mettler/Paar DMA-45 digital density meter (shown in Figure 2.3) consists of two U-shaped co-axial glass tubes. The inner tube, housed by the outer tube, accommodates the sample and is excited by an electronic system. An incorporated quartz clock measures the period of oscillation approximately every two seconds. The sample tube has two ports. Samples are introduced into the meter through the lower port by means of syringes. Detailed descriptions of the working principles and the meter calibration procedure appear in Amadi [2].

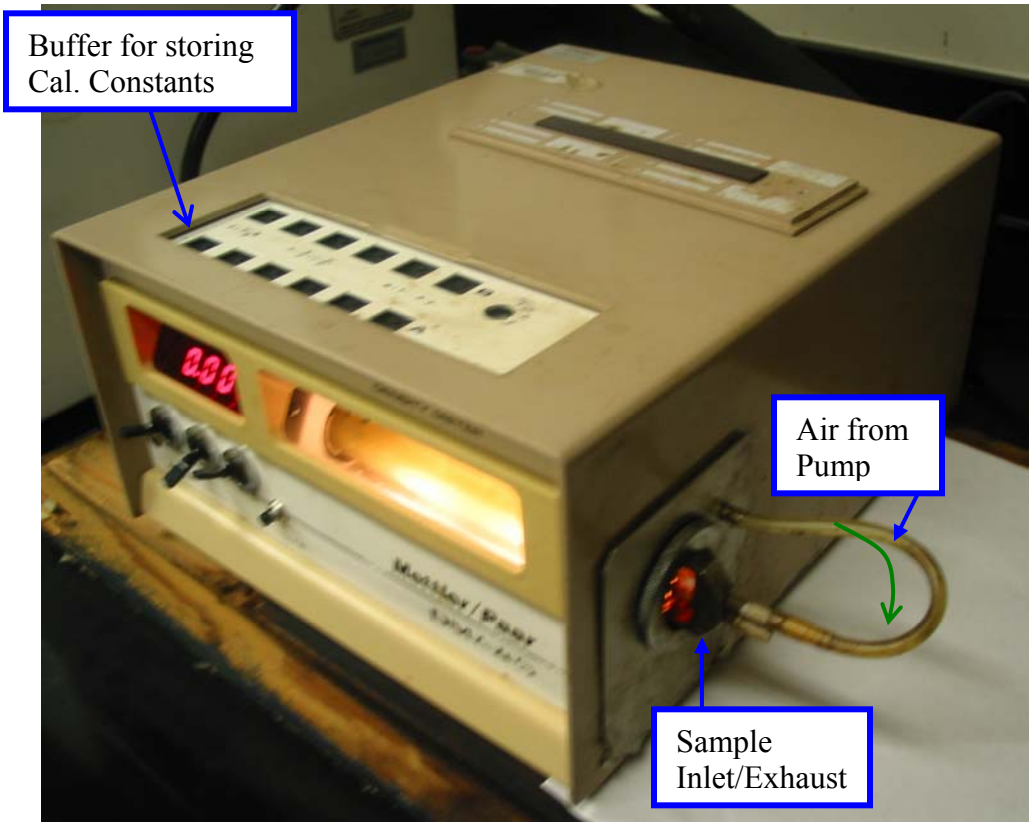

Figure 2.3. The Mettler/Paar digital density meter.

2.5 The Brookfield DV-II+ Programmable Viscometer

Three models of the Brookfield DV-II+ Programmable Viscometer were used for experiments in this study: the LVDV-II+, the LVDV-II+CP (Cone/Plate Viscometer) and the RVDV-II+. WinGather software installed in each of the data acquisition computers facilitated input and output communication with the viscometers. The LVDV-II+ and the RVDV-II+ viscometers, which have maximum torque capacities of 673.7 dyne-cm and 7187.0 dyne-cm respectively, were used for gel strength measurements. By virtue of a custom designed vane spindle and Small Sample Adapter, the LVDV-II+ and the RVDV-II+ viscometers can measure maximum gel strengths of 128.7dyne/cm^2 and 1372.7 dyne/cm^2, respectively [3] . The LVDV-II+ was also used for an asphaltene flocculation onset titration experiment.

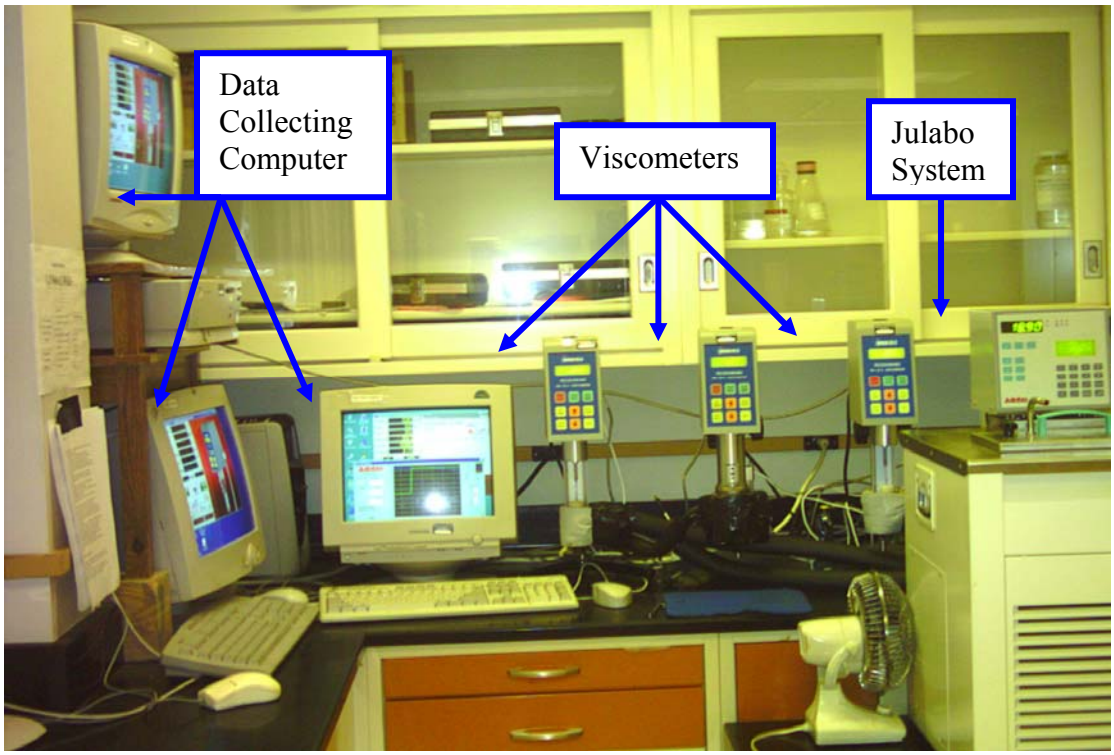

Figure 2.4. The Brookfield DV11 + Programmable Viscometer System.

A plate-shaped sample holder and a cone-shaped spindle (shown in Figure 2.5) characterize the LVDV-II+CP Viscometer. The equipment was used for measuring rheological parameters and wax appearance temperatures under static conditions. Accurate measurements are possible with the cone-plate viscometer when the gap between the spindle and the sample cup is properly set using a micrometer screw gage incorporated in the equipment**.** The setting procedure is detailed in the equipment manual.

A Julabo FP50 Heating/Cooling system (also shown in Figure 2.4) controlled remotely by means of EasyTemp software (installed in the data acquisition computer for the LVDV-11+CP viscometer) facilitated temperature control of the test sample.

Figure 2.5. Sample cups and spindles.

2.6 Bubble Point Pressure Measurement Apparatus

Figure 2.6 shows a schematic of the bubble point pressure measurement apparatus. The major components are a Tenney environmental test chamber, a JEFRI positive displacement pump, a 300 cc-capacity JEFRI floating-piston sample cylinder and a Heise digital pressure gauge.

The Tenney environmental test chamber is incorporated with heating/cooling devices. Heating is achieved by circulating chamber air through open-air nichrome wire heater elements, while cooling is achieved by re-circulating chamber air through a refrigerated cooling coil in the chamber conditioning section. The equipment has a temperature range of -73°C to 200°C and can be programmed for ramped temperature profiling.

The JEFRI positive displacement pump is a piston-cylinder arrangement designed to dispense high pressure fluids with a high degree of accuracy. It performs reliably, smoothly and safely to a maximum working pressure of 10,000 psi. Typical displacement volumes range between 5 to 1000 cc with a volume resolution of 0.0025 cc. High pressure seals positioned firmly between the cylinder and the piston (at the cylinder end) facilitate perfect confinement of the fluid within the cylinder. Thus the displaced fluid volume is proportional to the calibrated length of the piston inserted into the cylinder. Auxiliary control devices facilitate selection of desired fluid displacement rate, displacement acceleration, manual or automatic control of the pump, constant pressure operation, and digital display of pump displacement in millimeters or inches. Certified AW46 R&O hydraulic oil was used as the pressurizing fluid.

The 300 cc-capacity JEFRI floating-piston sample cylinder is a stainless steel high pressure cylinder with a maximum working pressure of 10,000 psi. The floating piston separates the sample and the pressurizing fluid thereby facilitating constant composition compression and expansion of the test sample within the cylinder. The end that accommodates the sample is marked “Process End” while the other end is the “Displacement Fluid End”. An external pump provides the displacement pressure.

The ANS crude oil sample is directly taken from a Welker Sample Cylinder connected to the JEFRI floating-piston sample cylinder (see Figure 2.6). This method of introducing the crude oil sample ensured that its composition is preserved.

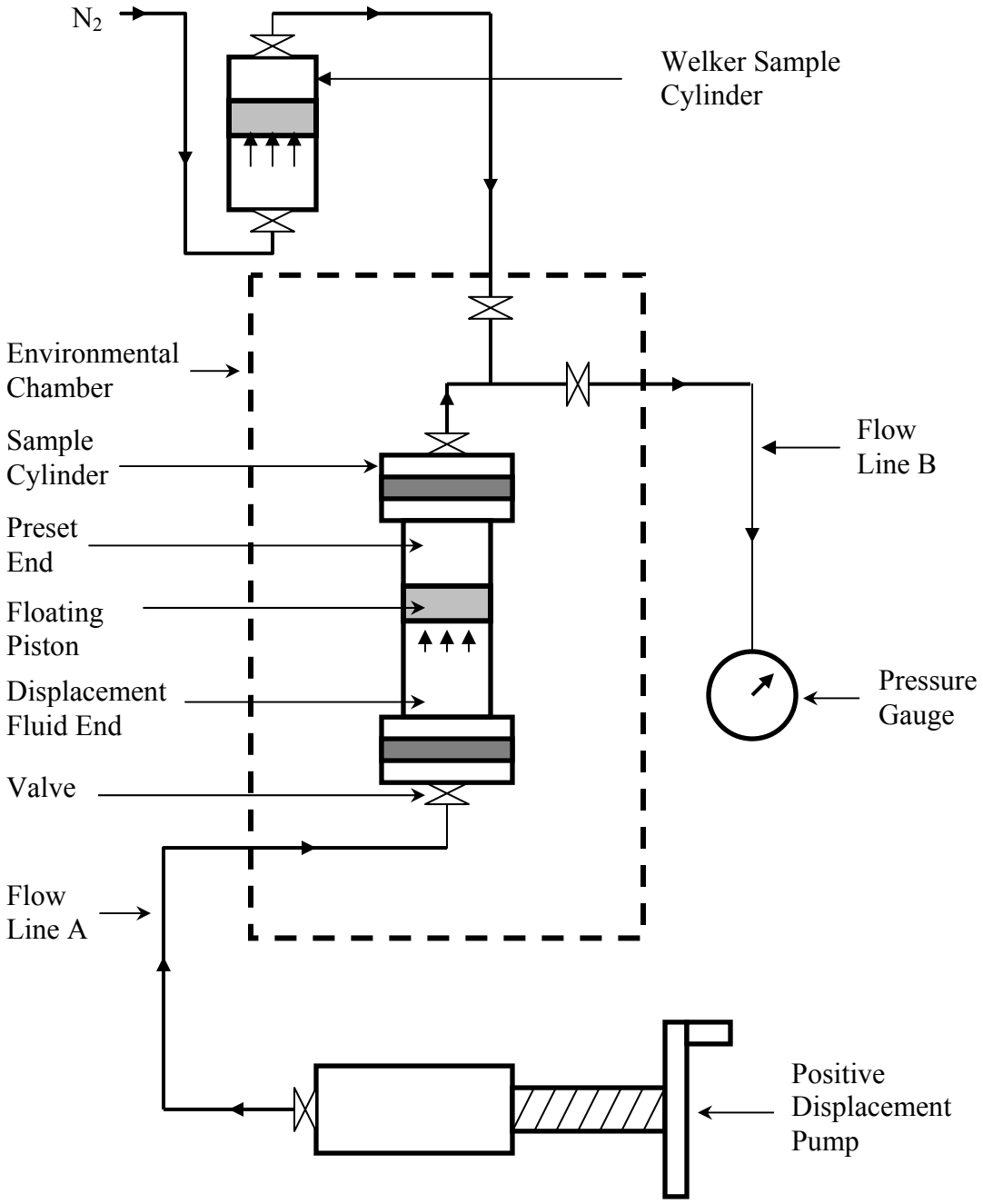

Figure 2.6. Schematic of the bubble point pressure measurement apparatus.

2.7 Static Asphaltene Deposition Test Apparatus

The static asphaltene deposition apparatus is shown in Figure 2.7. It is comprised chiefly of a glass filtration system, a vacuum source, 0.22 μm -pore-size 90mm-diameter cellulose acetate filter papers, and a Mettler-AE 160 mass balance with a resolution of 0.0001 gram.

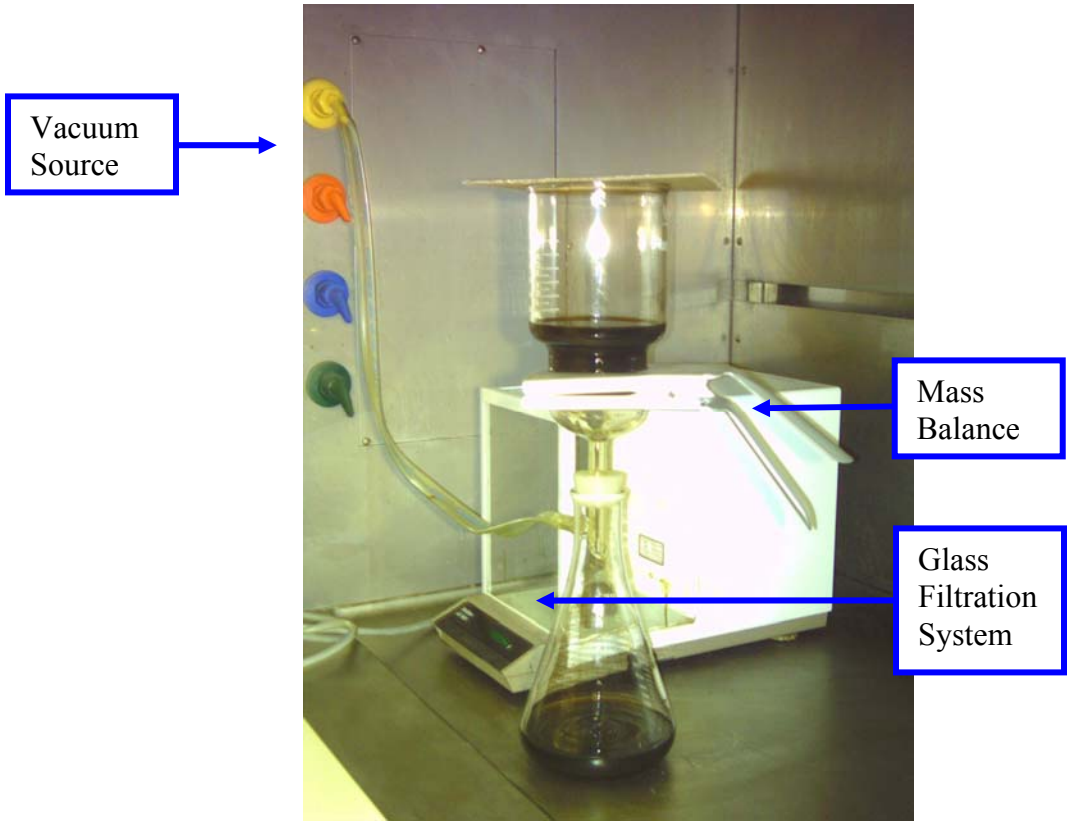

Figure 2.7. Static asphaltene deposition test apparatus.

2.8 Asphaltene Stability Test Apparatus

The apparatus shown in Figure 2.8 principally consists of a Cannon-Fenske viscometer (labeled 'B' in Figure 2.8 and also shown in Figure 2.9), a stop clock (labeled 'D' in Figure 2.8), a thermometer (labeled 'A' in Figure 2.8) and a constant temperature bath (labeled 'C' in Figure 2.8).

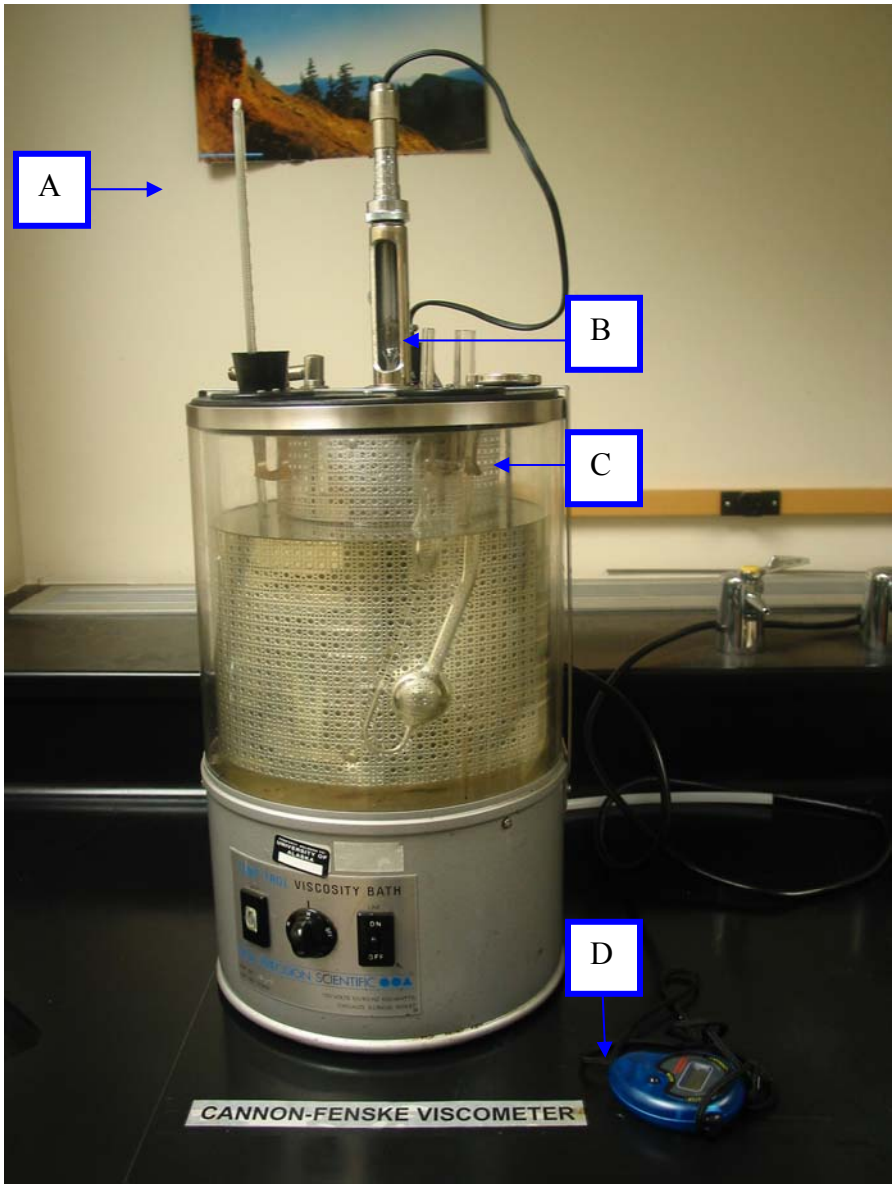

Figure 2.8. Asphaltene stability test apparatus.

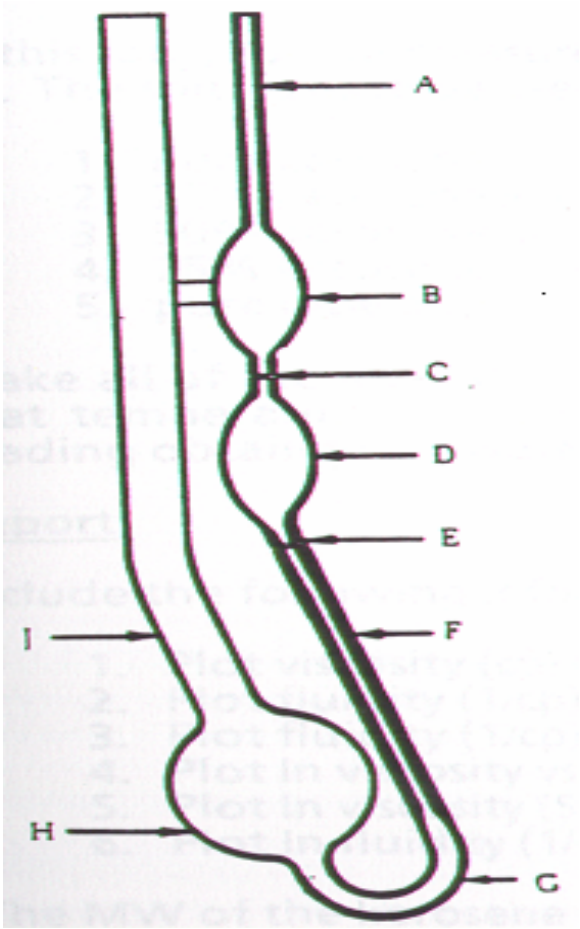

Figure 2.9. The Cannon-Fenske viscometer.

The efflux time, t, measured from the Cannon-Fenske viscometer; the viscometer constant, C; and viscometer coefficient, B are used to calculate fluid viscosity using the following equations.

$$\nu(cs) = Ct - \frac{B}{t} \qquad 2.4$$

Where:

$$B = \frac{t_1 t_2}{t_1^2 - t_2^2}\left(\nu_1 t_2 - \nu_2 t_1\right) \qquad 2.5$$

$$C = \frac{\nu t + B}{t^2} \qquad 2.6$$

Also, v_1 and v_2 are viscosities of standard fluids in centistokes, while t_1 and t_2 are the efflux times for v_1 and v_2 respectively.

2.9 Dynamic Solid Deposition Test Apparatus

Not many studies have been reported in the literature on solid deposition under dynamic conditions. Amadi [2] investigated solid deposition phenomena in ANS crude oil, cuts of the Laporte Light GTL sample and their blends at static conditions (atmospheric pressure). Researchers at the Petroleum Development Laboratory, UAF, custom designed a Dynamic Solid Deposition Test Apparatus for solid deposition studies under dynamic conditions. This set-up measures sample Wax Appearance Temperature (WAT). This set-up also allows investigation of how pressure and flow affect flocculated asphaltenes.

The apparatus (shown in Figures 2.10 through 2.13) consists of a JEFRI sample cylinder, a Temco inline filter with either a 50 micron or a 5 micron pore size filter element, a Heise pressure gauge of 10,000 psi capacity, a Validyne differential pressure transducer with a signal (ΔP) indicator, a Prep-100 pump, and 1/8-inch OD, 1/16-inch ID flow lines. A temperature probe and gauge are connected to the inline filter for instantaneous measurement of the sample temperature while it is being circulated.

The cylinder (Figure 2.13) accommodates the sample at one end, while the Isco pump (Figure 2.13) provides the desired line pressure, measured by the Heise gauge. The Isco pump uses water as pressuring fluid. The Prep-100 pump continuously circulates the sample through the inline filter while the Validyne differential pressure transducer measures the differential pressure across the filter. As with the bubble point measurement apparatus (above), the fluid sample was introduced directly from a Welker cylinder to ensure that its composition was preserved (Figure 2.13).

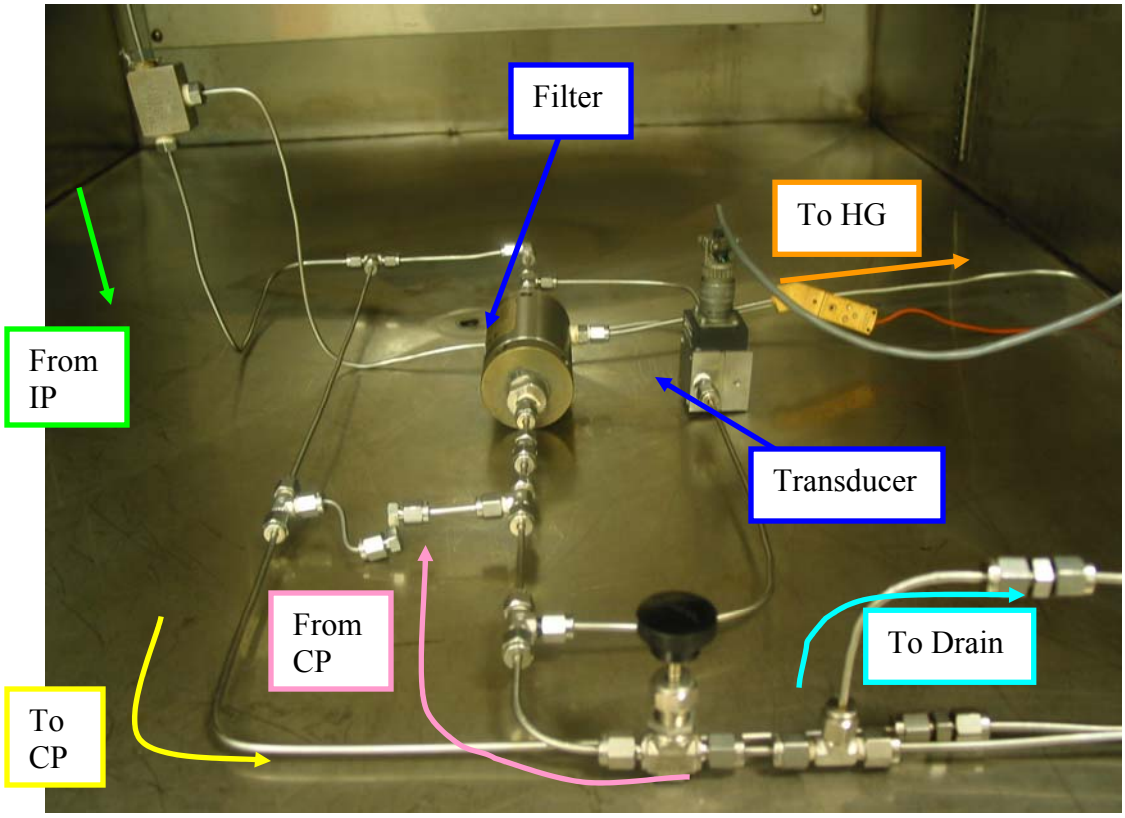

Figure 2.10. The flow loop of the dynamic solid deposition test apparatus
IP = Isco Pump, HG = Heise Gauge, CP = Circulating Pump (Prep-100 Pump).

The flow loop, including the inline filter and the differential pressure transducer, is housed in the Tenny environmental chamber, while the pressure and temperature gauges, circulating (prep-100) pump, Isco pump and sample cylinder are outside the chamber. The Prep-100 pump head, as well as all the lines linking the flow loop to the pump and the pressure gauges, are heavily insulated to avoid thermal communication between the circulating sample and the ambient temperature (see Figure 2.11).

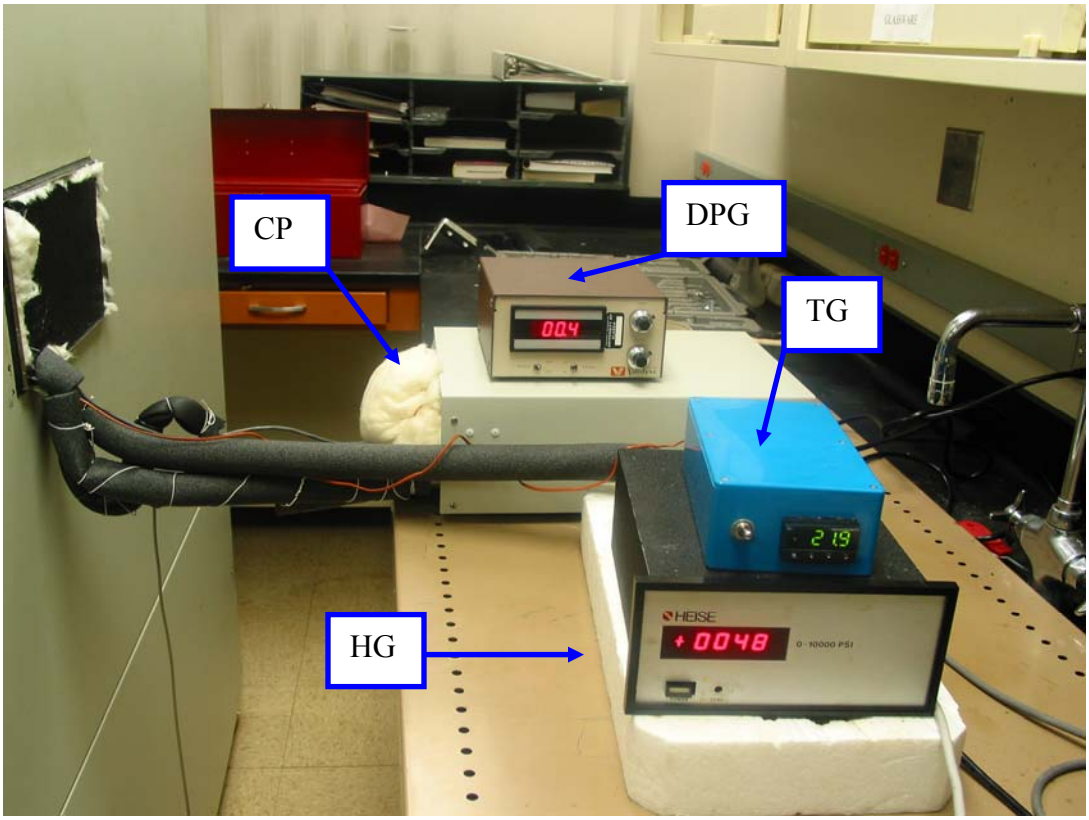

Figure 2.11. Dynamic solid deposition test apparatus showing the Prep-100 pump and the temperature and pressure gauges.

DPG = Differential Pressure Gauge (connected to the differential transducer),
HG = Heise Gauge, CP = Circulating Pump (Prep-100 Pump),
TG = Temperature Gauge (Connected to the inline filter)

The line connecting the sample cylinder and the loop is coiled inside the environmental chamber (see Figure 2.12 below) to avoid the thermal shock that might result if additional sample fluid flowed from the sample cylinder to the loop during the test. Hence, the coil serves as a fluid store, supplying the loop with additional fluid necessitated by temperature decrease during testing.

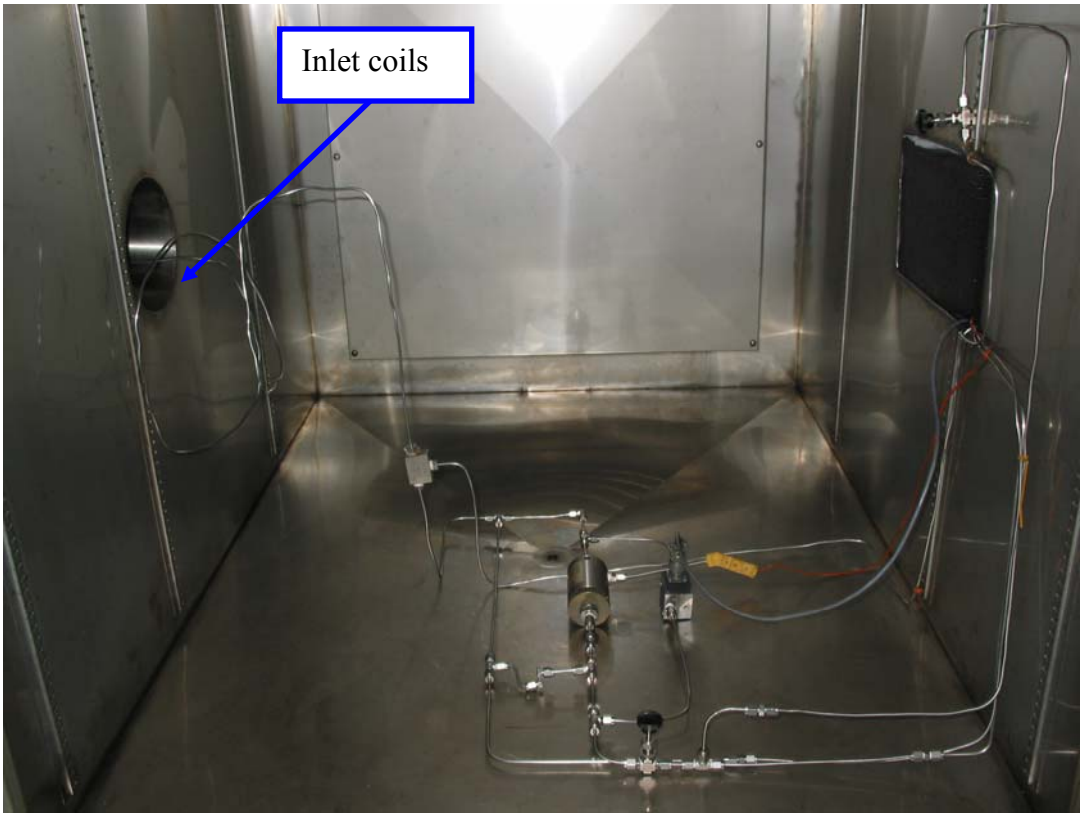

Figure 2.12. Dynamic solid deposition test apparatus showing the inlet coils.

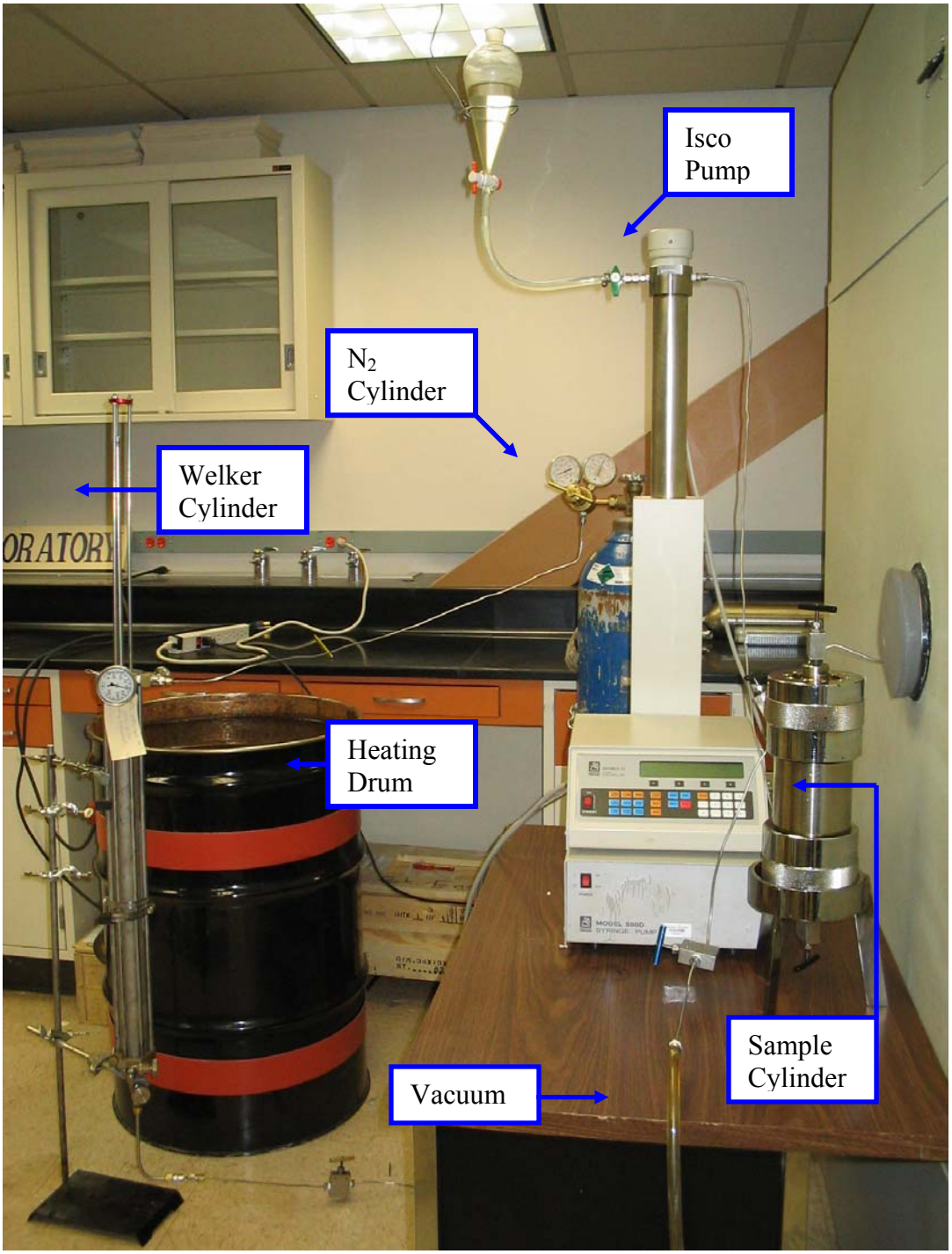

Figure 2.13. Dynamic solid deposition test apparatus showing Isco pump, sample cylinder, N_2 cylinder, heating drum, and Welker cylinder.

2.10 Koehler Apparatus for Measuring Wax Appearance Temperature (WAT)

The Koehler apparatus (Figure 2.14) is used to measure wax appearance temperature by the ASTM D3117 procedure. The major components include a thick-walled glass sample tube, a two-holed rubber (neoprene) stopper for sealing the top of the sample tube, a thermometer, a 200 mm-deep, 65 mm-internal diameter transparent glass flask, a motorized stirrer assembly, a retort stand for supporting the system, dry ice (carbon dioxide chips), a clock for monitoring the cooling rate and isopropanol.

The motorized stirrer assembly consists of a stainless steel wire and an electric motor. The electric motor moves the stainless steel wire up and down at a rate of about 50 to 60 cycles per minute. The carbon dioxide chips and the isopropanol formed the chilling mixture.

2.11 The LaPorte GTL Cuts

A Laporte light GTL sample (supplied by DOE) was distilled to generate a product that could be representative of a GTL sample produced at a North Slope GTL facility. The light GTL was distilled at atmospheric pressure in a Herzog HDA 627 automatic distillation apparatus.

Three final boiling points (distillate cuts) were determined to provide measurements across the range expected to begin generating high gel strengths and solid depositional problems (see table 2.1).

Table 2.1. Laporte Light GTL Distillate Cuts.

Final Boiling Point	Carbon Number (Theoretical maximum)	% Fraction of Light GTL Product
344ºC	nC20	92%
302ºC	nC17	86%
254ºC	nC14	73%

These GTL cuts have been designated as GTL 254, GTL 302 and GTL 344. The GTL cuts obtained from the distillation are mixed with TAPS crude oil in gravimetric ratios of GTL to crude oil of 1:3, 1:1 and 3:1. These ratios were designed so as to cover the effect of the entire range of GTL blending with crude oil.

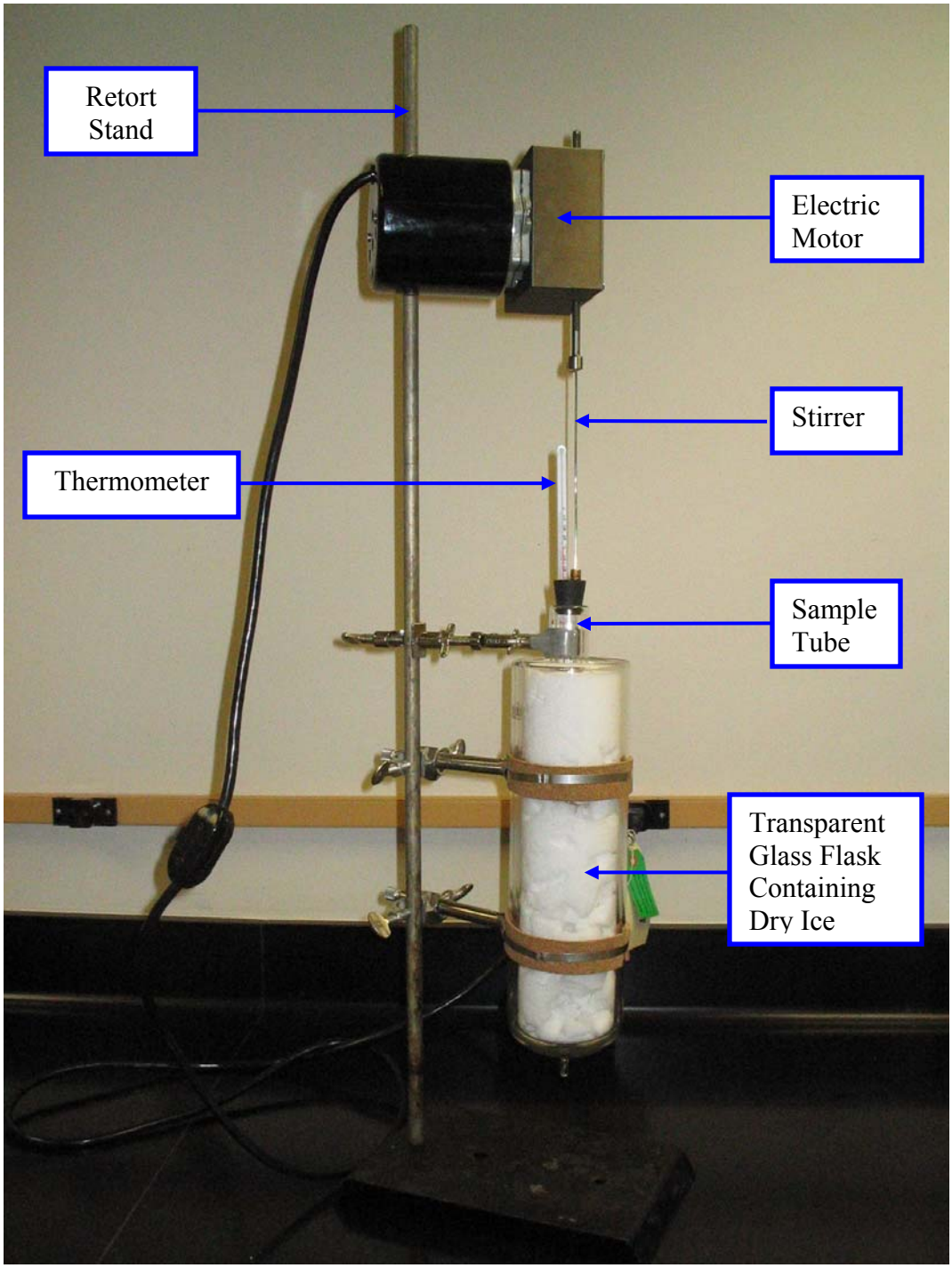

Figure 2.14. The Koehler apparatus.

References

1. Sharma, A. “Phase Behavior Analysis of Gas-To-Liquid (GTL) Products for Transportation through the Trans Alaska Pipeline System”; M.S. Thesis, University of Alaska Fairbanks, August 2003.

2. Amadi, S. “Experimental Study of Solid Deposition and Vapor Pressure in Gas-to-Liquid and Crude Oil Mixtures for Transportation through the Trans Alaska Pipeline System”; M.S. Thesis, University of Alaska Fairbanks, May, 2003.

3. Timmcke, M. D. “Rapid Evaluation of the Gel Strength of GTL Products during Prolonged Trans-Alaska Pipeline Shutdown”; M.S. Thesis, University of Alaska Fairbanks, December, 2002.

CHAPTER 3
GEL STRENGTH EFFECTS

Moving any GTL product or blend through the Trans-Alaska Pipeline System (TAPS) is dependent on the feasibility of a cold restart of fluid flow in the pipeline. Cold restart depends on gel strength. During pipeline shutdown at low temperatures (below 40°F), liquid movement is impeded by the liquid's gel structure. With decreasing temperature, the gel strength increases, resulting in increased viscosity. Under the arctic conditions typical of Alaska, it is important to determine the amount of pressure, known as the cold restart pressure, at which the liquid in the pipeline will yield. The discussion below corresponds to Task 2 in Section 1.3 above.

The gel strength of a fluid is a measure of the attractive forces between the particles of the fluid when under static (non-flowing) conditions. Gel strength depends mainly on fluid composition, temperature history, and ageing. When a fluid in a pipeline gels, much pressure is required to restart the flow of the fluid. Neglecting pressure losses and the effect of elevation, the pressure differential (ΔP) required to restart flow of a gelled fluid can be estimated using the following equation [1].

$$\Delta P = \frac{4\tau_S L}{D} \qquad 3.1$$

Where: τ_s = Gel yield strength, L = Length of pipe section, D = Pipe diameter.

Gel formation during a prolonged TAPS winter shutdown, scheduled or unscheduled, is unavoidable. Therefore, it is very important that the TAPS pumping system is able to provide enough pressure for restarting a commingled flow of ANS crude oil and GTL through the pipeline after a prolonged winter shutdown. Timmcke [2] developed a fast cold-ramp method for gel strength measurements at UAF. Timmcke defined a correlation factor relating the results from this technique and those from the conventional slow cold ramp method. The fast cold ramp method was employed in this work to determine the gel strengths of ANS crude oil, GTL and their blends at 20°F, 0°F and -20°F.

3.1 Gel Strength Measurement Procedure

The gel strength measurement procedure used in this test is a fast cold ramp procedure developed at the Petroleum Development Laboratory, UAF. In this procedure, the sample is cooled constantly at two degrees centigrade per hour, from 21°C to the desired measurement temperature (20°F, 0°F, or -20°F). It differs from the APSC-approved slow ramp procedure in which the sample is cooled slowly from the normal pipeline flowing temperature of 90°F to a simulated pipeline temperature of -20°F over a 21-day period. However, in addition to being faster, the fast cold ramp procedure is cheaper than the slow cold ramp procedure. Timmcke [2] proposed a correlation between the gel strength results obtained using the fast and the slow cold ramp techniques.

The Brookfield LVDV11+ and RVDV11+ Viscometers were used for the fast cold ramp gel strength measurements. The sample was ramped at a constant rate of 2°C/hr from 21°C to the desired test temperature (20°F, 0°F, or -20°F). At the end of the ramping period, the spindle speed was set at 0.1 RPM and the torque values recorded automatically as a function of time. At the end of data acquisition, a plot of torque percent versus time was prepared to obtain the gel strength of the sample at the temperature.

3.2 Gel Strength Results

The gel strength of the ANS crude oil, AKGTL and their blends were measured at three different temperatures (20°F, 0°F and -20°F) using the fast cold ramp procedure. Figure 3.1 is a representative graph of viscometer maximum torque capacity (VMTC) versus time. Other graphs are included in **Appendix A.** The gel strength values were obtained by multiplying the VMTC (128.7dyne/cm^2 for the LVDV-II+ viscometer and 1372.7 dyne/cm^2 for the RVDV-II+ viscometer) by the percentage of VMTC observed in the test. Brookfield stipulated in the viscometer manual that only torque readings that are at least 10% of VMTC are acceptable. Although this rule was strictly adhered to in this work, whenever the readings from both viscometers were less than 10%, the larger of the two values was recorded as the gel strength value. The results, shown in Table 3.1 and Figure 3.2, indicate that gels formed at higher temperatures were weaker than those formed at lower temperatures. Also, the gels formed by the blends were weaker than those formed by the ANS crude oil at the same temperature. Therefore,

addition of AKGTL to the ANS crude oil leads to a decrease in gel strength. The pressure differentials required to restart flow of the gelled fluids through a unit mile of TAPS were also calculated using Equation 3.1. The pressure differentials were generally calculated based on a unit mile of TAPS because the distances between pump stations are not uniform (see Table 1.1). The calculations showed that to restart flow through a mile-long section of TAPS filled with gelled ANS crude oil at -20°F, a differential pressure of about 65 psi is required across the one-mile long section. The pressure requirement decreased as temperature increased because, as mentioned earlier, the gels formed at higher temperatures are weaker than those formed at lower temperatures.

Table 3.1. Gel Strength Results (Fast Cold Ramp).

Sample	Temp. (°F)	Viscometer	% VMTC	τ_s (dyne/cm^2)	Required ΔP (psi/mile)
TAPS Crude oil	20	LV	4.20	5.405	0.428
	0	LV	>100	>128.7	–
	-20	RV	60.00	823.620	65.231
20% AKGTL	20	LV	1.10	1.416	0.112
	0	LV	41.00	52.767	4.179
	-20	RV	41.00	562.807	44.574
25% AKGTL	20	LV	0.20	0.257	0.020
	0	LV	25.80	33.205	2.630
	-20	RV	18.10	248.459	19.678
33.3% AKGTL	20	LV	0.10	0.129	0.010
	0	LV	21.50	27.671	2.192
	-20	LV	>100	>128.7	–
50% AKGTL	20	LV	0.10	0.129	0.010
	0	LV	2.70	3.475	0.275
	-20	LV	76.00	97.812	7.747
AKGTL	20	LV	0.00	0.000	0.000
	0	LV	0.10	0.129	0.010
	-20	LV	0.30	0.386	0.031

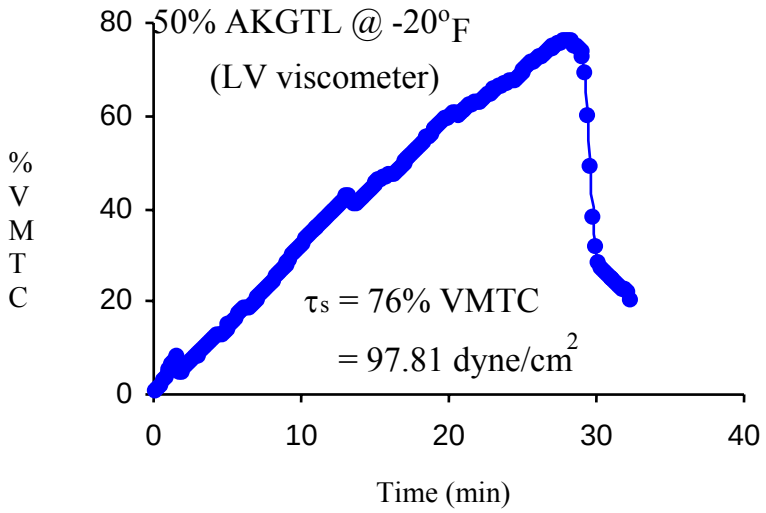

Figure 3.1. Representative gel strength curve (LV viscometer).

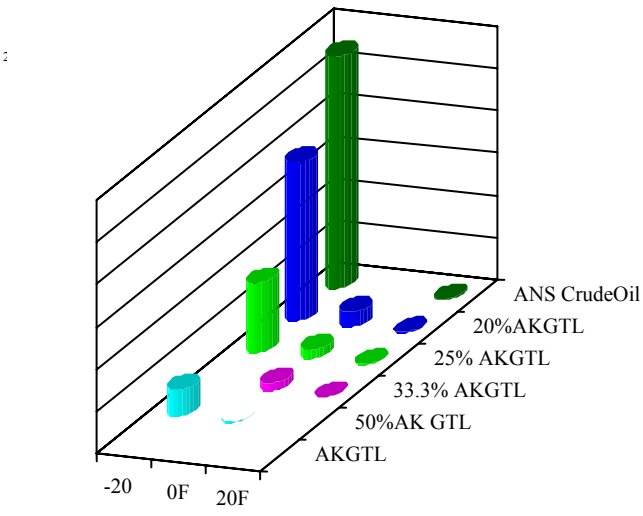

Figure 3.2. Gel strength results (fast cold ramp).

The gel strength results obtained in this work using AKGTL, and those obtained by Timmcke [2], using Laporte GTL cuts, are compared in Table 3.2 and in figures 3.3 through figures 3.5.

Table 3.2. Comparison of the Fast Cold Ramp
Gel Strength Results for AKGTL and Timmcke [2].

Sample	Gel strength (dyne/cm^2) at:		
%AKGTL Content	-20°F	0°F	20°F
0	823.62		5.405
20	562.807	52.767	1.416
25	248.459	33.205	0.257
33.33		27.671	0.129
50	97.812	3.475	0.129
100	0.386	0.129	0
% GTL 254 Content			
0	193.5	18.8	0
25	87.8	8.5	0
50	36.7	0	
100	0	0	0
% GTL 302 Content			
0	193.5	18.8	0
25	581.3	36.8	0
50	831.8	27.3	0
100	>1372	0	0
% GTL 344 Content			
0	193.5	18.8	0
25	>1372	201.8	0
50		805.8	9.9
100		>1372	84

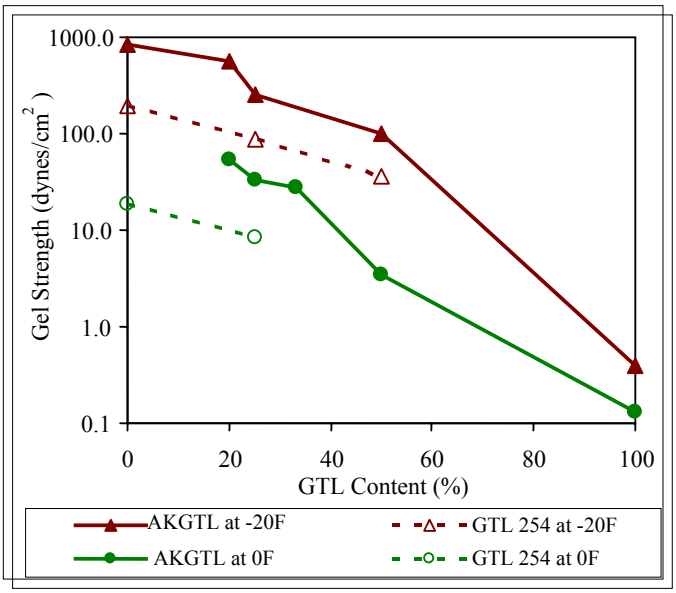

Figure 3.3. Comparison of fast cold ramp gel strength results from AKGTL and GTL 254 Cut.

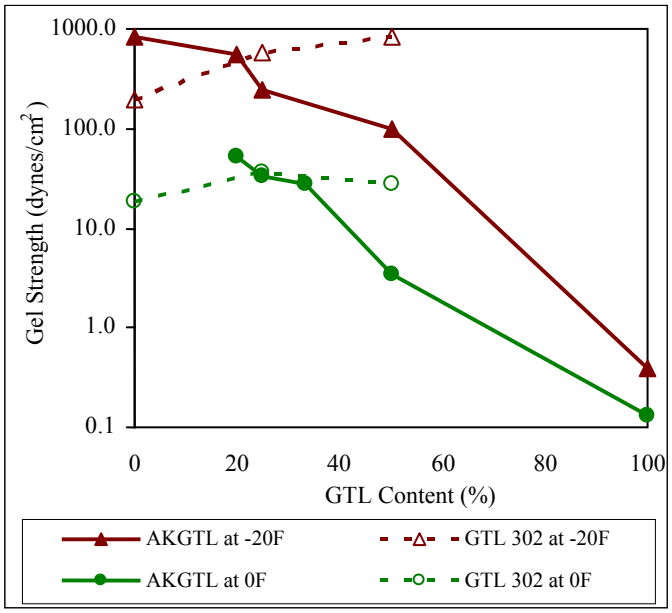

Figure 3.4. Comparison of fast cold ramp gel strength results from AKGTL and GTL 302 Cut.

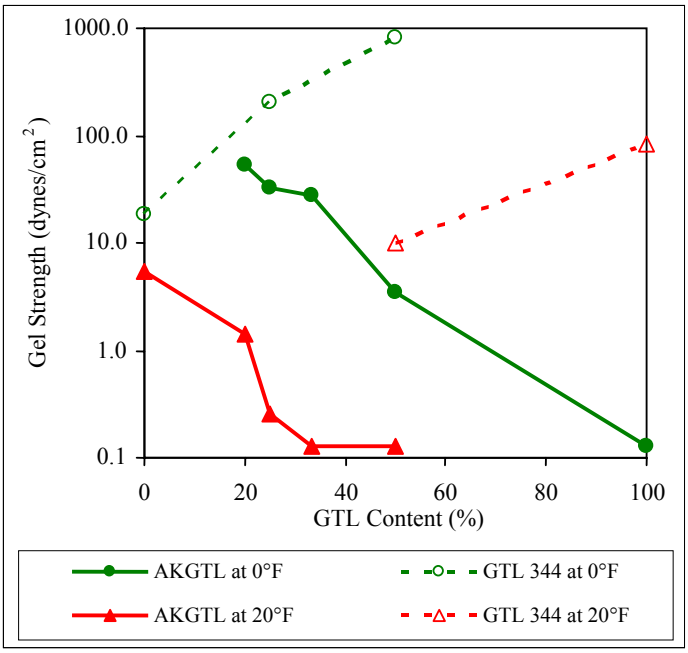

Figure 3.5. Comparison of fast cold ramp gel strength results from AKGTL and GTL 344 cut.

From Table 3.2 and figures 3.3 through 3.5, it is clear that while the results obtained from this work always showed a consistent trend, the trend of results based on Timmcke [2] are not consistent. For example, gel strength increased with increasing amount of GTL 302 cut at -20°F. On the other hand, the results for GTL 254 at -20°F decreased with increasing amounts of GTL content.

References

1. Perkins, T. K. and Turner, J. B.: "Starting Behavior of Gathering Lines and Pipeline Filled with Gelled Prudhoe Bay Oil"; SPE Paper No. 2997 Presented at the SPE 45th Annual Fall Meeting, Houston; 4 – 7 October 1971.

2. Timmcke, M. D: "Rapid Evaluation of the Gel Strength of GTL Products during Prolonged Trans-Alaska Pipeline Shutdown"; M.S. Thesis, University of Alaska Fairbanks, December, 2002.

CHAPTER 4
DENSITY, RHEOLOGY AND VISCOSITY EFFECTS

4.1 Introduction

One main focus of this study is to select tests and evaluate the properties of GTL and crude oil blend samples to assess the effects of their transportation through the Trans-Alaska Pipeline System. The properties (density, viscosity and rheology) that are measured as functions of temperature are necessary to determine the pressure drop in the pipeline system. The horse power requirements to move the product mixtures in the pipeline can be calculated from the pressure drop data. These properties are also used to evaluate for cold flow problems. The density and viscosity data are used in the phase behavior studies for determining the phase in which the blends would exist at pipeline conditions.

Crude oil samples were taken from the TAPS at pipeline conditions and preserved in constant pressure Welker cylinders, which are designed to maintain fluid samples at pipeline pressure conditions. Blends of GTL and crude oil samples were gravimetrically prepared in the ratios of: 1:1, 1:2, 1:3, and 1:4 for density, rheology and viscosity measurements at different temperatures.

4.2 Density Measurement

The calibration constants buffer was set to the values corresponding to the desired temperature. With the temperature bath set to the desired temperature, an appropriate volume of sample was introduced into the sample tube using a syringe. The sample inlet port was then closed with a syringe and about ten to fifteen minutes allowed for the sample to attain the set temperature. After the stabilized density reading was recorded, the syringe was removed from the sample inlet port and the sample disposed of by switching on the in-house pump to blow air through the sample tube. Finally, the sample tube was cleaned with toluene and acetone in succession, and dried with an air stream from the in-house pump to get the system ready for another test.

4.3 Density Measurement Results

The density of each sample was measured at different temperatures from 0°C to 50°C, inclusive. As expected, the density values decreased with increasing temperature. Addition of AKGTL to

the samples caused a reduction in density, because the blends contain more light ends than the pure crude oil. The results are shown in Table 4.1 and Figure 4.1. The trend of the results also agreed with the trend of the results obtained by Inamdar [1] using the Laporte Light GTL cuts. A comparison of the two sets of results (Figures 4.2 – 4.4) shows that the AKGTL consistently had higher density than all the cuts of the Laporte Light GTL sample. The blends prepared with the AKGTL also had higher density than those prepared with the cuts of the Laporte Light GTL sample. This trend of results is not unexpected, because the AKGTL used in this work is a syncrude, and possibly has a broader range of components than the cuts of the Laporte light GTL sample.

Table 4.1. Density Results.

Temp. (°C)	Sample					
	AKGTL	50% AKGTL	33.33% AKGTL	25% AKGTL	20% AKGTL	TAPS Crude Oil
	Density (g/cc)					
0.0	0.7655	0.8354	0.8453	0.8488	0.8584	0.8753
5.0	0.7619	0.8320	0.8416	0.8452	0.8547	0.8716
10.0	0.7582	0.8285	0.8378	0.8416	0.8511	0.8678
15.0	0.7545	0.8250	0.8343	0.8380	0.8474	0.8639
20.0	0.7510	0.8215	0.8307	0.8344	0.8439	0.8603
22.0	0.7495	0.8201	0.8292	0.8329	0.8425	0.8587
25.0	0.7473	0.8183	0.8272	0.8310	0.8406	0.8568
30.0	0.7439	0.8149	0.8239	0.8274	0.8372	0.8560
35.0	0.7421	0.8133	0.8222	0.8257	0.8356	0.8544
40.0	0.7371	0.8085	0.8173	0.8208	0.8306	0.8492
45.0	0.7332	0.8048	0.8137	0.8168	0.8269	0.8455
50.0	0.7319	0.8040	0.8127	0.8160	0.8261	0.8445

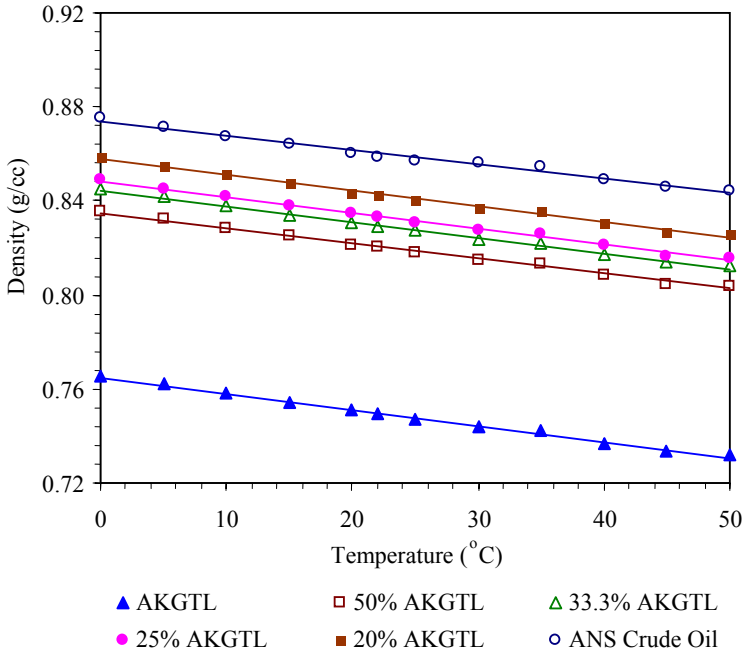

Figure 4.1. Density vs. temperature for AKGTL, ANS crude oil and their blends.

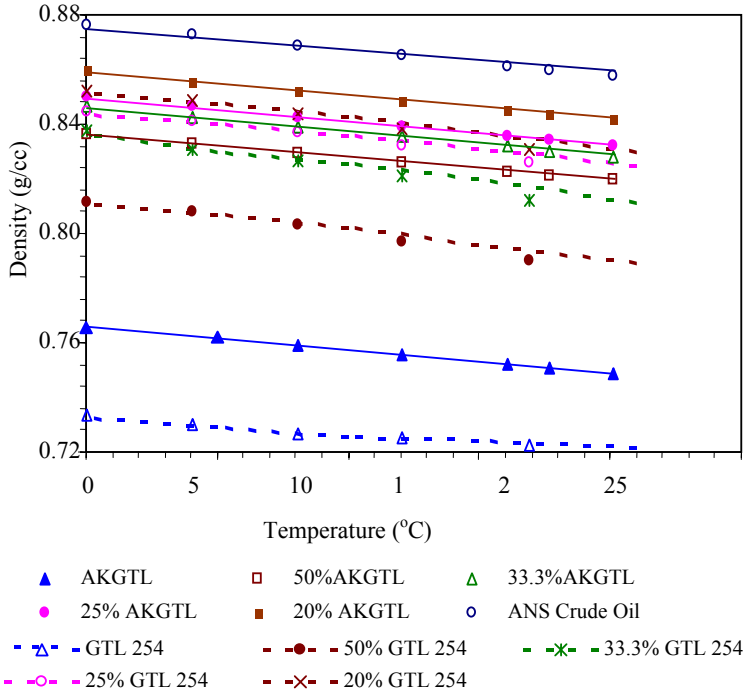

Figure 4.2. Comparison of the densities of AKGTL and GTL 254 Cut.

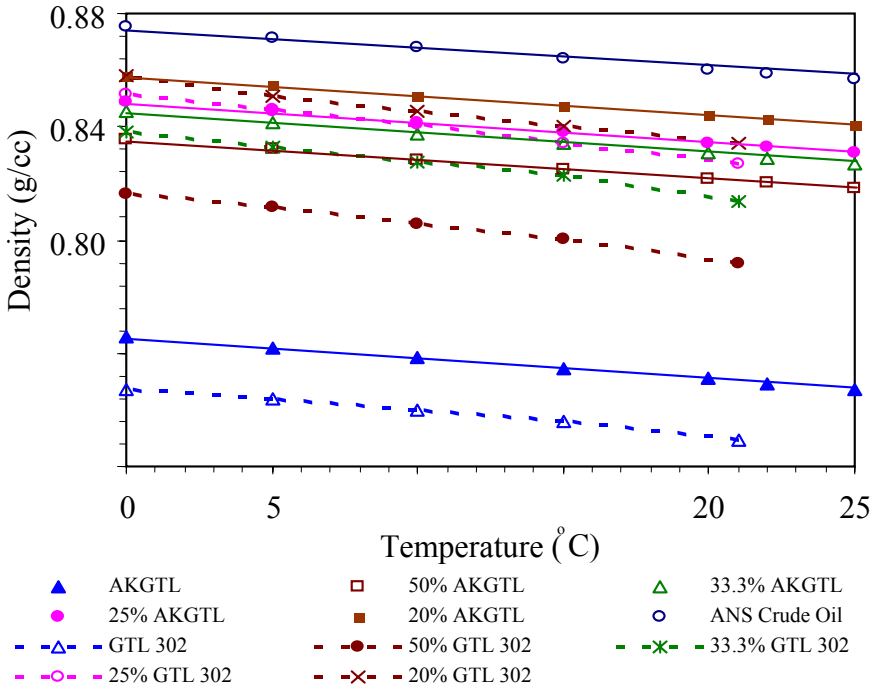

Figure 4.3. Comparison of the densities of AKGTL and GTL 302 Cut.

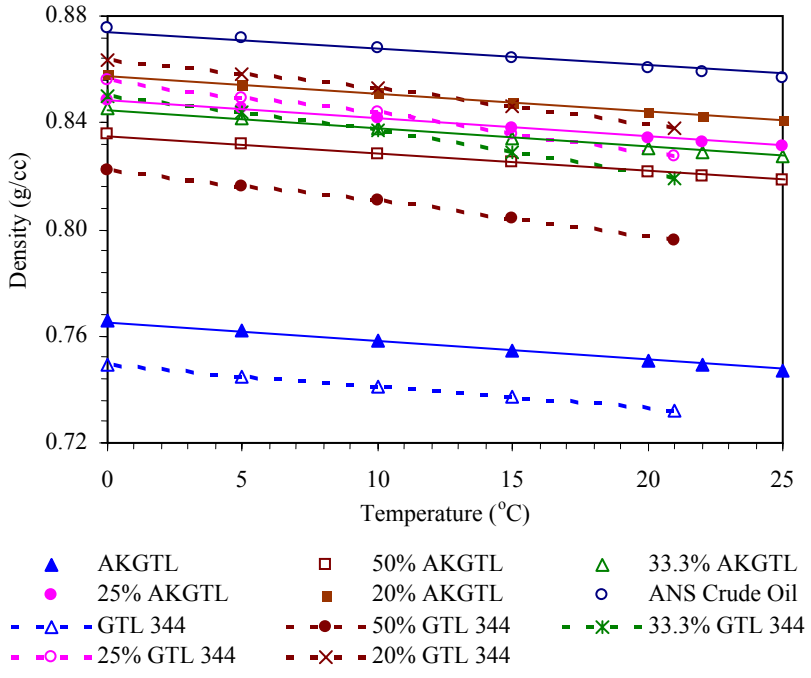

Figure 4.4. Comparison of the densities of AKGTL and GTL 344 Cut.

4.4 Rheology

When a fluid is flowing, a force exists in the fluid that opposes the flow. This force, known as shear stress, can also be seen as the frictional force between the two adjacent layers of fluid. Similarly, the relative velocity with which an individual layer moves with neighboring layers is known as shear rate. Shear stress is a function of pressure, and shear rate is a function of geometry and average velocity of a fluid. The relationship between shear stress and shear rate defines the flow behavior of the fluid.

A fluid's rheology depends on its shear stress-shear rate relationship. A linear relationship between shear stress and shear rate on a Cartesian plot which passes through the origin indicates that a fluid exhibits Newtonian characteristics. Non-Newtonian fluid behavior can be characterized by either the Bingham plastic or power-law fluid flow model (among others), depending on the fluid's shear stress-shear rate relationship. Figure 4.5 shows a rheogram of behavior for Newtonian, Bingham plastic and power-law fluids.

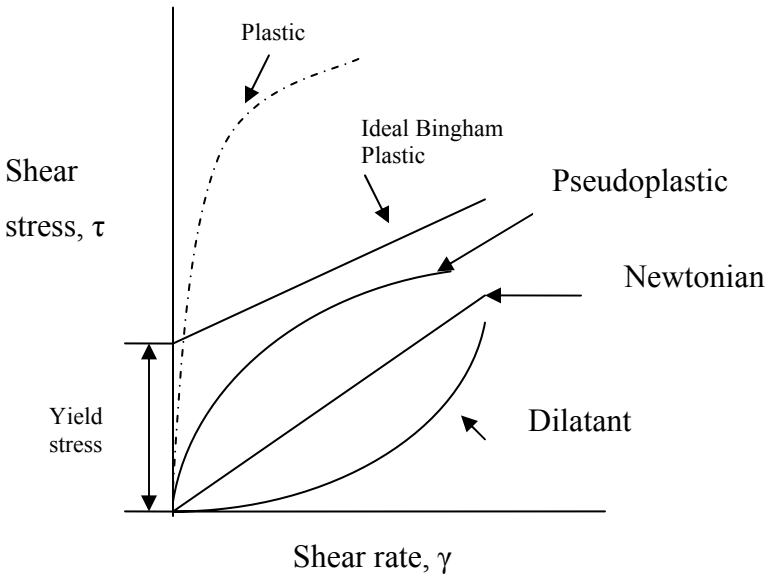

Figure 4.5. Rheogram of Newtonian, Bingham plastic and power-law fluids.

The constitutive equations of these fluid models are given in equations 4.1, 4.2 and 4.3, respectively.

For Newtonian fluids:

$$\tau = \mu\gamma \tag{4.1}$$

The absolute or true Newtonian viscosity (μ) is constant for Newtonian fluids.

For Bingham plastic fluids:

$$\tau = \mu_p\gamma + \tau_o \tag{4.2}$$

Where:

τ	=	shear stress
τ_o	=	yield stress
γ	=	shear rate
μ	=	absolute or effective Newtonian viscosity
μ_p	=	Bingham plastic viscosity

The plastic viscosity (μ_p) of Bingham plastic fluids is described as that part of resistance to flow caused by mechanical friction. Primarily, it is affected by (a) solids concentration, (b) size and shape of solids, and (c) viscosity of the fluid phase. An increase in plastic viscosity indicates an increase in the percent by volume of solids, a reduction in size of the solid particles, a change in the shape of the particles, or a combination of all these. Yield point is that part of the resistance to flow caused by the attractive forces between particles.

For power-law fluids:

$$\tau = k(\gamma)^n \tag{4.3}$$

"n" and "k" are called the power-law index and consistency index parameters, respectively, of the power-law model. The parameter n shows the degree of deviation of fluid from Newtonian fluid characteristics. Based on the value of n, fluids can be classified as follows:

n = 1	--------- Newtonian	examples: air, water, high viscosity fuels
n < 1	--------- Pseudoplastic	examples: grease, printer's ink, soap
n > 1	--------- Dilatant	examples: clay, starch in water, peanut butter

4.5 Rheology and Viscosity Measurements

Brookfield's cone plate viscometer was used to determine the viscosity of the fluid samples. The readings within the 10% to 100% torque range were accepted for accuracy, as suggested in the manual. For viscous fluids at lower temperatures, the 100% torque is achieved at comparatively lower shear rates. Hence less data points are obtained at low temperatures as well as for viscous fluids. These shear stress values are plotted against shear rate values. Regression coefficient (R^2) is used to decide the best fit curve. Flow behavior parameters n & k and viscosities are determined with the help of these curves. AKGTL, crude oil and their blends are then classified as Newtonian or non Newtonian fluids based on the best fits and values of n and k.

4.6 Rheology and Viscosity Results

Crude oil

TAPS crude oil shows Newtonian behavior at higher temperatures (>20°C). At lower temperatures it shows Bingham plastic behavior with some yield point. Viscosity of crude oil is determined by the slope of the shear stress vs. shear rate plot. The experimental results are plotted on the Cartesian graph. The representative rheograms at temperatures 50°C, 30°C and 10°C are shown in figures 4.6 through 4.8. The classification of crude oil behavior based on temperature appears in Table 4.2. The table also summarizes the absolute viscosities for Newtonian behavior and plastic viscosities (PV) and the yield values for Bingham plastic behavior.

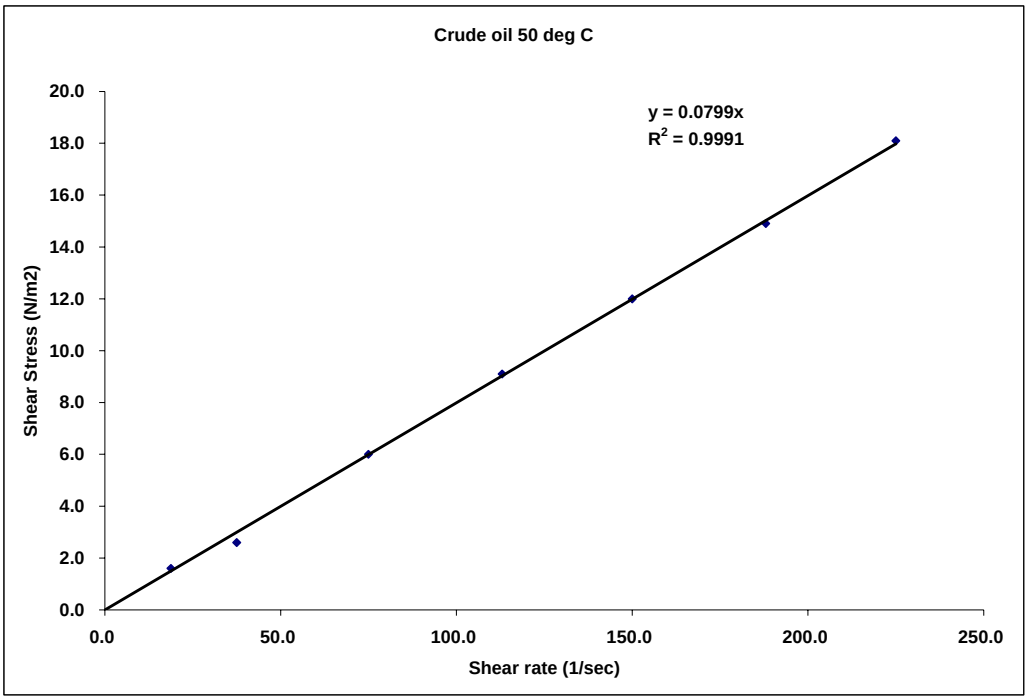

Figure 4.6. Rheogram for crude oil at 50°C.

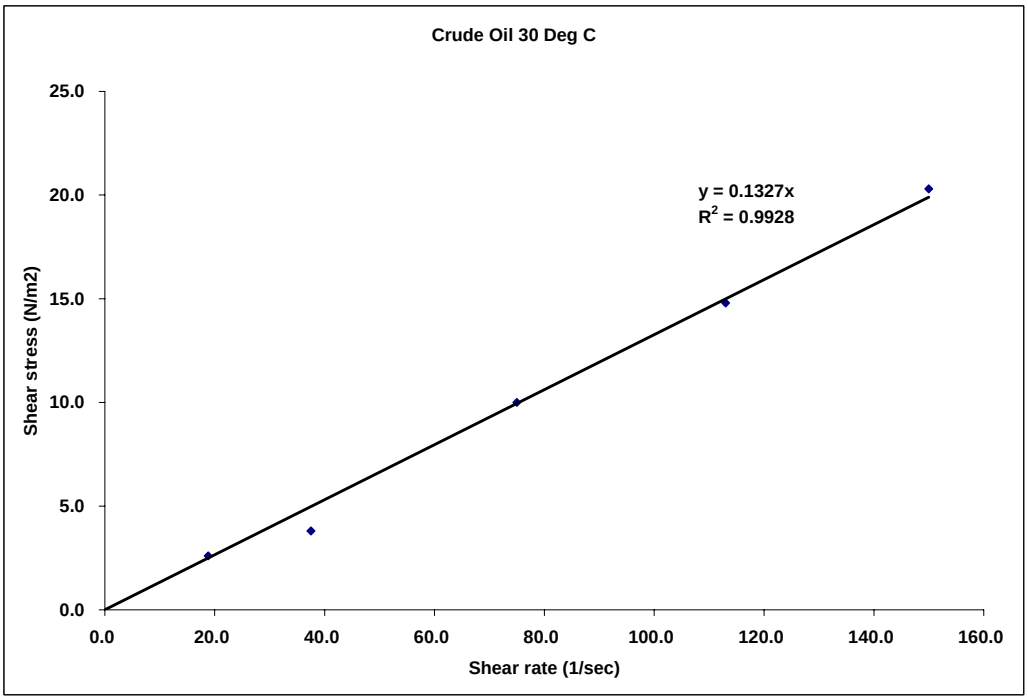

Figure 4.7. Rheogram for Crude oil at 30°C.

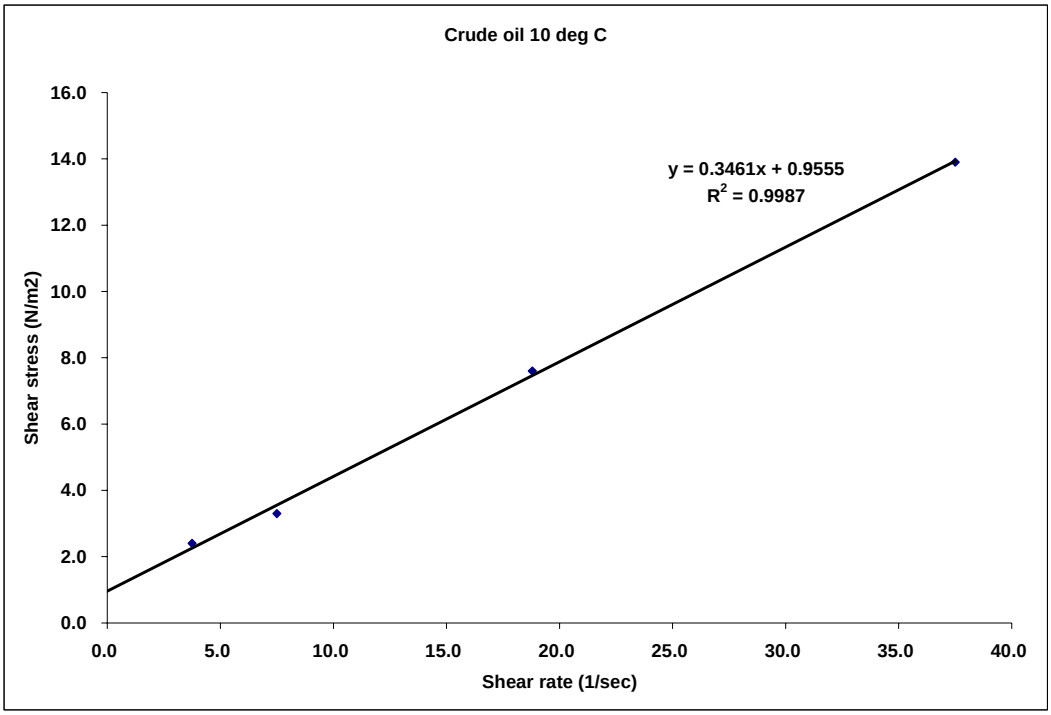

Figure 4.8. Rheogram for crude oil at 10°C.

Table 4.2. Flow behavior of crude oil, its viscosity and yield point at different temperatures.

Fluid	Temperature		Flow Behavior	abs viscosity/PV	YP
	°C	°F		centipoise	$N.s^n/m^2$
Crude oil	50	122	Newtonian	7.99	
	45	113	Newtonian	8.97	
	40	104	Newtonian	10.06	
	35	95	Newtonian	11.39	
	30	86	Newtonian	13.27	
	25	77	Newtonian	15.12	
	20	68	Newtonian	18.35	
	15	59	Bingham	25.54	0.3991
	10	50	Bingham	34.61	0.9555
	5	41	Bingham	56.21	1.3611
	0	32	Bingham	109.84	1.9066
	-5	23	Bingham	318.16	2.2934

AKGTL

From the experimental results, the rheograms of the AKGTL field sample were plotted on a Cartesian graph. Log-log plots (log γ vs. log γ) were used to determine the n and k values. From the plots and values of n, researchers concluded that GTL shows pseudoplastic behavior at all the temperatures considered. The representative rheograms and the log-log plots at temperatures 50°C, 30°C, 10°C and -10°C are shown in figures 4.9 through 4.12. The n and k values appear in Table 4.3.

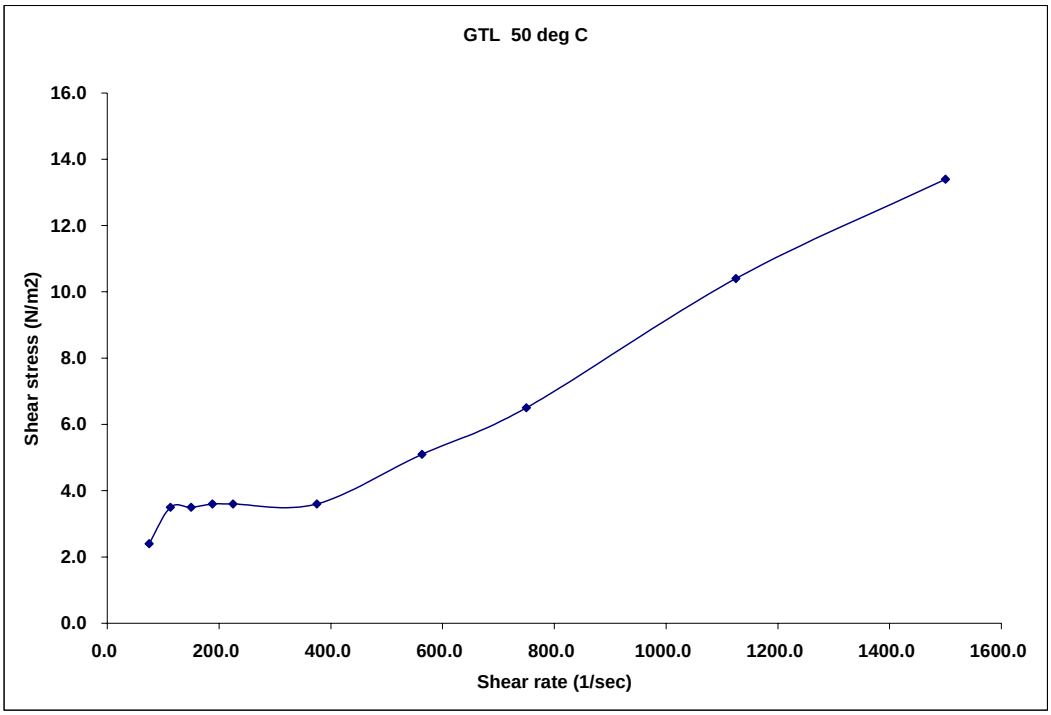

Figure 4.9a. Rheogram for AKGTL at 50°C

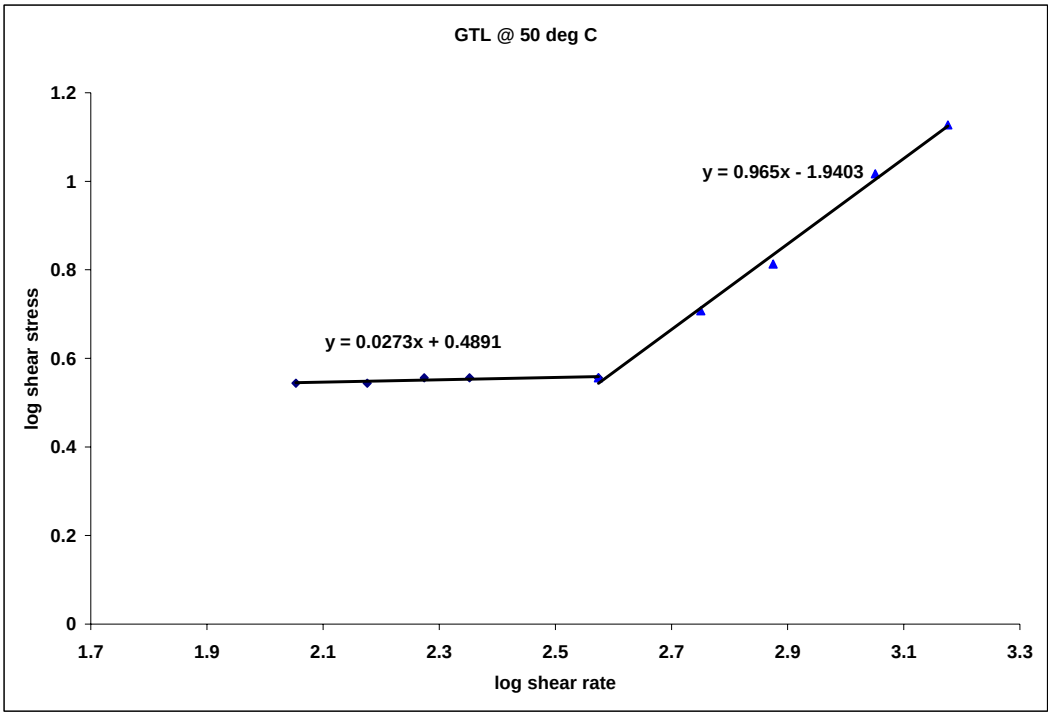

Figure 4.9b. Log-log plot for AKGTL to find n and k values (at 50°C)

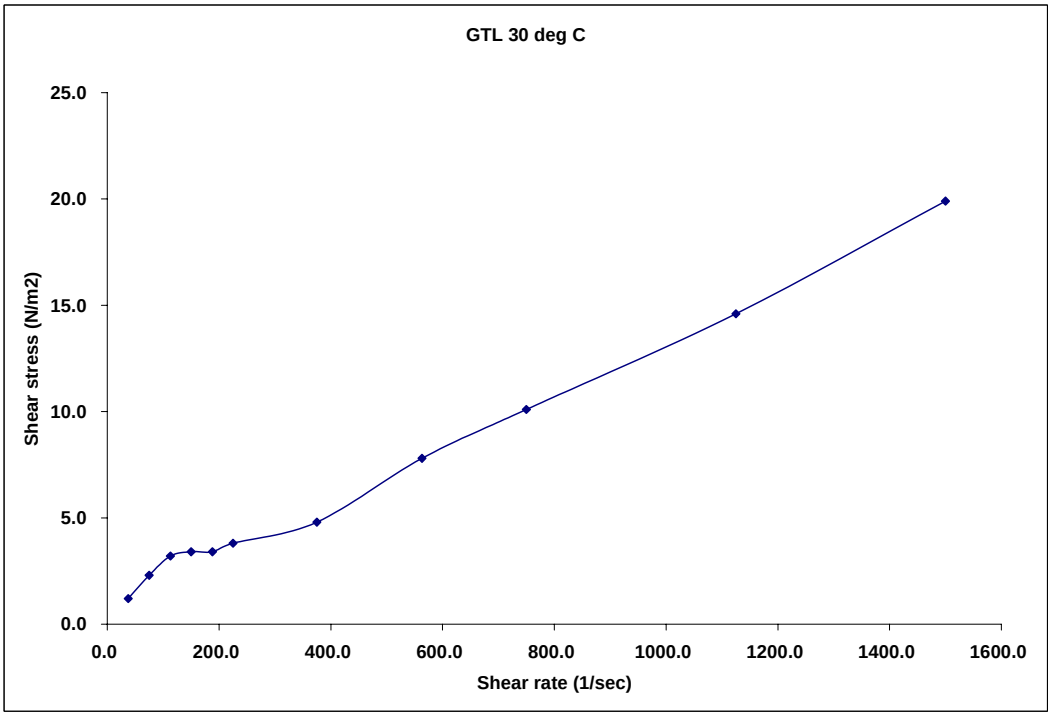

Figure 4.10a. Rheogram for AKGTL at 30°C.

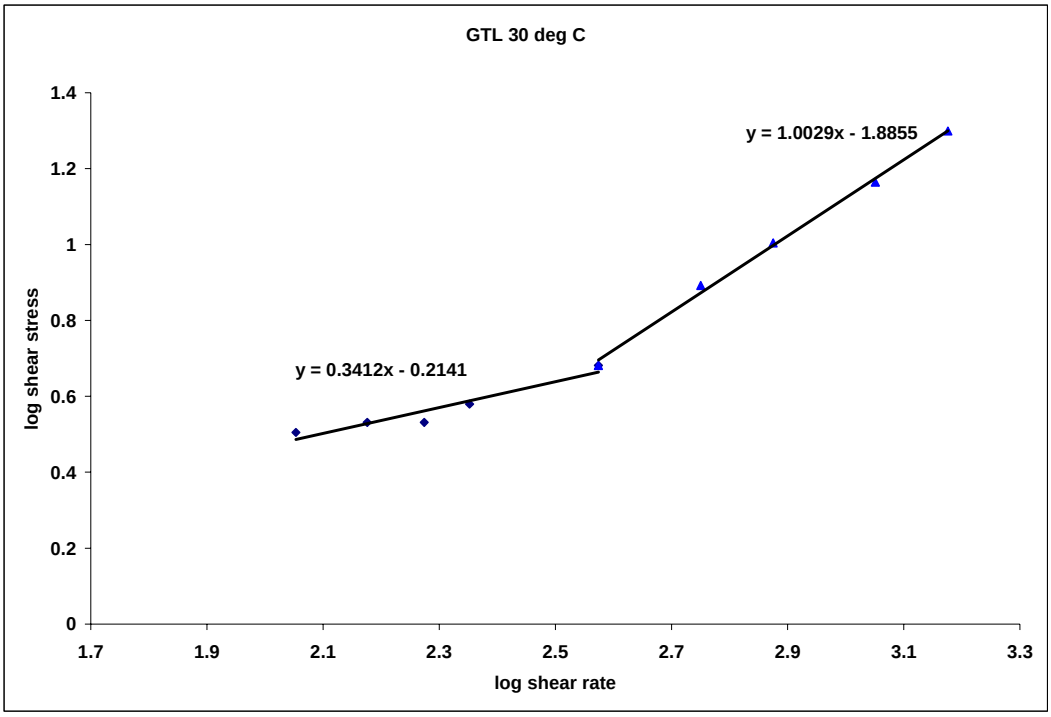

Figure 4.10b. Log-log plot for AKGTL to find n and k values (at 30°C).

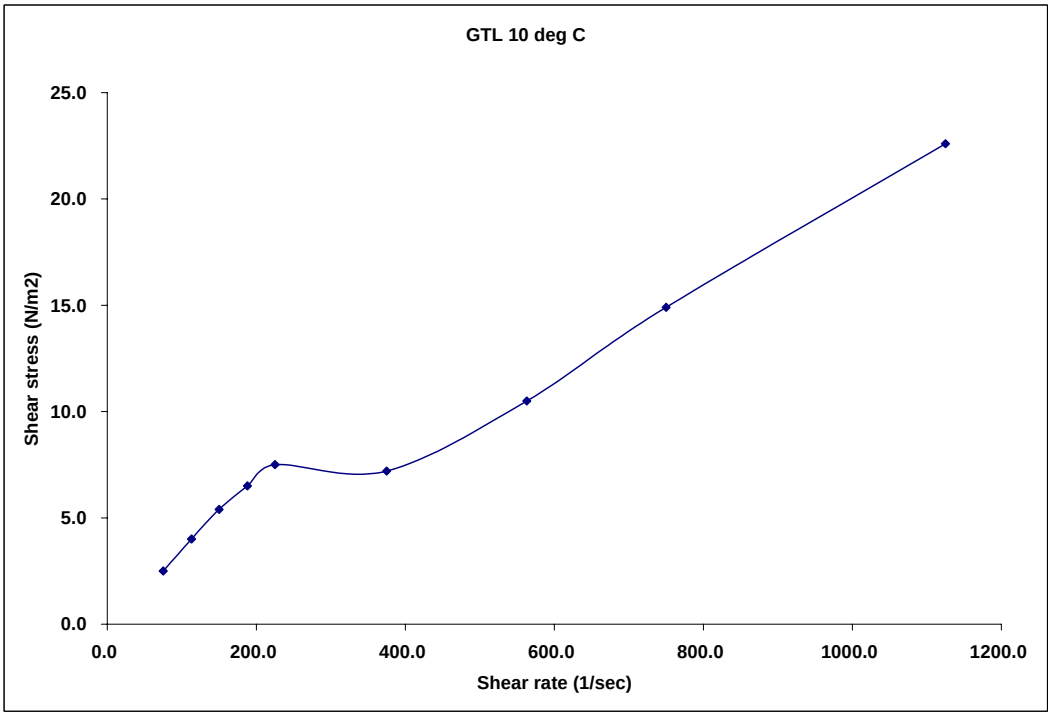

Figure 4.11a. Rheogram for AKGTL at 10°C.

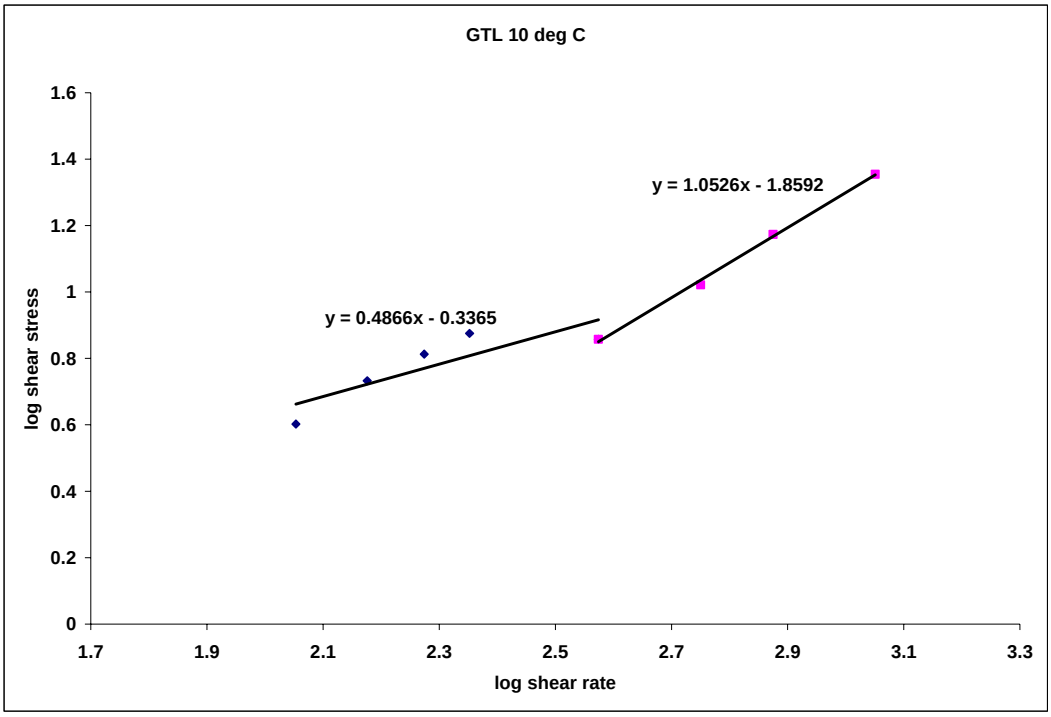

Figure 4.11b. Log-log plot for AKGTL to find n and k values (at 10°C).

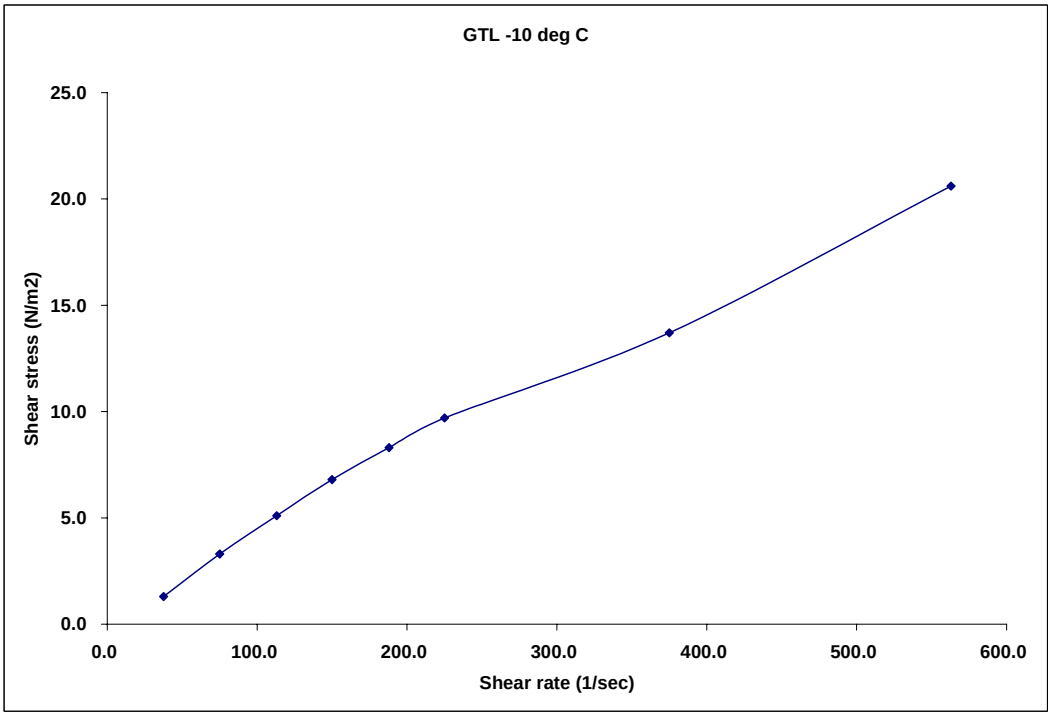

Figure 4.12a. Rheogram for AKGTL at -10°C.

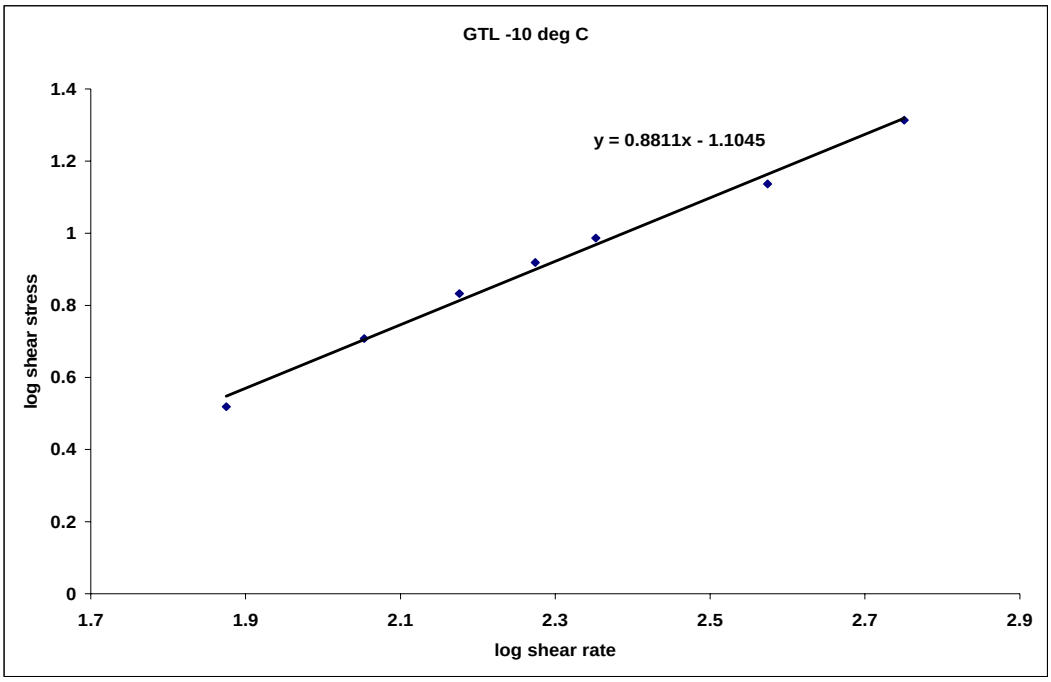

Figure 4.12b. Log-log plot for AKGTL to find n and k values (at -10°C).

Table 4.3. Flow behavior parameters for AKGTL.

Fluid	Temperature		Behavior	n		k (lbf.s^n/100ft^2)	
	°C	°F		rps < 375 1/sec	rps > 375 1/sec	rps < 375 1/sec	rps > 375 1/sec
AK GTL	50	122	Pseudoplastic	0.0273	0.965	6.4407	0.0240
	45	113	Pseudoplastic	0.0573	0.9956	6.0762	0.0218
	40	104	Pseudoplastic	0.1291	1.0716	3.8863	0.0138
	35	95	Pseudoplastic	0.2747	1.0195	1.7875	0.0223
	30	86	Pseudoplastic	0.3412	1.0029	3.4193	0.0272
	25	77	Pseudoplastic	0.4389	1.0316	0.7489	0.0243
	22	71.6	Pseudoplastic	0.3948	0.9584	1.1149	0.0407
	20	68	Pseudoplastic	0.5015	0.9635	0.6128	0.0417
	15	59	Pseudoplastic	0.4302	0.9797	1.4974	0.0432
	10	50	Pseudoplastic	0.4866	1.0526	0.9624	0.0458
	5	41	Pseudoplastic	0.7018	0.9571	0.3404	0.0628
	0	32	Pseudoplastic	0.8302		0.0653	
	-5	23	Pseudoplastic	0.8108		0.2159	
	-10	14	Pseudoplastic	0.8811		0.1642	
	-15	5	Pseudoplastic	0.9750		0.1158	
	-20	-4	Pseudoplastic	0.8783		0.2262	

AKGTL/Crude Oil Blends

Blends of GTL and crude oil show Newtonian, pseudoplastic and Bingham plastic behavior depending on the given temperature. At higher temperatures (above room temperature) pseudoplastic behavior is observed; at intermediate temperatures (around room temperature) Newtonian behavior can be seen; whereas at lower temperatures (around 0°C and below) Bingham plastic behavior is apparent. Tables 4.4 through 4.7 summarize these findings.

Table 4.4. Flow behavior and related parameters for 1:1 AKGTL/crude oil blend.

Fluid	Temperature		Behavior	n	K	Viscosity/PV	YP
	°C	°F			$lbf.s^n/100ft^2$	cp	N/m^2
1:1 (GTL:crude oil)	50	122	Pseudoplastic	0.8528	0.1645		
	45	113	Pseudoplastic	0.8590	0.1711		
	40	104	Pseudoplastic	0.8946	0.1558		
	35	95	Pseudoplastic	0.8933	0.1693		
	30	86	Pseudoplastic	0.9250	0.1570		
	25	77	Pseudoplastic	0.9728	0.1343		
	20	68	Pseudoplastic	0.9879	0.1329		
	15	59	Newtonian			7.36	
	10	50	Newtonian			8.73	
	5	41	Newtonian			10.76	
	0	32	Newtonian			13.96	
	-5	23	Bingham			18.79	0.5251
	-10	14	Bingham			27.14	0.8679
	-15	5	Bingham			47.47	0.3387
	-20	-4	Bingham			77.67	0.9536

Table 4.5. Flow behavior and related parameters for 1:2 AKGTL/crude oil blend.

Fluid	Temperature		Behavior	n	K	Viscosity/PV	YP
	°C	°F			$lbf.s^n/100ft^2$	cp	N/m^2
1:2 (GTL :crude oil)	50	122	Pseudoplastic	0.8573	0.1741		
	45	113	Pseudoplastic	0.8397	0.2132		
	40	104	Pseudoplastic	0.8268	0.2459		
	35	95	Pseudoplastic	0.8494	0.2454		
	30	86	Pseudoplastic	0.9335	0.1776		
	25	77	Pseudoplastic	0.9754	0.1554		
	20	68	Newtonian			6.54	
	15	59	Newtonian			7.60	
	10	50	Newtonian			8.82	
	5	41	Newtonian			10.80	
	0	32	Newtonian			14.63	
	-5	23	Bingham			18.95	0.4401
	-10	14	Bingham			27.98	0.9164
	-15	5	Bingham			43.33	1.0931
	-20	-4	Bingham			82.92	2.2153

Table 4.6. Flow behavior and related parameters for 1:3 AKGTL/crude oil blend.

Fluid	Temperature		Behavior	n	K	Viscosity/PV	YP
	°C	°F			$lbf.s^n/100ft^2$	cp	N/m^2
1:3 (GTL :crude oil)	50	122	Pseudoplastic	0.9225	0.1226		
	45	113	Pseudoplastic	0.9218	0.1385		
	40	104	Pseudoplastic	0.9482	0.1330		
	35	95	Pseudoplastic	0.9682	0.1363		
	30	86	Newtonian			6.27	
	25	77	Newtonian			6.88	
	22	71.6	Newtonian			7.04	
	20	68	Newtonian			7.31	
	15	59	Newtonian			8.58	
	10	50	Newtonian			11.17	
	5	41	Newtonian			14.44	
	0	32	Bingham			18.55	0.3180
	-5	23	Bingham			27.08	0.0027
	-10	14	Bingham			33.71	2.4322
	-15	5	Bingham			57.49	2.4164
	-20	-4	Bingham			81.76	5.1775

Table 4.7. Flow behavior and related parameters for 1:4 AKGTL/rcude oil blend.

Fluid	Temperature		Behavior	n	K	Viscosity/PV	YP
	° C	° F			$lbf.s^n/100ft^2$	cp	N/m^2
1:4 (GTL:crude oil)	50	122	Pseudoplastic	0.8097	0.2917		
	45	113	Pseudoplastic	0.8954	0.2086		
	40	104	Pseudoplastic	0.9668	0.1645		
	35	95	Newtonian			7.47	
	30	86	Newtonian			8.47	
	25	77	Newtonian			9.43	
	22	71.6	Newtonian			9.49	
	20	68	Newtonian			13.05	
	15	59	Newtonian			16.15	
	10	50	Bingham			21.05	0.2891
	5	41	Bingham			28.44	1.1055
	0	32	Bingham			45.09	1.9808
	-5	23	Bingham			86.87	2.1609
	-10	14	Bingham			186.36	3.8637

4.7 Pressure Drop Considerations

The total pressure drop in TAPS while transporting fluid from Pump Station 1 to the Valdez Marine terminal is due to friction, elevation change and some other minor causes, such as fittings losses. Pressure losses due to acceleration are neglected since it is assumed that the flow rate is constant. For calculation purpose, TAPS is divided into five segments between Pump Station 1 (PS-1) on the slope and the Valdez terminal (VDZ). Only the operating pump stations are considered here. The center line elevation from sea level of each pump, elevation change between two consecutive pump stations, and the distance of each pump station from PS1 are given in Table 4.8, which also shows the assumed values of minor losses used for calculations. These minor losses are considered constant for all fluids. The data in Table 4.8 were calculated using the appropriate model, based on the rheological evaluation results (either Newtonian or power-law). Pressure drop per mile is evaluated at various temperatures based on the daily throughput of 1.02 million barrels per day (MMBPD).

Table 4.8. Center line elevation from sea level of each pump, elevation change between two consecutive pump stations, distance of each pump station from PS1, and minor losses.

Stations	Elevation (ft)	Elev. change between two consecutive pump stations (ft)	Distance between two consecutive pump stations (miles)	Total Distance from PS1 (miles)	Minor losses (Assumed) (psi)
PS-1	39			0	
PS-3	1383	1344	104.27	104.27	60.5
PS-4	2763	1380	39.79	144.06	52
PS-7	904	-1859	270.02	414.08	61
PS-9	1509	605	134.66	548.74	59
VDZ	166	-1343	251.46	800.32	62

Total pressure drops along TAPS at various temperatures for AKGTL samples, crude oil and their blends appear in tables 4.9 through 4.11.

Using data in tables 4.9 through 4.11, pressure drop along TAPS can be found at various temperatures if we assume that particular temperature is constant throughout TAPS length. In reality, temperatures along TAPS vary; average pressure drop at current TAPS temperature conditions between pump stations are shown in Table 4.12. These average temperatures are assumed to remain constant throughout the particular pipe segment in consideration.

Table 4.9. Total pressure drop for Newtonian fluids flowing through TAPS at various temperatures.

Fluid	Temperature		Total pressure drop				
	°C	°F	PS1 - PS3	PS3 - PS4	PS4 - PS7	PS7 - PS9	PS9 – VDZ
Crude oil	50	122	932.83	701.89	367.99	772.21	489.82
	45	113	941.73	705.66	388.73	783.21	509.30
	40	104	953.51	711.55	410.67	796.61	530.35
	35	95	967.85	718.97	435.79	812.58	554.62
	30	86	981.46	724.77	467.33	829.37	584.26
	25	77	993.06	729.50	495.54	843.97	610.66
	20	68	1013.56	738.63	540.52	868.72	653.14
	15	59	1037.20	749.00	593.43	897.50	703.02
1:1(GTL:crude oil)	15	59	908.87	685.43	351.01	750.81	470.73
	10	50	923.55	692.34	380.93	768.05	499.18
	5	41	941.81	700.63	420.12	789.91	536.27
	0	32	965.31	710.87	473.12	818.60	586.19
1:2 (GTL:crude oil)	20	68	906.82	686.78	332.51	745.36	454.46
	15	59	919.80	693.09	357.81	760.36	478.62
	10	50	933.17	699.51	384.36	775.92	503.93
	5	41	951.40	707.89	422.77	797.60	540.34
	0	32	978.93	719.78	485.51	831.34	599.39
1:3 (GTL:crude oil)	30	86	901.11	683.37	325.38	739.61	447.26
	25	77	910.27	688.21	340.76	749.67	462.19
	20	68	917.36	692.20	351.27	757.17	472.55
	15	59	931.46	698.93	379.47	773.62	499.41
	10	50	953.92	708.85	429.31	800.86	546.43
	5	41	977.74	719.29	482.68	829.87	596.74
1:4 (GTL:crude oil)	35	95	919.91	693.62	355.09	759.87	476.31
	30	86	929.81	698.00	377.05	771.88	497.02
	25	77	940.55	703.38	397.00	784.09	516.18
	20	68	968.24	715.18	461.07	818.23	576.40
	15	59	989.37	724.56	507.71	843.81	620.42

Table 4.10. Total pressure drop for power-law fluids (blends) flowing through TAPS at various temperatures.

Fluid	Temp	Temp	Total Pressure Drop				
	°C	°F	PS1 - PS3	PS3 - PS4	PS4 - PS7	PS7 - PS9	PS9 - VDZ
1:1 (GTL:crude oil)	50	122	1017.97	719.18	682.07	901.98	775.51
	45	113	1009.67	716.31	658.74	890.87	753.91
	40	104	1032.62	726.46	709.61	918.70	801.91
	35	95	1033.72	728.68	701.36	917.77	795.03
	30	86	1059.04	738.94	763.25	949.69	852.93
	25	77	1074.49	746.12	795.40	967.98	883.44
	20	68	1079.40	749.19	600.25	972.75	888.93
1:2 (GTL:crude oil)	50	122	1065.69	740.65	785.54	959.35	873.32
	45	113	1076.27	745.07	810.64	972.53	896.87
	40	104	1085.46	749.93	826.12	982.64	911.89
	35	95	1101.06	757.72	855.18	1000.38	939.77
	30	86	1107.94	760.98	869.08	1008.44	953.00
	25	77	1121.64	767.45	896.93	1024.52	979.49
1:3 (GTL:crude oil)	50	122	1074.46	745.24	800.62	969.06	887.92
	45	113	1084.84	749.50	825.65	982.07	911.37
	40	104	1097.40	755.80	848.94	996.34	933.72
	35	95	1119.72	766.15	895.42	1022.77	977.83
1:4 (GTL:crude oil)	50	122	1110.74	762.88	871.24	1010.97	955.38
	45	113	1116.51	765.38	884.32	1018.03	967.70
	40	104	1130.78	772.21	912.73	1034.65	994.77

Table 4.11. Total pressure drop for power-law fluids (GTL) flowing through TAPS at various temperatures.

Fluid	Temp	Temp	Total Pressure Drop (rps>375 1/sec), psi				
	°C	°F	PS1 - PS3	PS3 - PS4	PS4 - PS7	PS7 - PS9	PS9 – VDZ
AK GTL	50	122	839.59	624.04	386.79	706.90	488.40
	45	113	849.40	628.27	409.19	718.93	509.48
	40	104	828.18	621.64	345.23	689.62	450.57
	35	95	867.50	638.52	435.50	737.96	535.47
	30	86	878.01	643.21	458.54	750.64	557.24
	25	77	877.45	644.27	449.24	748.26	549.15
	22	71.6	901.39	654.23	506.15	778.10	602.51
	20	68	911.70	658.73	529.39	790.68	624.41
	15	59	911.33	659.90	520.34	788.49	616.57
	10	50	911.15	661.22	511.31	786.44	608.78
	5	41	932.81	670.88	558.86	812.61	653.68
GTL254	21	69.8	811.62	609.35	339.10	676.02	442.19
	15	59	822.75	614.62	361.69	689.07	463.68
	10	50	833.09	619.27	384.07	701.50	484.85
	5	41	861.63	631.37	450.58	736.79	547.32
GTL302	21	69.8	837.14	622.24	385.77	704.86	487.06
	15	59	852.41	630.47	410.52	721.45	511.19
	10	50	865.33	636.94	434.49	736.13	534.20
	5	41	886.44	646.39	480.63	761.59	577.79
GTL344	21	69.8	856.84	630.78	430.55	728.99	529.22
	15	59	870.97	638.12	455.12	744.69	552.98
	10	50	875.04	641.06	457.10	748.13	555.44
	5	41	904.90	653.88	525.64	784.84	619.91

Table 4.12. Average TAPS temperature between pump stations.

	Temperature	
Pipe segments	°C	°F
PS1-PS3	35	95
PS3-PS4	30	86
PS4-PS7	20	68
PS7-PS9	15	59
PS9-VDZ	15	59

4.8 Power Requirement for Transporting Fluids between Pump Stations

The hydraulic horsepower required to flow liquid from one point to the other is a function of the pressure drop between the points, and the fluid flow rate. Researchers calculated the hydraulic horsepower required to flow fluid between two consecutive pump stations. In this study, the flow

rate is assumed constant at 1.02 MMBPD. Pressure drop varies with temperature and fluid behavior. Details on pump specifications and efficiency were not considered in this analysis. The results appear in tables 4.13 through 4.15. Hydraulic horsepower required between pump stations at the present average temperature conditions for AKGTL, crude oil and their blends is shown in Figure 4.13

Table 4.13. Hydraulic horsepower required between pump stations for transporting Newtonian fluids through TAPS at various temperatures.

Fluid	Temp	Temp	Hydraulic horsepower (hp)				
	°C	°F	PS1 - PS3	PS3 - PS4	PS4 - PS7	PS7 – PS9	PS9 – VDZ
Crude oil	50	122	16191.25	12182.81	6387.29	13403.25	8501.83
	45	113	16345.70	12248.27	6747.15	13594.22	8839.87
	40	104	16550.07	12350.36	7127.95	13826.72	9205.29
	35	95	16799.01	12479.24	7563.98	14104.04	9626.52
	30	86	17035.21	12579.80	8111.45	14395.48	10141.03
	25	77	17236.68	12661.89	8601.09	14648.88	10599.34
	20	68	17592.37	12820.43	9381.79	15078.50	11336.59
	15	59	18002.78	13000.50	10300.16	15577.95	12202.34
1:1 (GTL:crude oil)	15	59	15775.33	11897.04	6092.57	13031.79	8170.48
	10	50	16030.05	12017.05	6611.79	13331.01	8664.22
	5	41	16346.99	12160.80	7292.11	13710.58	9307.99
	0	32	16754.86	12338.60	8211.93	14208.44	10174.51
1:2 (GTL:crude oil)	20	68	15739.65	11920.56	5771.48	12937.28	7888.09
	15	59	15964.98	12030.01	6210.58	13197.70	8307.51
	10	50	16197.12	12141.40	6671.30	13467.75	8746.77
	5	41	16513.43	12286.86	7337.98	13843.97	9378.71
	0	32	16991.29	12493.32	8427.02	14429.68	10403.69
1:3 (GTL:crude oil)	30	86	15640.70	11861.30	5647.64	12837.53	7763.14
	25	77	15799.55	11945.38	5914.57	13012.09	8022.22
	20	68	15922.69	12014.52	6097.04	13142.23	8202.07
	15	59	16167.44	12131.37	6586.41	13427.72	8668.30
	10	50	16557.29	12303.60	7451.56	13900.62	9484.48
	5	41	16970.77	12484.84	8377.87	14404.02	10357.63
1:4 (GTL:crude oil)	35	95	15966.87	12039.20	6163.30	13189.09	8267.28
	30	86	16138.82	12115.24	6544.41	13397.57	8626.85
	25	77	16325.24	12208.53	6890.75	13609.43	8959.31
	20	68	16805.81	12413.42	8002.86	14202.03	10004.60
	15	59	17172.61	12576.20	8812.32	14646.00	10768.63

Table 4.14. Hydraulic horsepower required between pump stations for transportation of power-law fluids (blends) through TAPS at various temperatures.

Fluid	Temp	Temp	Hydraulic horsepower (hp)				
	°C	°F	PS1 - PS3	PS3 - PS4	PS4 - PS7	PS7 - PS9	PS9 - VDZ
1:1(GTL:crude oil)	50	122	17668.93	12482.83	11838.80	15655.71	13460.49
	45	113	17524.94	12433.09	11433.82	15462.95	13085.68
	40	104	17923.21	12609.18	12316.76	15945.87	13918.72
	35	95	17942.28	12647.73	12173.55	15929.70	13799.35
	30	86	18381.86	12825.90	13247.72	16483.82	14804.36
	25	77	18650.04	12950.39	13805.79	16801.27	15333.99
	20	68	18735.25	13003.76	10418.57	16884.13	15429.26
1:2(GTL:crude oil)	50	122	18497.18	12855.57	13634.60	16651.43	15158.23
	45	113	18680.95	12932.22	14070.38	16880.27	15566.97
	40	104	18840.46	13016.54	14339.03	17055.68	15827.65
	35	95	19111.12	13151.75	14843.34	17363.60	16311.60
	30	86	19230.63	13208.44	15084.63	17503.50	16541.26
	25	77	19468.45	13320.69	15568.08	17782.59	17001.11
1:3(GTL:crude oil)	50	122	18649.40	12935.16	13896.41	16819.99	15411.67
	45	113	18829.58	13009.13	14330.90	17045.88	15818.63
	40	104	19047.62	13118.40	14735.07	17293.49	16206.69
	35	95	19435.05	13298.17	15541.77	17752.20	16972.23
1:4(GTL:crude oil)	50	122	19279.18	13241.30	15122.08	17547.50	16582.55
	45	113	19379.30	13284.72	15349.26	17670.01	16796.45
	40	104	19626.99	13403.34	15842.24	17958.45	17266.34

Table 4.15. Hydraulic horsepower required between pumpstations for transportation of power-law fluids (GTL) through TAPS at various temperatures.

Fluid	Temp	Temp	Hydraulic horsepower (hp)				
	° C	°F	PS1 – PS3	PS3 - PS4	PS4 - PS7	PS7 - PS9	PS9 – VDZ
AK GTL	50	122	14572.76	10831.54	6713.53	12269.70	8477.18
	45	113	14743.02	10904.99	7102.29	12478.54	8843.02
	40	104	14374.78	10789.88	5992.23	11969.85	7820.63
	35	95	15057.25	11082.89	7558.97	12808.75	9294.27
	30	86	15239.61	11164.21	7958.99	13028.96	9672.04
	25	77	15229.93	11182.67	7797.52	12987.58	9531.59
	22	71.6	15645.42	11355.55	8785.22	13505.47	10457.81
	20	68	15824.43	11433.63	9188.60	13723.90	10837.84
	15	59	15818.04	11454.00	9031.62	13685.91	10701.87
	10	50	15814.84	11476.89	8874.90	13650.35	10566.71
	5	41	16190.83	11644.48	9700.14	14104.49	11346.02

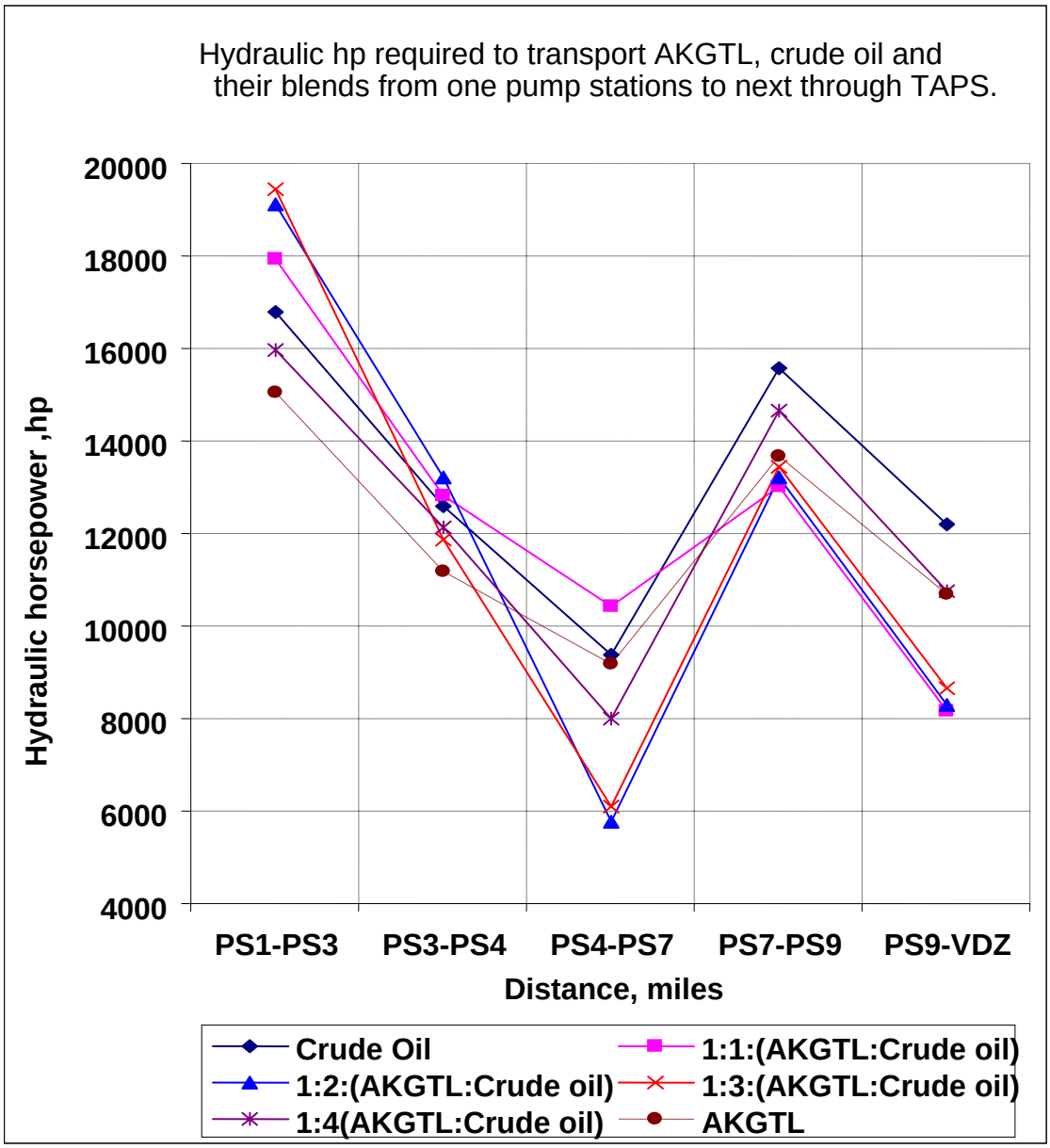

Figure 4.13. Hydraulic horsepower required betweenpump stations for transporting AKGTL, crude oil and their blends through TAPS at present temperature. conditions.

Reference(s)

1. Inamdar, A. A.: "Study of Rheology of Gas-to-Liquid (GTL) Products, ANS Crude Oil and their Blends for Transportation through Trans-Alaska Pipeline System"; M.S. Thesis, University of Alaska Fairbanks; August 2004.

CHAPTER 5
PHASE BEHAVIOR EFFECTS

This project's phase behavior study involved experiments on D.B. Robinson's phase behavior apparatus. Phase behavior experiments were conducted to obtain the bubble point pressure of the GTL and TAPS crude oil blends. The bubble point pressure determines the phase in which the fluid would exist under typical pipeline conditions, that is, as single liquid phase or as two distinct phases, liquid and gas. Whether one or two phases are present significantly affects both the flow behavior and the hydraulics of GTL-crude oil blends flowing through TAPS. Bubble point measurements are also instrumental in verifying the accuracy of the equation of state (EOS) for predicting the phase properties.

5.1 Overview of the Phase Behavior Study

Specific knowledge of hydrocarbon properties such as density, compressibility and saturation pressure are crucial in designing pipeline and processing equipment. Knowledge of these properties are obtained either by laboratory studies or by the use of correlations. A phase behavior study was designed to investigate the nature of specific fluids under pipeline conditions. One major concern in pipeline transport of a fluid rich in lighter hydrocarbons is the two-phase flow. Is it possible that a vapor phase might exist at the pipeline terminal? If so, are the gas handling capacities at the Valdez terminal sufficient to process the pipeline gas? To address these questions, the saturation pressure of the various GTL and TAPS crude oil blends were determined in the laboratory. Researches compared these results with the pipeline conditions, to determine if the fluid would exist as a two-phase or a single-phase liquid. Phase behavior study is also important in verifying the accuracy of a model designed to predict various other fluid properties at high-pressure conditions.

Because the nature of a fluid flowing through TAPS varies over time, a successful model must predict the behavior of fluids of different compositions. By designing such a model for a range of fluids studied under laboratory conditions we can predict the phase behavior of other similar fluids (slight change in composition) on which phase behavior experiments have not been conducted.

5.2 Compositional Analysis

Identifying the composition of a complex hydrocarbon mixture is very important for a phase behavior study. The entire phase behavior modeling depends on the accurately determining the sample composition. Sample compositions were measured using an HP Gas Chromatograph and Mass Spectroscope (GCMS). The compound total ion concentrations were recorded as peaks by the Chem station program. The abundance rate was obtained as a function of retention time. The area under the peaks serves to measure the composition of the respective compounds. Numerous peaks in the chromatograph indicate the chemically complex nature of the fluid. Specifying the weight percent composition of every compound in the fluid does not yield significant useful information. The result of the compositional analysis is best presented with all compounds of the same carbon number grouped together. The lower the concentration of lighter hydrocarbons, the more the phase envelope shifts toward the right. The crude oil delivered in Welker cylinders has a higher bubble point pressure, due to the presence of lighter hydrocarbons, compared to GTL samples at the same temperature.

5.3 Experimental Apparatus

The experimental apparatus consisted of individual components assembled to measure the bubble point pressure of this study's crude oil and GTL samples. The apparatus also facilitated phase behavior experiments, including constant composition expansion, a differential liberation test, separator test and constant volume depletion. For this study, only saturation pressures were measured for developing the phase envelope of the complex mixtures. The phase behavior apparatus is primarily composed of the following components.

1) A Pyrex glass tube
2) Moving piston
3) Positive displacement pump
4) Air Bath
5) Sample cylinders
6) Pressure gauge
7) Thermocouple

The DBR JEFRI PVT cell consisted of a moving piston installed in a Pyrex glass tube. The JEFRI PVT Cell incorporated various design features that enhance the accuracy of measurement and observation as well as provide ease of operation and maintenance. The fluids under study were contained within a transparent glass cylinder, which is secured between two full-length sight glass windows. The space surrounding the glass tube is filled with an inert, transparent fluid, which exerts an overburden stress on the glass, equal and opposite to the pressure on the process fluid, (see Figure 5.1). This allows unimpaired visibility of the entire contents of the PVT cell. The full-length sight glass windows and their respective seals are contacted only by the overburden fluid, reducing the need for component cleaning and seal replacement to a minimum. The maximum working pressure of the JEFRI PVT Cell was set to 10,000 psig and the maximum temperature is set to 390F.

The cylinder-piston design of the JEFRI pumps facilitates the dispensing of high-pressure fluids with a high degree of accuracy. JEFRI pumps are built to work reliably and smoothly to a working pressure of up to 20,000 psi. Standard capacity range from 5 to 1000 cc with a volume resolution as low as 0.0025 cc. The JEFRI pump uses a finely machined piston of precise diameter to displace a fluid, which is confined within a cylinder. The fluid is confined by a system of high-pressure seals, which are held firmly within the end of the cylinder. Desired flow rates can be maintained by adjusting the set points. The displaced fluid volume is proportional to the calibrated length of the piston inserted into the cylinder.

The AKGTL samples used in this study were procured from BPX Alaska under a confidentiality agreement with the University of Alaska Fairbanks. Due to a delay in procuring the AKGTL, a light GTL sample from LaPorte (which is a direct product of Fischer-Tropsch process), supplied by US DOE, was used for the initial phase behavior studies in this work.

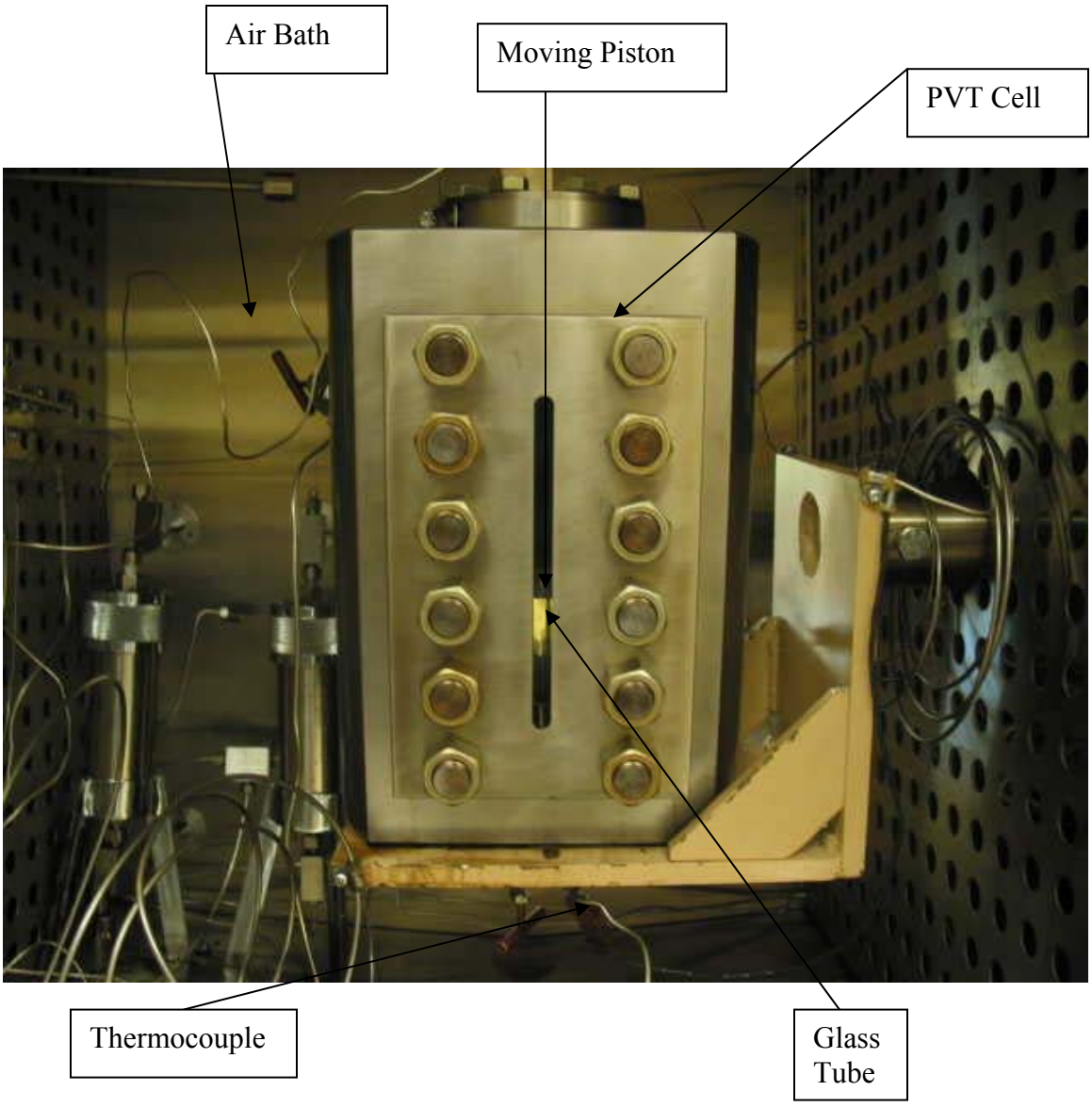

Figure 5.1. D.B. Robinson phase behavior apparatus.

The JEFRI positive displacement pump was used to monitor pressure in the PVT cell, (see Figure 5.2).

Figure 5.2. JEFRI high pressure positive displacement pump.

5.4 Bubble Point Pressure of AKGTL and TAPS Crude Oil

The sample bubble point pressures were measured by a constant composition expansion procedure at different temperatures. The AKGTL and ANS crude oil blends were prepared volumetrically. A representative PV diagram is shown in Figure 5.3. The remaining PV diagrams are in Appendix B. The bubble point pressures were obtained from the breaks in the PV diagrams. At the bubble point, the slope of the PV diagram changed abruptly. Pressure – Temperature (PT) diagrams were also prepared for each of the samples. TAPS operating conditions were also plotted on each of the PT diagrams. A representative PT diagram is shown in Figure 5.4, which also shows that the range of TAPS operating conditions (indicated in red) is well above the bubble point curve (indicated in blue). These results suggest that the GTL-crude oil blend of Figure 5.4 will remain as single phase liquid for the entire range of TAPS operating conditions. Additional PT diagrams are shown in Appendix B.

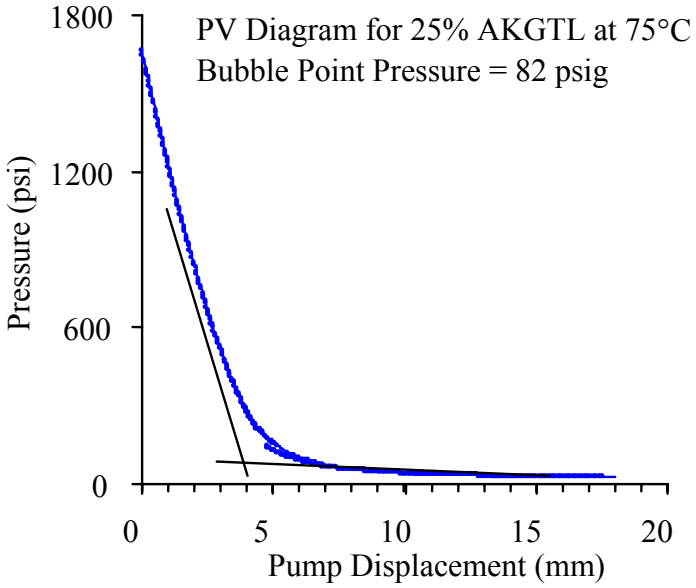

Figure 5.3. Representative PV diagram (pressure vs. pump displacement).

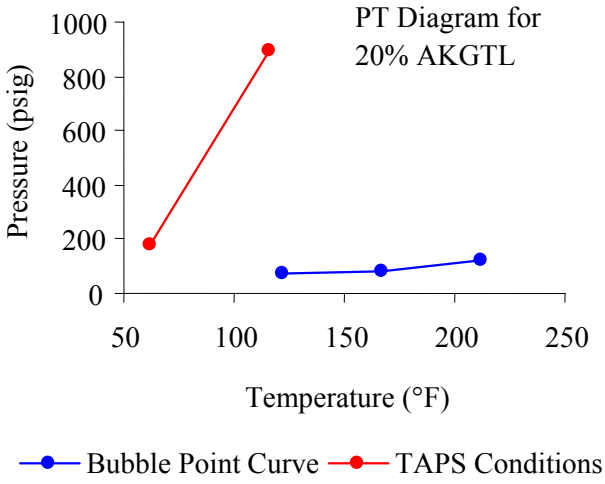

Figure 5.4. Representative pressure-temperature (PT) diagram.

Results showed that within the TAPS average operating temperature range (116.45 – 62.1°F, January – October; 2004), the bubble point pressures of all the samples were well below the average minimum TAPS operating pressure (175.75 psi; January – October, 2004); these findings suggest that there is no possibility of vapor formation as the blends are transported

through the TAPS. In other words, the blends will successfully flow through the TAPS as single phase (compressed) liquid and there would be no problem of pump cavitation, which is associated with the presence of vapor in a pipeline.

5.5 Bubble Point Pressure of LaPorte GTL Cuts

The following TAPS crude oil/GTL blend ratios were studied to determine the saturation pressure (boiling point) and for saturation pressure modeling.

1. Blend of TAPS crude oil and GTL 254 in ratios of 3:1, 1:1, and 1:3
2. Blend of TAPS crude oil and GTL 302 in ratios of 3:1, 1:1, and 1:3
3. Blend of TAPS crude oil and GTL 344 in ratios of 3:1, 1:1, and 1:3

The pressure in the crude oil Welker cylinders were maintained at 850 psig. The crude oil was transferred into the sample cylinders for phase behavior study. The pressure in the PVT cell was plotted against the pump displacement in millimeters (mm), to obtain the sample bubble points. The sample bubble point was taken as the point from where the slope of the pressure-displacement curve approaches 1. A base volume of 20cc of crude oil was charged in the PVT cell, and GTL samples were added and mixed inside the cell in various ratios.

In order to gain confidence in the accuracy of the DBR PVT cell, initial saturation pressures of CO_2 were measured (Figure 5.5). These results were compared with saturation pressures for CO_2 as published in the literature. The equipment was checked for leaks and recalibrated to agree with the measured values and the published data. The CO_2 testing results are shown in Table 5.1.

Table 5.1. Vapor pressure measurements of CO_2.

Temperature °F	Vapor Pressure psia (experimental)	Vapor Pressure psia (CRC handbook of chemistry and physics)
71.6	869	847.1
77.0	947	933.3
86.99	------	1069 (critical point)

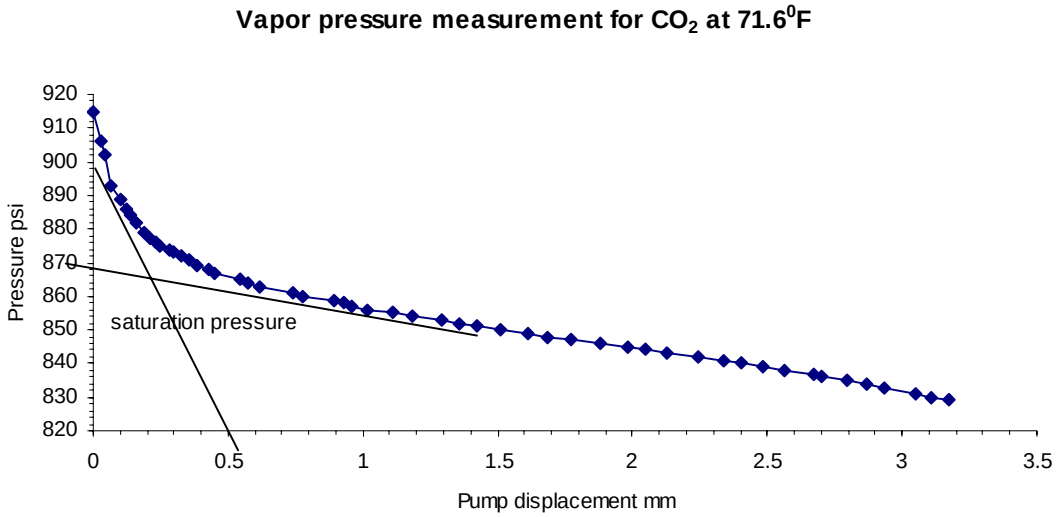

Figure 5.5. CO_2 vapor pressure measurements.

After equipment calibration, the bubble points of mixtures of GTL and TAPS crude oil at various blending ratios were determined.

5.5.1 Saturation Pressures for TAPS Crude Oil/GTL 254 Blend Ratio of 3:1

Figures 5.6 through 5.8 show plots of the saturation pressures or bubble point pressures for GTL 254 blended with TAPS crude oil in a ratio of 3:1, for a range of temperatures. In these pressure-displacement diagrams, the bubble point pressure is indicated by an abrupt change in the slope. Table 5.1 shows the pipeline pressure and temperature data [1]. The saturation pressure or the bubble point of the mixture was observed to be less than the pipeline conditions, as shown in Table 5.2. These results suggest that a blend of TAPS crude with GTL 254 will always exist as a single-phase liquid when passed through the TAPS. However, the composition of the GTL that would be produced on the North Slope of Alaska is not yet fixed; therefore the mathematical modeling of the saturation pressures based on the experimental results becomes essential for predicting the phase behavior properties of any fluid type that would be transported through TAPS.

Table 5.2. Pipeline Operating Parameters[1].

Date	Discharge		Valdez	
	Pressure psi	Temperature °F	Pressure psi	Temperature °F
31 May-2003	938	117	189	62.4
1 June-2003	910	117	212	60.9
5 June-2003	893	119	178	62.0

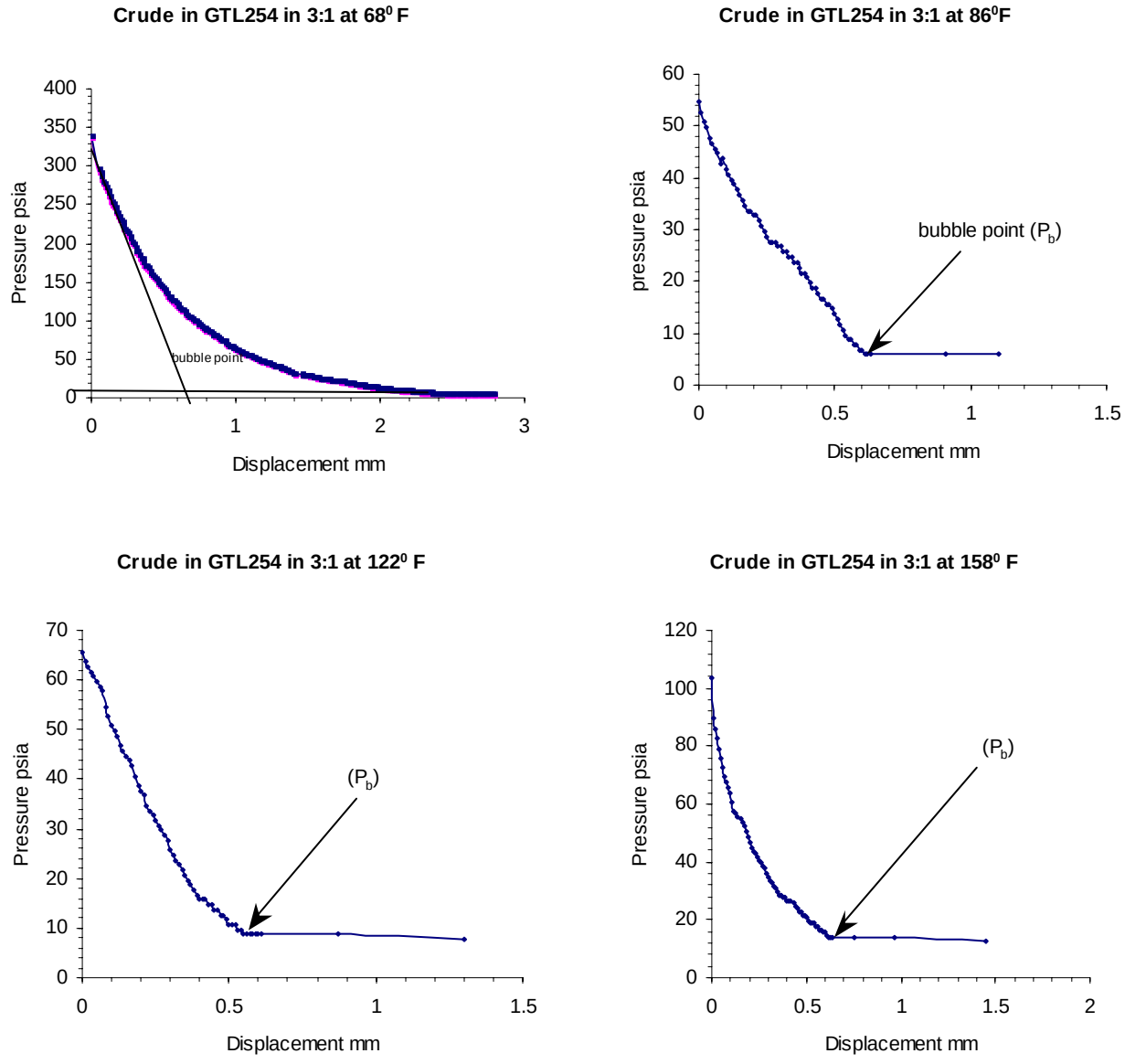

Figure 5.6. Bubble point measurements for TAPS crude/GTL 254 blend of 3:1.

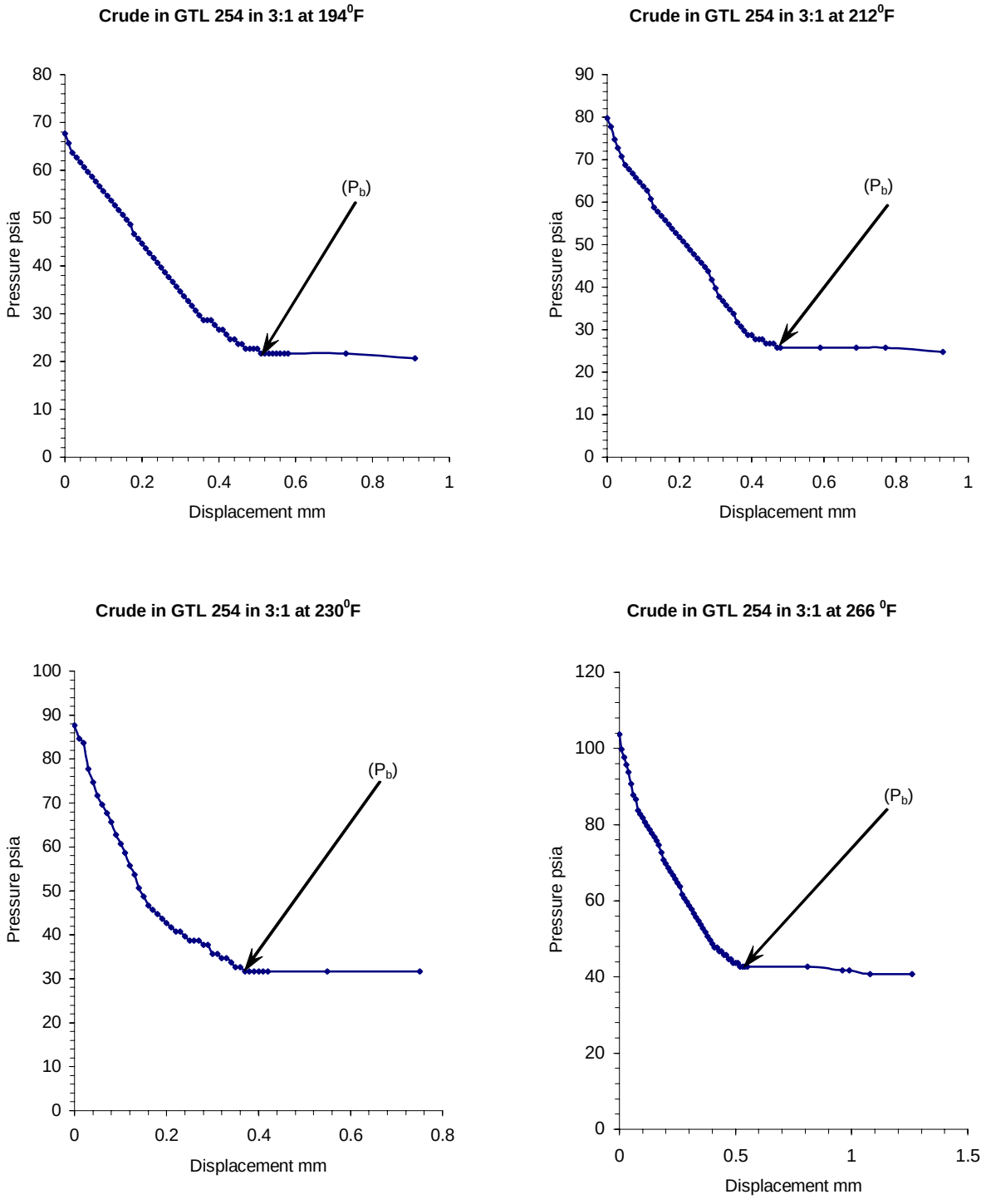

Figure 5.7. Bubble point measurements for TAPS crude/GTL 254 blend of 3:1.

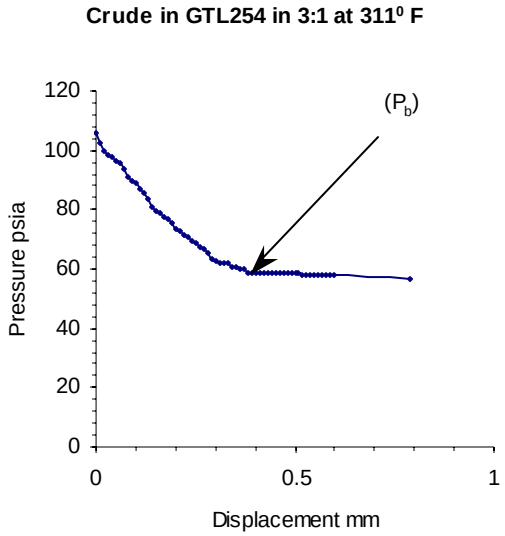

Figure 5.8. Bubble point measurements for TAPS crude/GTL 254 blend of 3:1.

Table 5.3. Bubble point measurements for TAPS crude/GTL 254 blend of 3:1.

Temperature^{0}F	**Pressure Pisa**
71.6	3.7
86	6.7
122	8.7
158	13.7
194	21.7
212	25.7
230	31.7
266	42.7
311	58.7

5.5.2 Saturation Pressures for TAPS Crude Oil/GTL 254 Blend Ratio of 1:1

Figures 5.9 through 5.11 show plots for the saturation pressures of GTL 254 blended with TAPS crude oil in a ratio of 1:1. The saturation pressure, or the bubble point, of the mixture was also observed to be less than standard pipeline conditions (Table 5.4). Note also that increasing the GTL 254 ratio decreases the bubble point pressure of the commingled fluid. The results presented above suggest that a blend of TAPS crude with GTL 254 in a 1:1 ratio will always exist as a single-phase liquid when passed through the TAPS.

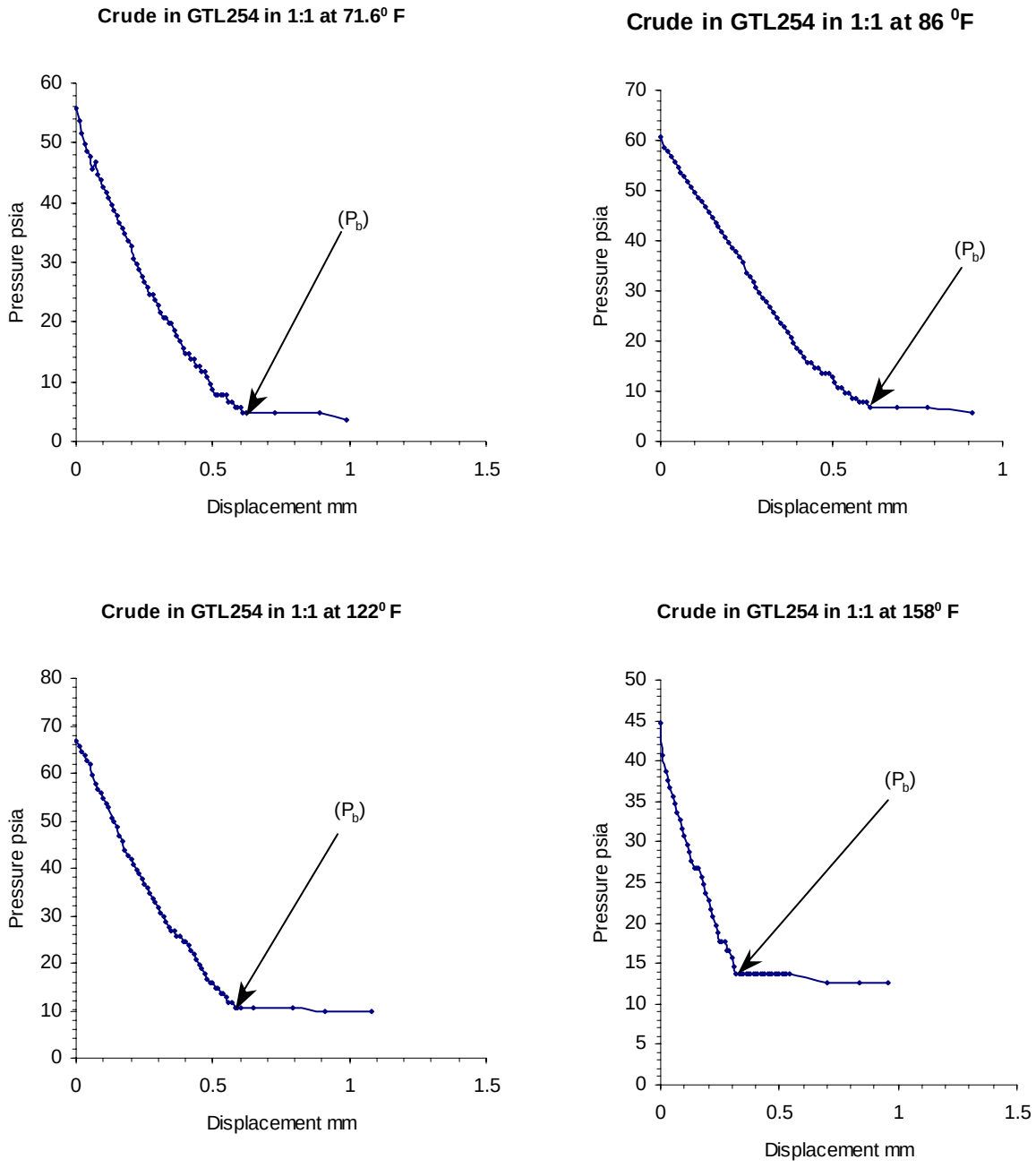

Figure 5.9. Bubble point measurements for TAPS crude/GTL 254 blend of 1:1.

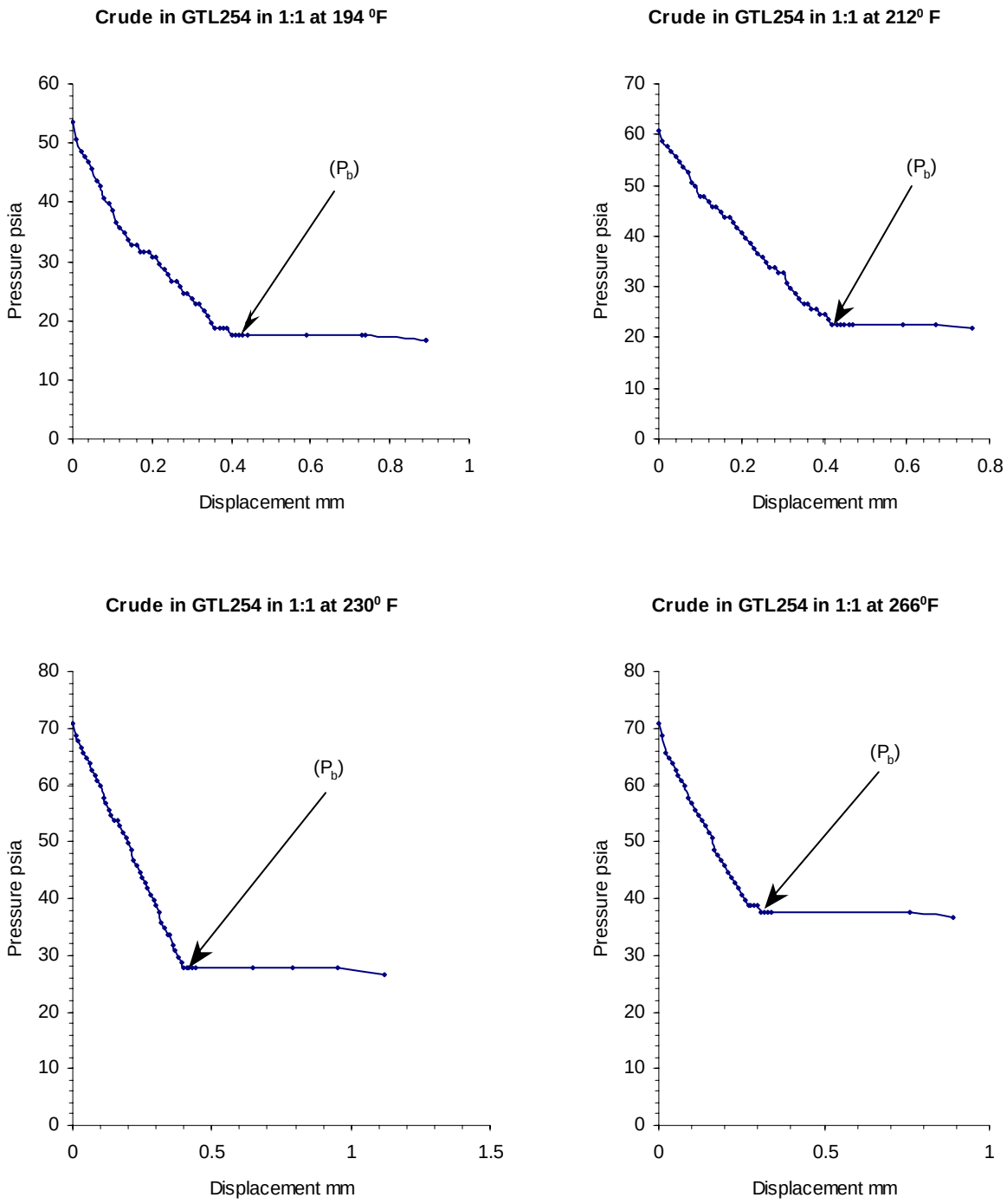

Figure 5.10. Bubble point measurements for TAPS crude/GTL 254 blend of 1:1.

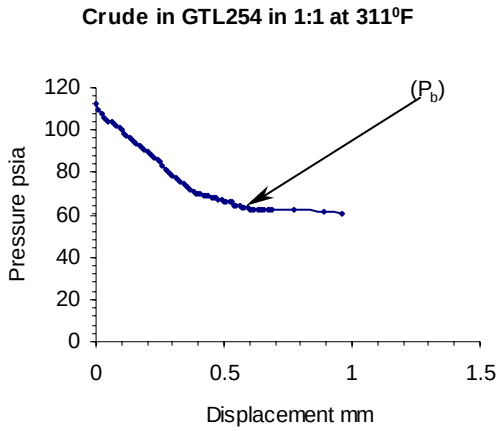

Figure 5.11. Bubble point measurements for TAPS crude/GTL 254 blend of 1:1.

Table 5.4. Bubble point measurements for TAPS Crude/GTL 254 Blend of 1:1.

Temperature°F	Pressure psia
71.6	4.7
86	6.7
122	10.7
158	13.7
194	17.7
212	22.7
230	27.7
266	37.7
311	62.7

5.5.3 Saturation Pressures for TAPS Crude Oil/GTL 254 Blend Ratio of 1:3

Figures 5.12 and 5.13 show saturation pressure measurements for a blend of TAPS crude in GTL 254 in a ratio of 1:3. The ratio of TAPS crude in this case was very low as compared to GTL 254, and the bubble point pressures were extremely low (Table 5.5). The reason for the bubble point pressure being so low is that the GTL samples used were not obtained and transported to the laboratory in constant pressure Welker cylinders; instead these were obtained in DOE-supplied drums. Most of the light ends in the sample may have been lost over time. However, phase behavior modeling attempts to address this problem, as reliable prediction of TAPS crude and GTL mixture (of current composition) using an EOS model ensures some certainty in accurately predicting behavior for similar mixtures if GTL composition changed slightly.

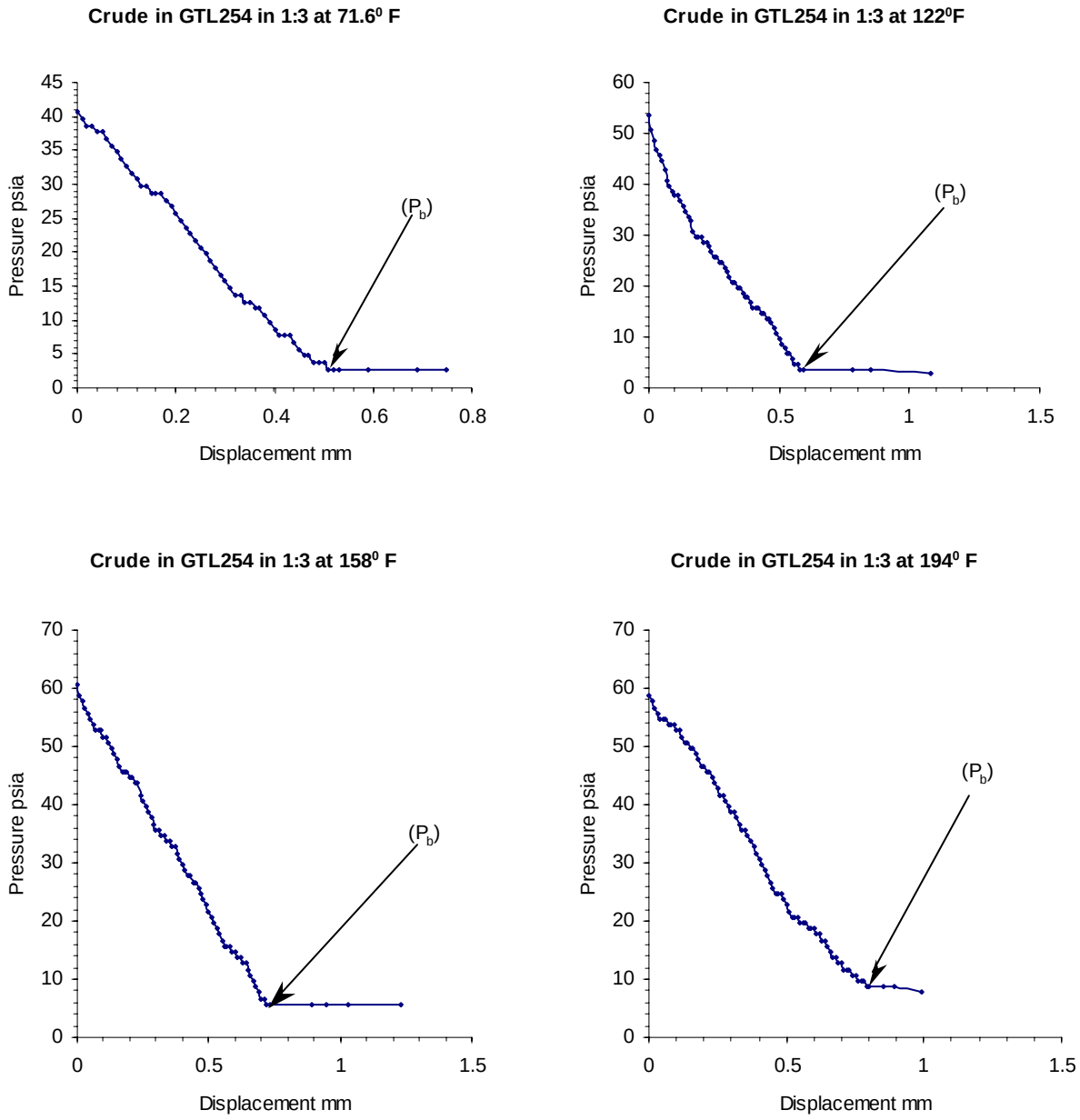

Figure 5.12. Bubble point measurements for TAPS crude/GTL 254 blend of 1:3.

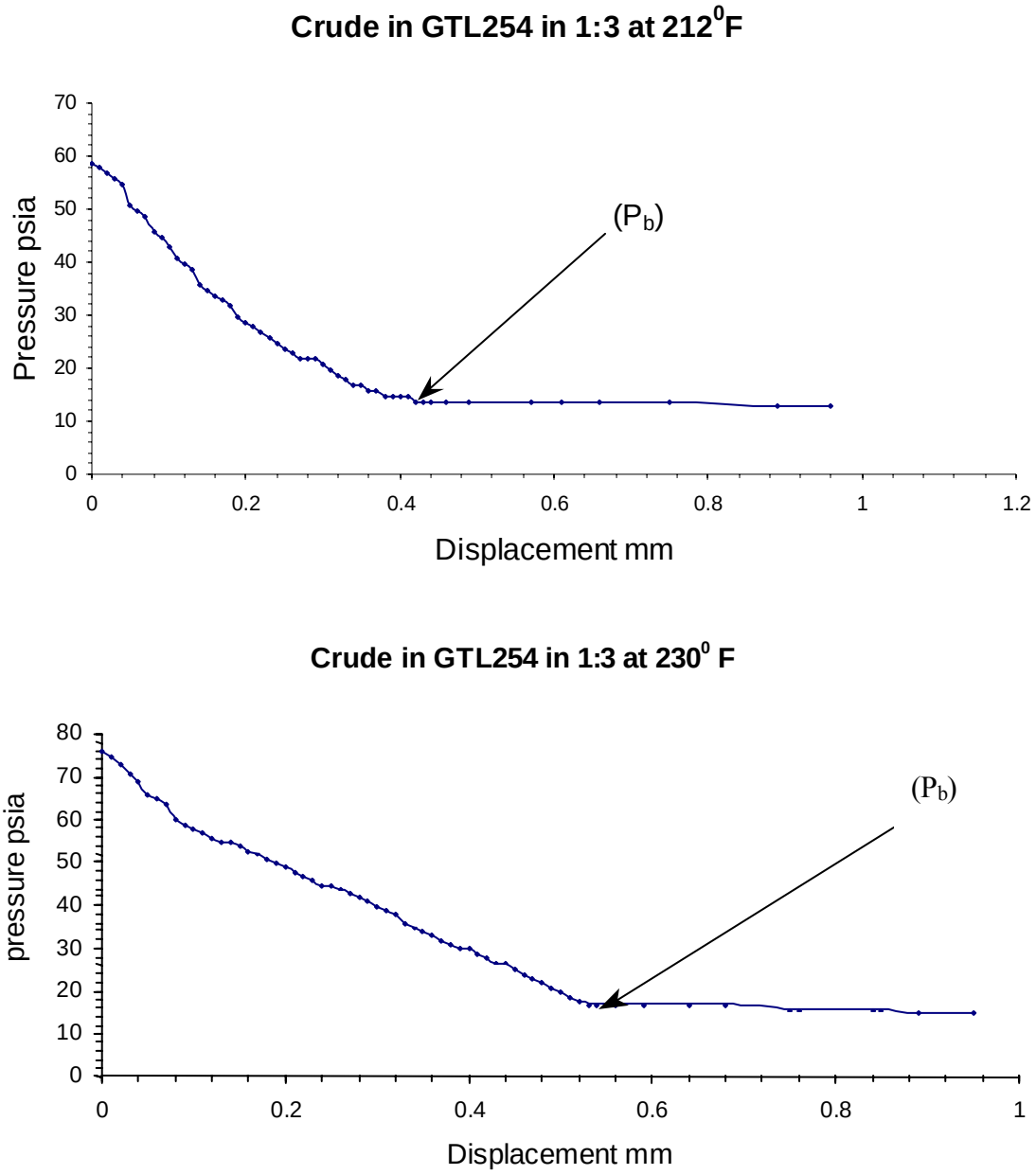

Figure 5.13. Bubble point measurements for TAPS crude/GTL 254 blend of 1:3.

Table 5.5. Bubble point measurements for TAPS crude/GTL 254 blend of 1:3.

Temperature°F	Pressure pisa
71.6	2.7
122	3.7
158	5.7
194	8.7
212	13.7
230	16.7

5.5.4 Saturation Pressures for TAPS Crude Oil/GTL 302 Blend Ratio of 3:1

Saturation pressure trends similar to those discussed above were observed when TAPS crude was mixed with GTL 302 (figures 5.14 and 5.15). The bubble point pressures were still observed to be lower than the pipeline conditions (see Table 5.6). It can be stated that a blend of crude oil and GTL 302 in a ratio of 3:1 will always exist as single-phase liquid at pipeline conditions.

Table 5.6: Bubble point measurements for TAPS crude/GTL 302 blend of 3:1.

Temperature°F	**Pressure psia**
69.44	3.7
95.54	7.7
117.14	9.7
153.86	12.7
197.96	20.7
271.76	48.7

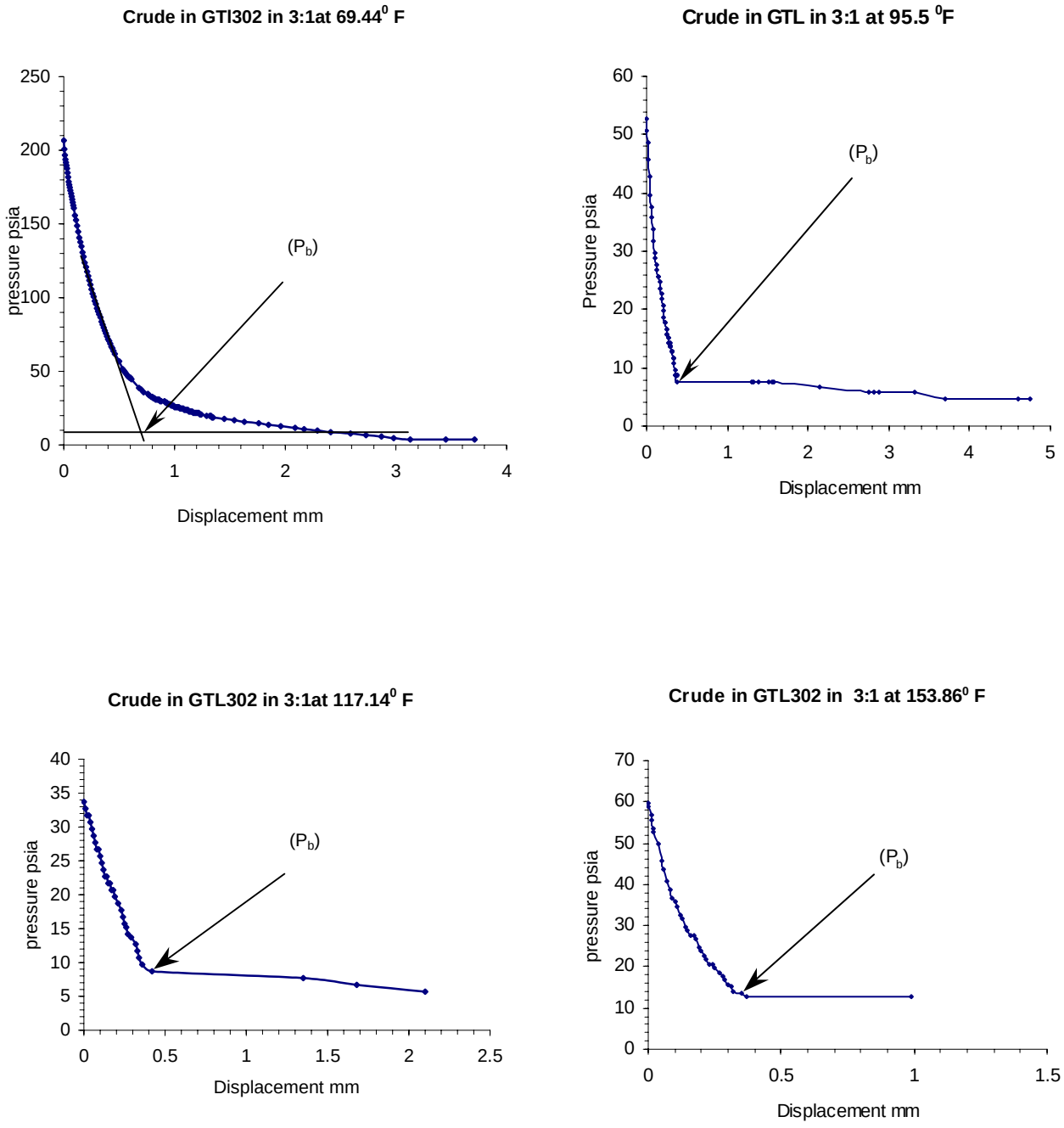

Figure 5.14. Bubble point measurements for TAPS Crude/GTL 302 blend of 3:1.

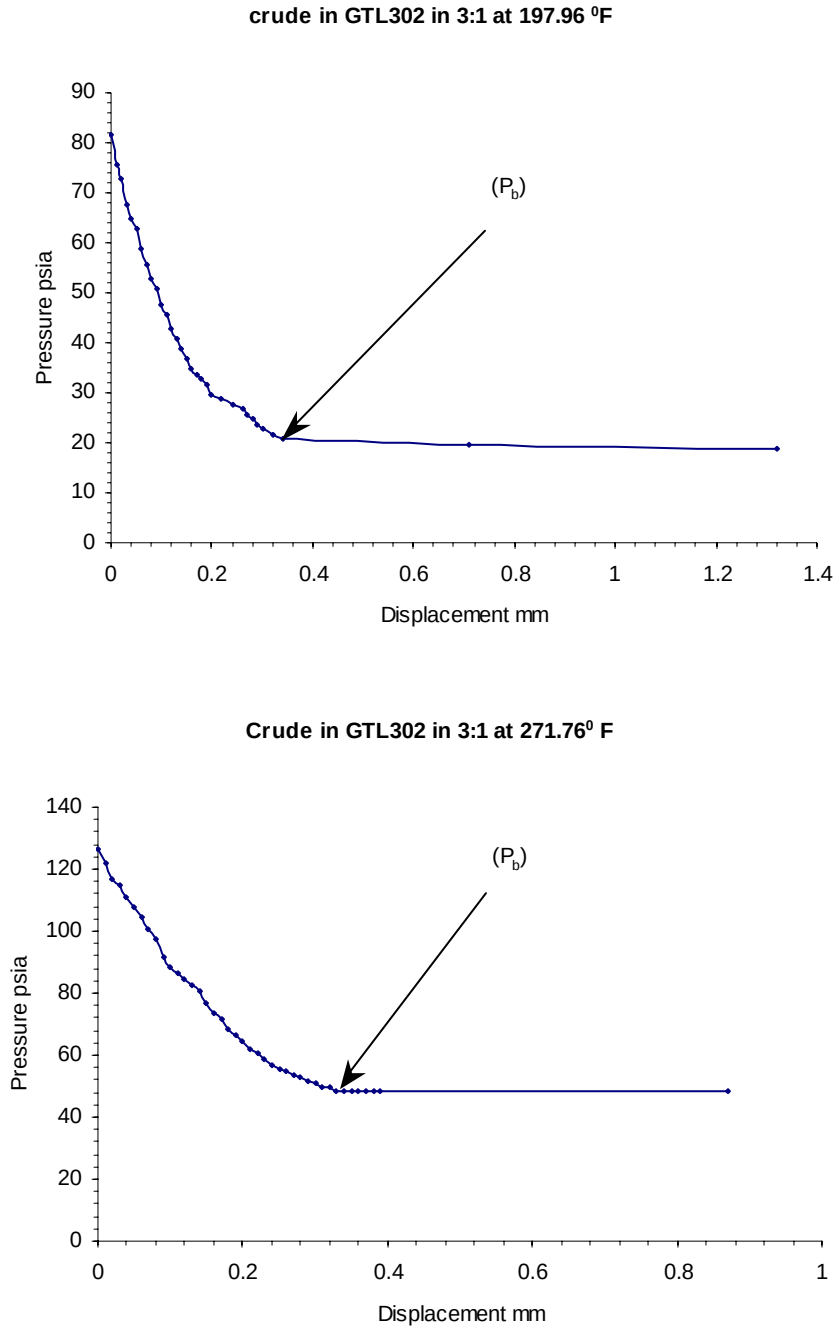

Figure 5.15. Bubble point measurements for TAPS Crude/GTL 302 blend of 3:1.

5.5.5 Saturation Pressures for TAPS Crude Oil/GTL 302 Blend Ratio of 1:1

The plots in Figure 5.16 show saturation pressure for a 1:1 blend of crude/GTL 302. It was observed that the change in saturation pressure with respect to ratio followed the same trend as that of GTL 254. However the bubble point pressure obtained for the GTL 302 blends were

much lower than those obtained from GTL 254 blends. This indicates that the bubble point decreases as a fluid having heavier hydrocarbons is added to TAPS crude oil. While testing this blend for its bubble point pressure, the O-Rings on the isolation piston failed; therefore the readings were limited to a temperature of 194.18°F (see Table 5.7).

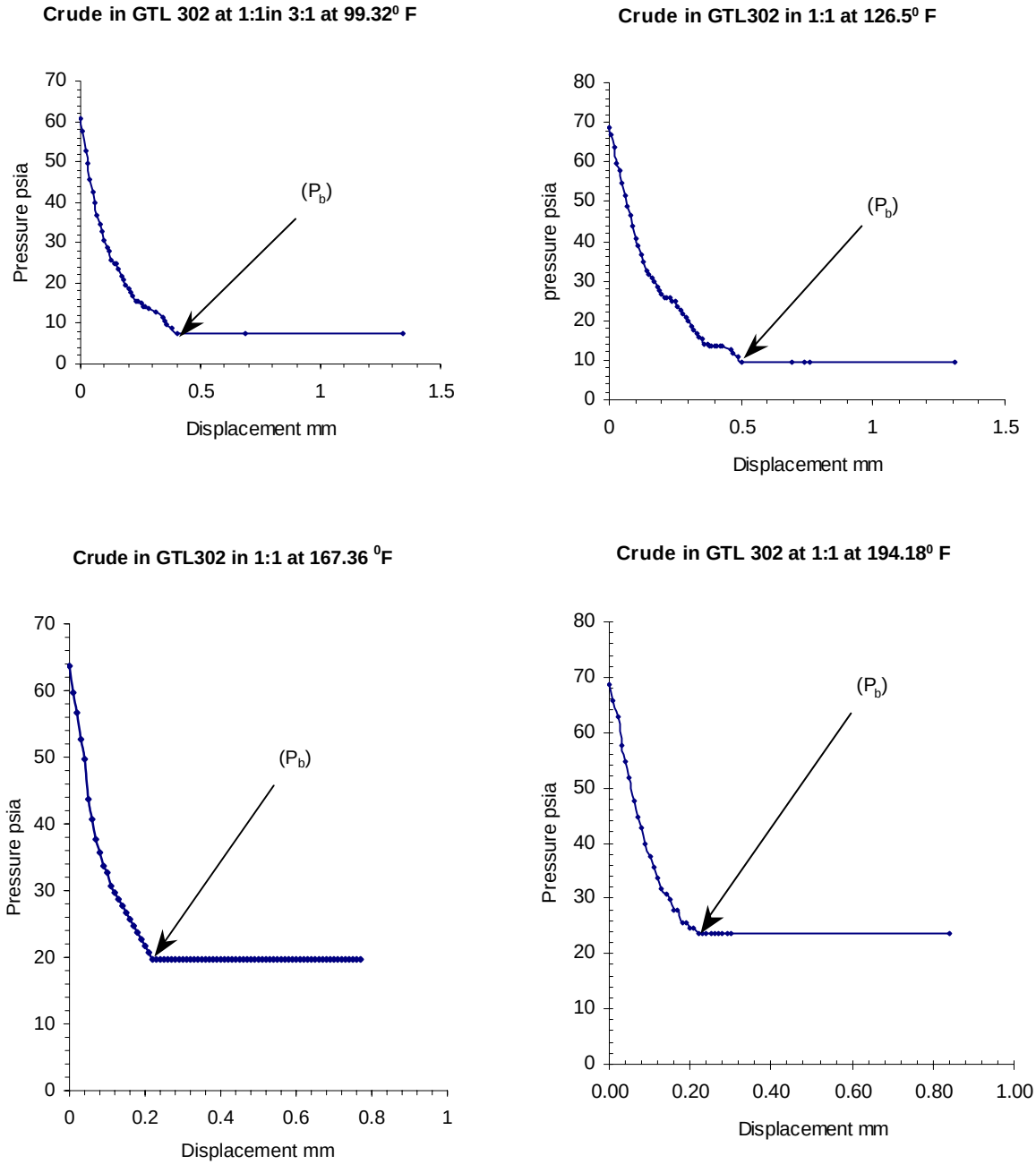

Figure 5.16: Bubble point measurements for TAPS Crude/GTL 302 blend of 1:1

Table 5.7. Bubble point measurements for TAPS Crude/GTL 302 blend of 1:1.

Temperature°F	Pressure psia
99.32	7.7
126.5	9.7
167.36	19.7
194.18	23.7

5.5.6 Saturation Pressures for TAPS Crude Oil/GTL 302 Blend Ratio of 1:3

Saturation pressure measurements obtained for a 1:3 blend of crude/GTL 302 are shown in figures 5.17 and 5.18. Very similar trends were observed for a mixture of crude oil in GTL 302. The bubble point pressure was less than that of the pipeline conditions (Table 5.8).

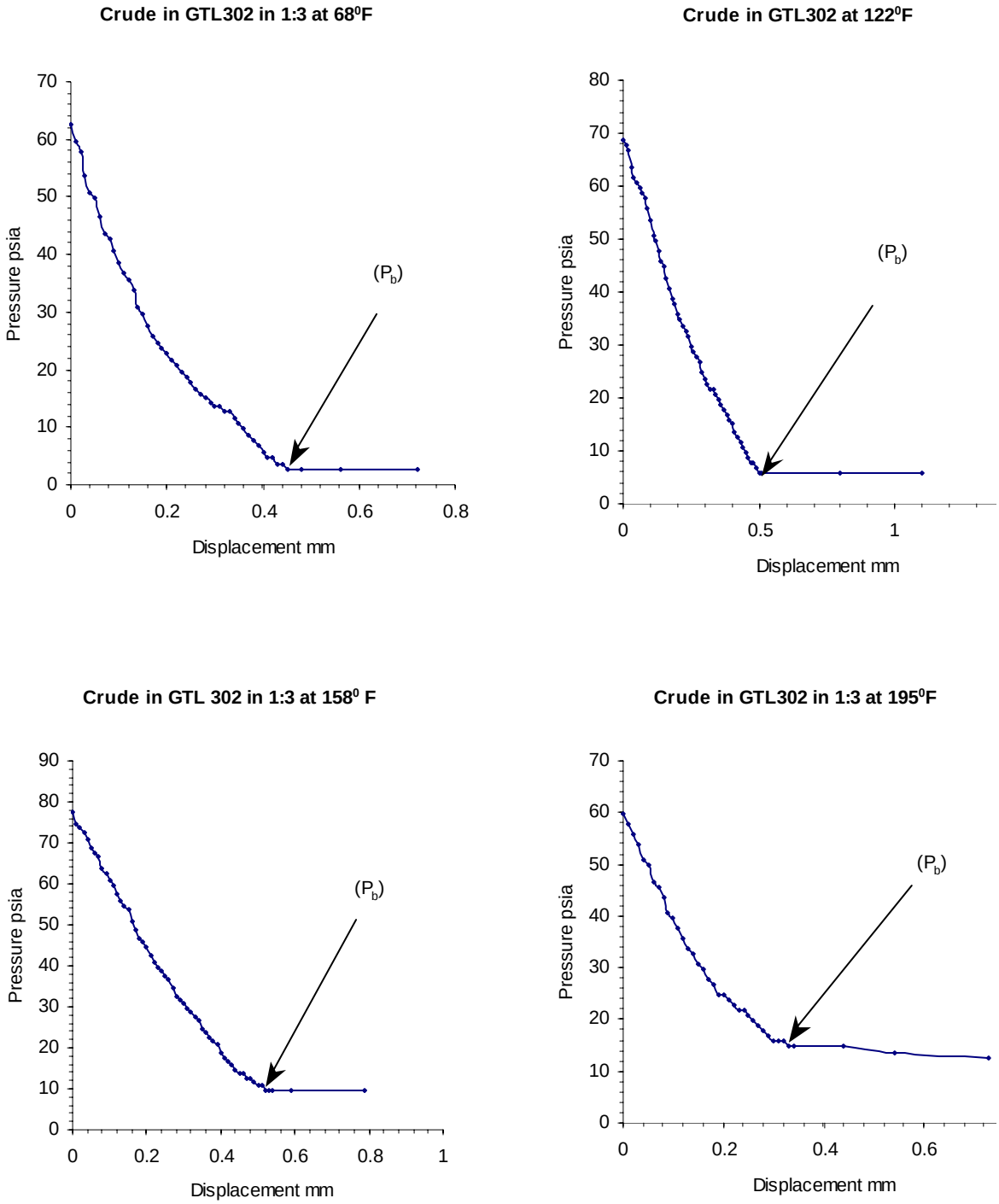

Figure 5.17. Bubble point measurements for TAPS crude/GTL 302 blend of 1:3.

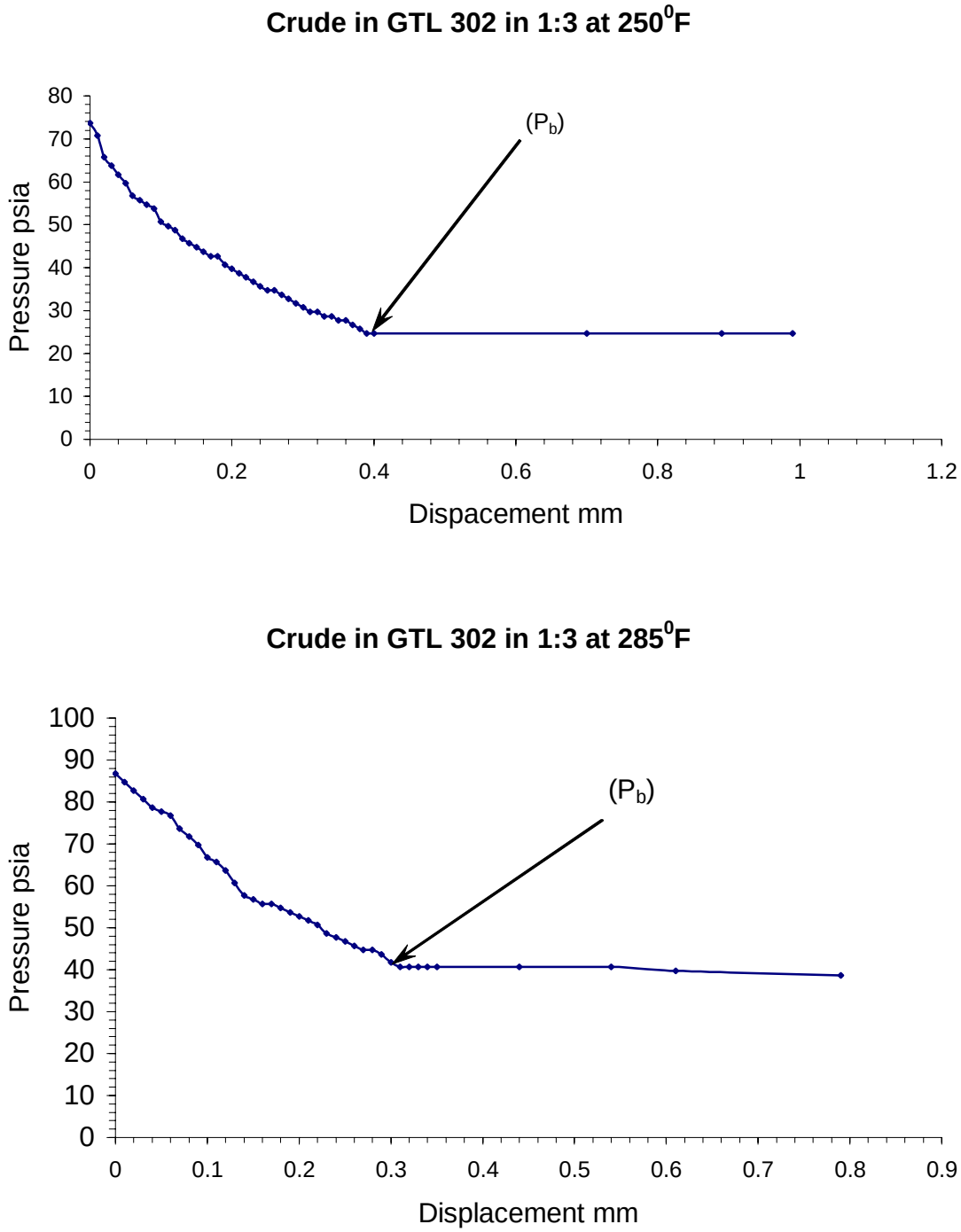

Figure 5.18. Bubble point measurements for TAPS crude/GTL 302 blend of 1:3**.**

Table 5.8. Bubble point measurements for TAPS Crude/GTL 302 blend of 1:3.

Temperature°F	Pressure psia
68	2.7
122	5.7
158	9.7
195	14.7
250	24.7
282	40.7

5.5.7 Saturation Pressures for TAPS Crude Oil/GTL 344 Blend Ratio of 3:1

Plots in figures 5.19 and 5.20 show bubble point measurements for TAPS crude oil in GTL 344 in 3:1. The measured bubble points for this blend are also below those of pipeline conditions (see Table 5.9). Hence, it can be stated that this blend will also exist as a single phase liquid under pipeline conditions. However, as mentioned earlier, there is still some uncertainty about the nature of GTL that would flow through the TAPS; a prediction model based on an equation of state is necessary to predict the phase properties of the blends that may flow through TAPS.

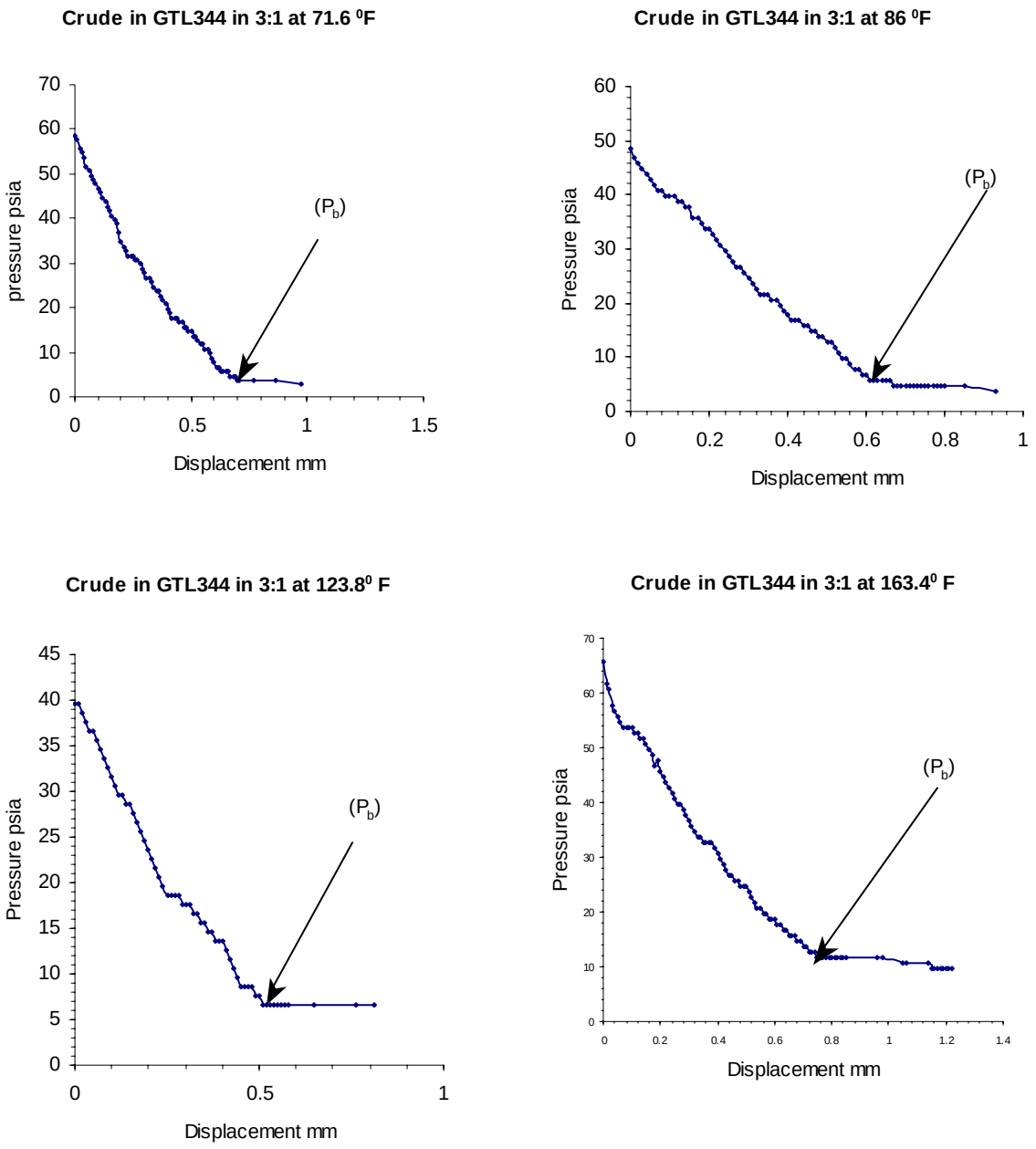

Figure 5.19. Bubble point measurements for TAPS crude/GTL 344 blend of 3:1.

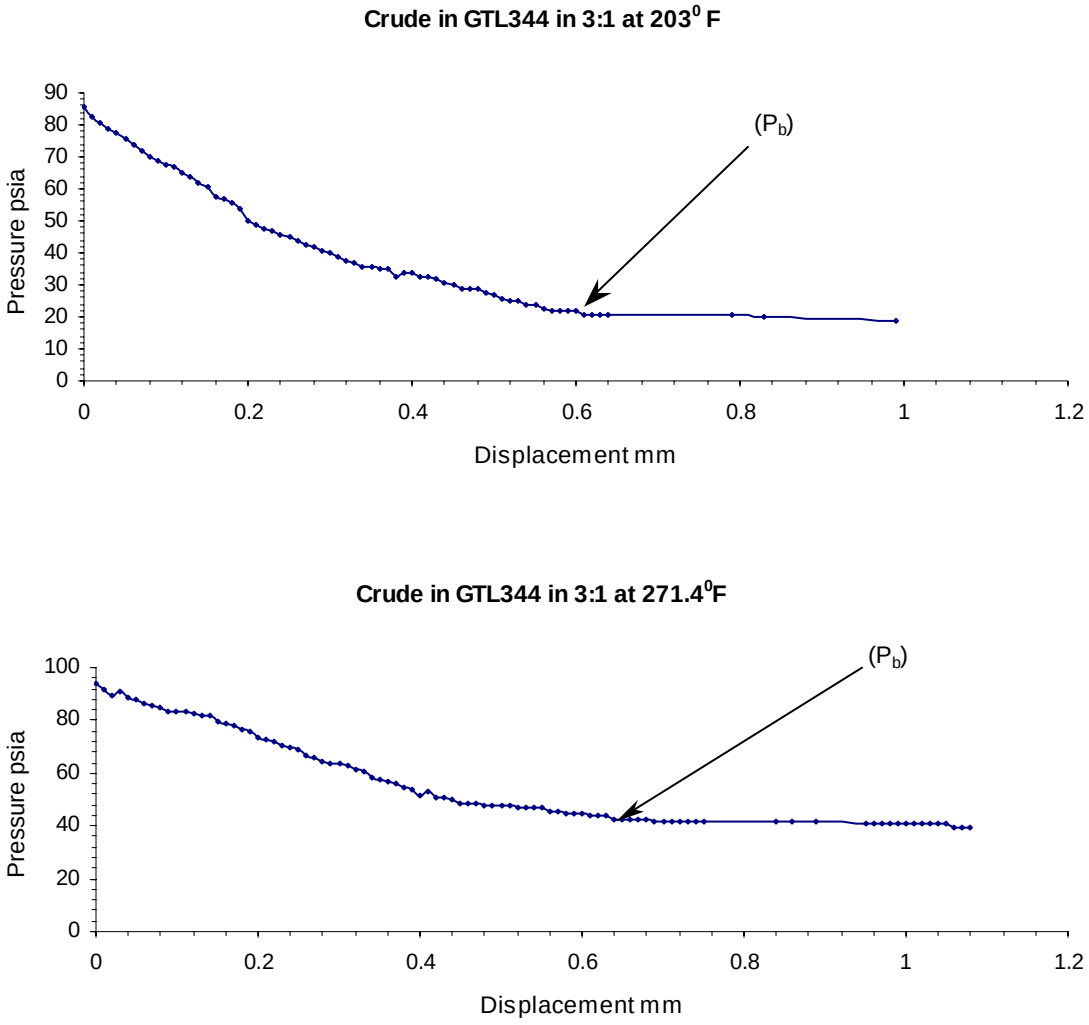

Figure 5.20. Bubble point measurements for TAPS crude/GTL 344 blend of 3:1.

Table 5.9. Bubble point measurements for TAPS crude/GTL 344 Blend of 3:1.

Temperature°F	Pressure psia
76.5	2.7
98.6	4.7
138.2	6.7
174.2	12.7
208.6	16.7
273.2	41.7

5.5.8 Saturation Pressures for TAPS Crude Oil/GTL 344 Blend Ratio of 1:1

Figures 5.21 and 5.22 show bubble point measurements for TAPS crude oil/GTL 344 in a 1:1 mixture. Results show that the mixture will exist as a single-phase liquid at pipeline conditions (Table 5.10). Even though the GTL samples have lost some of the light ends (these samples have been handled for over six years in various experiments), experimental phase behavior of these samples, as well as TAPS crude samples, is still significantly valuable. Such data can be used to evaluate and select a good model based on an appropriate equation of state (EOS). A rigorously evaluated and selected model will be very useful in determining the phase behavior characteristics of at least a similar type of GTL that would flow through TAPS.

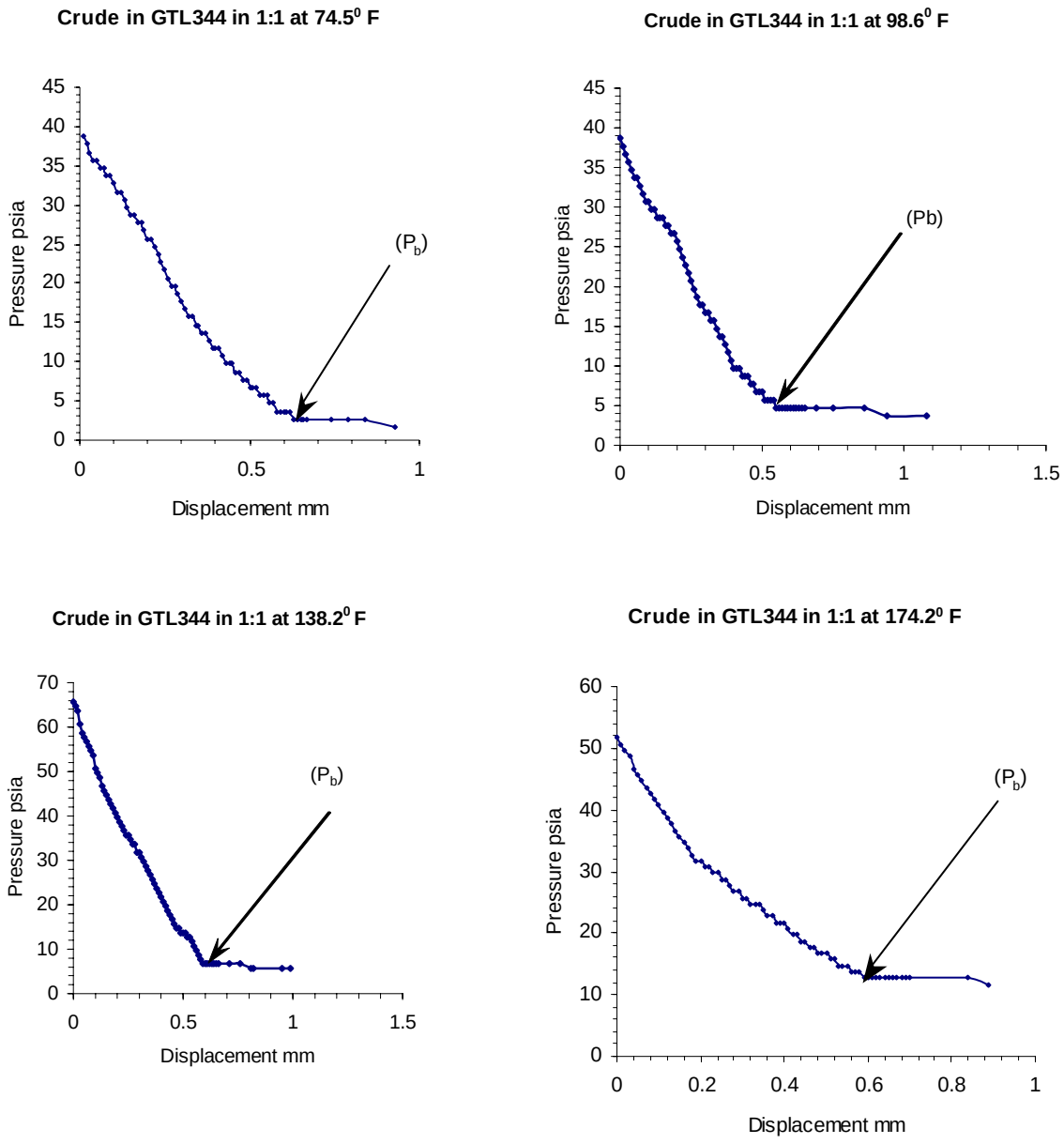

Figure 5.21. Bubble point measurements for TAPS crude/GTL 344 blend of 1:1.

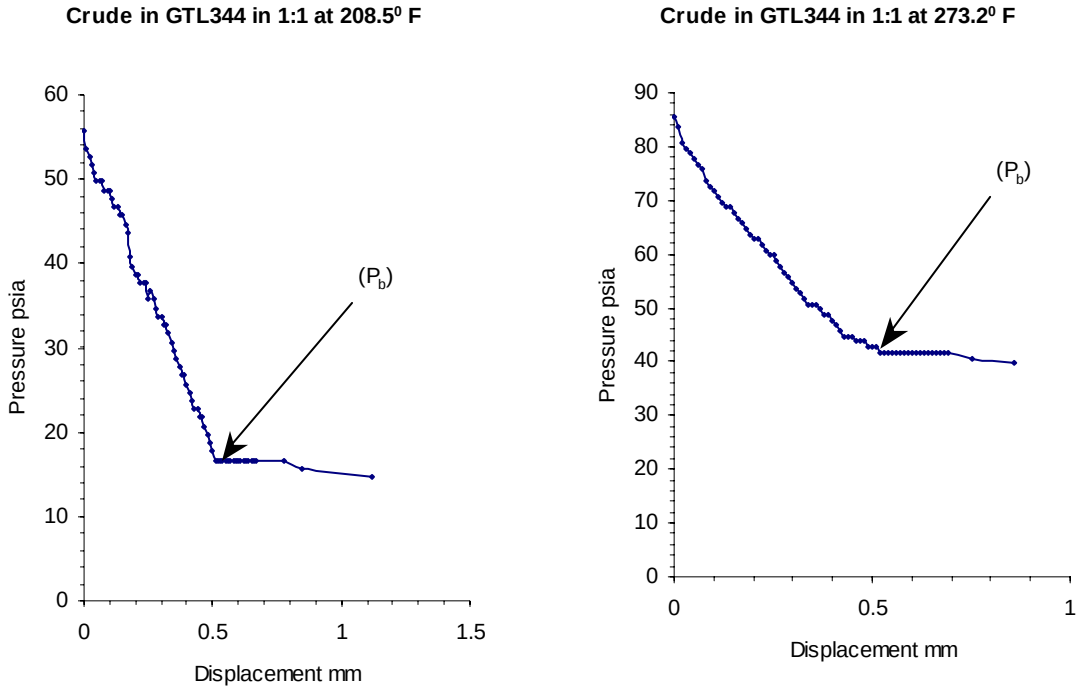

Figure 5.22. Bubble point measurements for TAPS crude/GTL 344 blend of 1:1.

Table 5.10. Bubble point measurements for TAPS crude/GTL 344 blend of 1:1.

Temperature°F	Pressure psia
71.6	3.7
86.0	4.7
123.8	6.7
163.4	11.7
203.0	20.7
271.4	41.7

The bubble point pressures obtained in this work are compared in tables 5.12 through 5.14 and figures 5.23 through 5.25 for AKGTL and different cuts of the Laporte light GTL sample.

Table 5.11. Comparison of bubble point pressure results for AKGTL and GTL 254.

Temp (°F)	Bubble Pt. Pressure (psia)		Temp (°F)	Bubble Pt. Pressure (psia)	
	25% AKGTL	50% AKGTL		25% GTL 254	50% GTL 254
122	86.7	84.7	122	8.7	10.7
167	96.7	94.7	158	13.7	13.7
212	137.7	135.7	194	21.7	17.7
			212	25.7	22.7

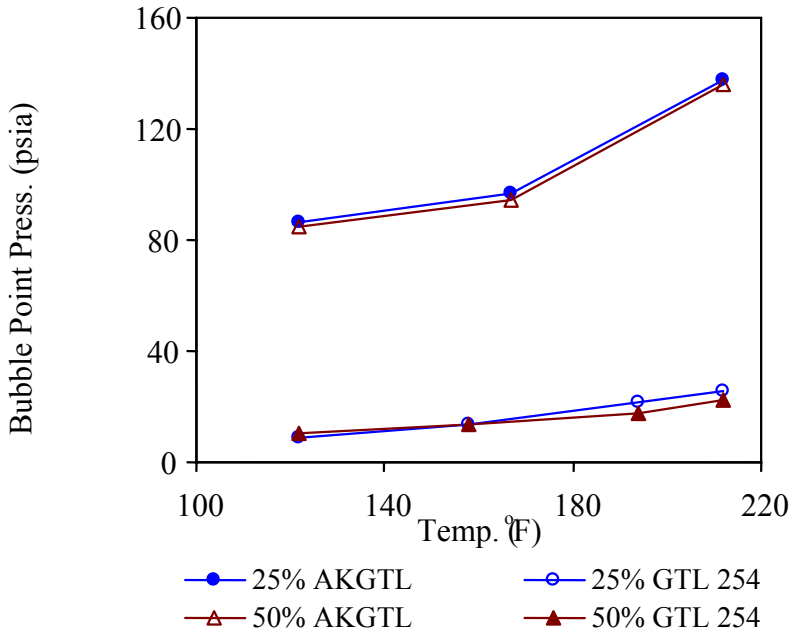

Figure 5.23. Comparison of bubble point pressure results for AKGTL and GTL 254.

Table 5.12. Comparison of bubble point pressure results for AKGTL and GTL 302.

Temp (°F)	BP Press. (psia)		Temp (°F)	BP (psia) (25% GTL 302)	Temp (°F)	BP (psia) (50% GTL 302)
	25% AKGTL	50% AKGTL				
122	86.7	84.7	117.14	8.7	126.5	9.7
167	96.7	94.7	153.86	13.7	167.36	19.7
212	137.7	135.7	197.96	21.7	194.18	23.7

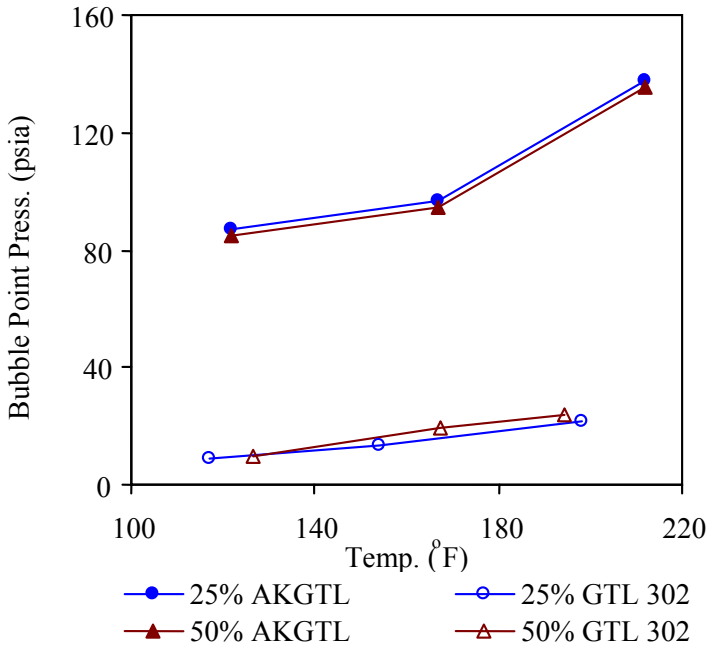

Figure 5.24. Comparison of bubble point pressure results for AKGTL and GTL 302.

Table 5.13. Comparison of bubble point pressure results for AKGTL and GTL 344.

Temp (°F)	BP Press. (psia)		Temp (°F)	BP (psia) (25% GTL 302)	Temp (°F)	BP (psia) (50% GTL 302)
	25% AKGTL	50% AKGTL				
122	86.7	84.7	98.6	4.7	86.0	4.7
167	96.7	94.7	138.2	6.7	123.8	6.7
212	137.7	135.7	174.2	12.7	163.4	11.7
			208.6	16.7		
			203.0	20.7		

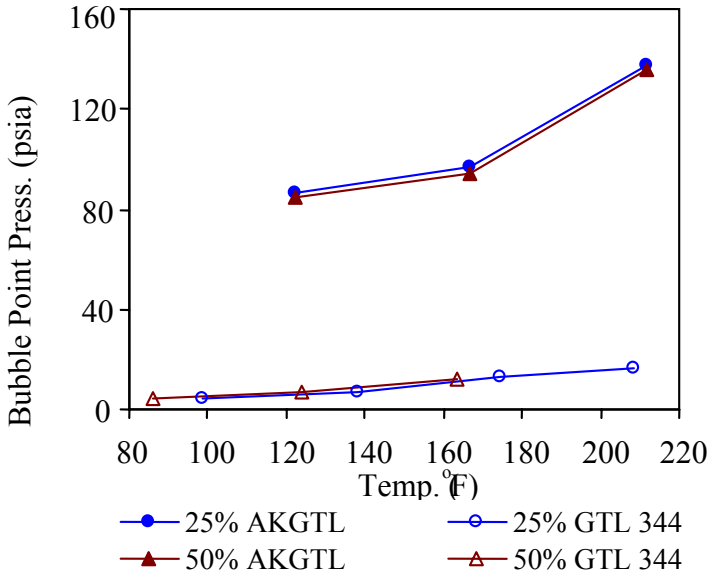

Figure 5.25. Comparison of bubble point pressure results for AKGTL and GTL 344.

Tables 5.12 through 8.14 and figures 5.23 through 5.25 show that the bubble point pressures obtained using the AKGTL are consistently higher than those obtained using cuts of the Laporte Light GTL sample. This difference is due to the compositional differences in the fluids. The AKGTL is a syncrude and has a broader range of composition.

5.6 Saturation Pressure Modeling

Saturation pressures obtained in the laboratory (as discussed in section 5.1) were modeled to predict the behavior of GTL and crude oil mixtures under various conditions. The main purpose of modeling this fluid's phase behavior was to establish the accuracy and reliability of the developed equation of state (EOS) model to predict various other fluid phase behavior properties at high pressure and temperature conditions. The Soave-Redlich-Kwong (SRK) and Peng-Robinson (PR) equations of state were used to determine the two-phase envelope. Generally, a model based on a saturation pressure match that matches several points on a phase envelope will successfully predict the fluid behavior under constant composition expansion and the separator tests. A phase behavior model will also predict properties such as compressibility, density, viscosity, thermal conductivity, and so on, for the fluid's vapor and liquid phases. These properties are very important parameters for the pressure drop calculations. A good phase

behavior model will also be capable of simulating solid deposition at various temperatures and pressure conditions.

The phase behavior modeling was conducted using the Computer Modeling Group's WinProp simulator, a commercial simulator often used for generating fluid properties for reservoir simulators. The WinProp simulator uses two major equations of state (The Soave-Redlich-Kwong and the Peng-Robinson) for modeling saturation pressures of GTL and crude oil blends. The composition of the GTL cuts were measured in the GC/MS laboratory and the composition of the crude oil was supplied by the Alyeska Pipeline Service Company. The compositions are the main input into the phase behavior simulator. The two-phase envelope was constructed using either of the two equations of state, and the results were compared with the experimental data. If the simulated data did not match, the model was "fine-tuned" by changing the eccentric factor correlation, and, in some cases, the critical properties correlations as well. A correlation that matched the laboratory-obtained data well was considered a good phase behavior model.

Figures 5.26 through 5.34 show the saturation pressures obtained in the laboratory and those calculated using the equations of state for TAPS crude oil and cuts of LaPorte GTL blends. These figures show the phase envelopes on pressure-temperature (PT) diagrams for several GTL and crude oil blends. In these figures, "phase envelope" refers to the area bounded by the red curve (Soave-Redlich-Kwong EOS) or the blue curve (Peng-Robinson EOS). In all figures, the red and the blue curves follow each other very closely, which suggests that either of the two EOS can be used for phase behavior prediction. The area enclosed by the phase envelope represents the two phase region; that is, the given blend will exist in two phases (liquid and gas) if pressure and temperature fall within that envelope. All other pressures and temperatures outside this envelope will result in the blend existing as a single phase.

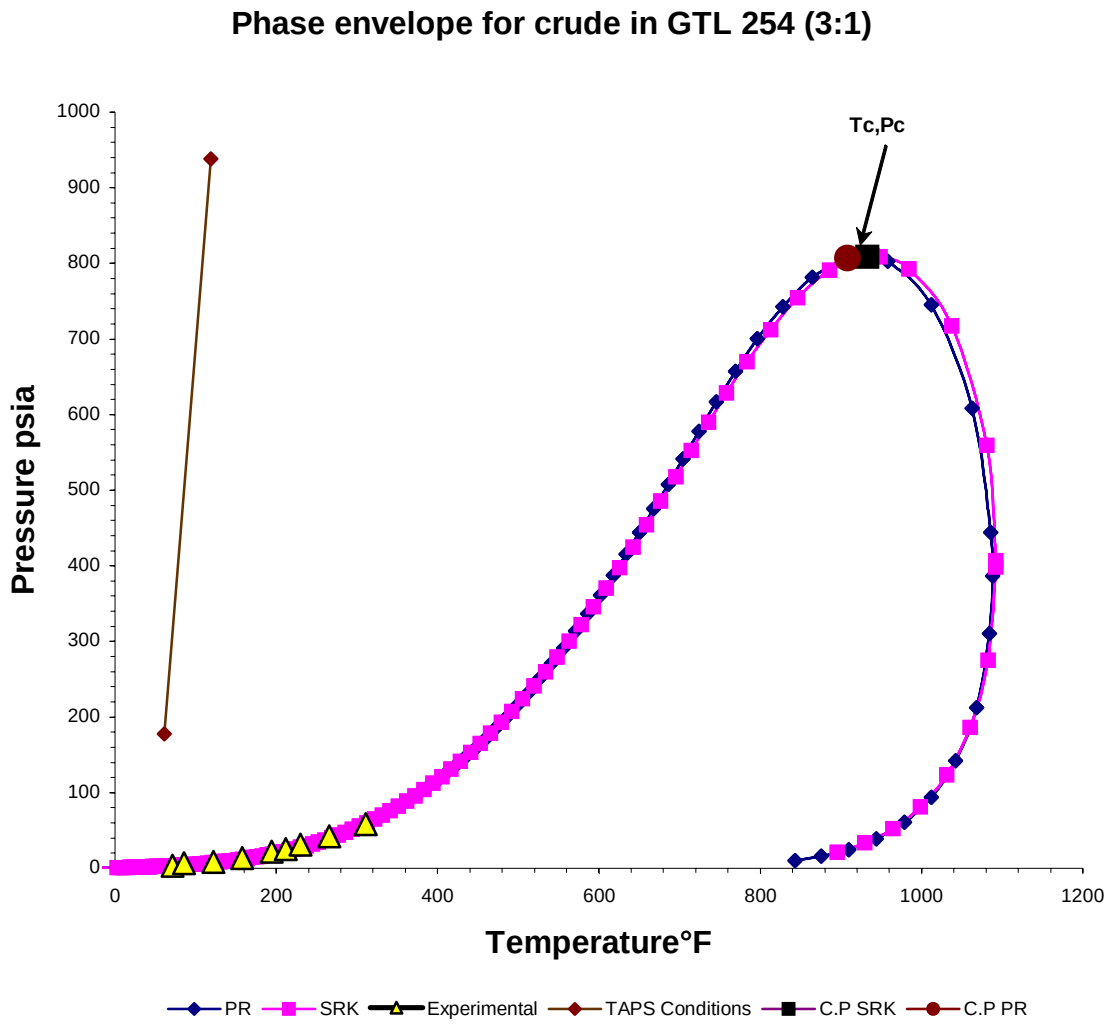

Figure 5.26. Phase envelope for TAPS Crude/GTL 254 blend (3:1).

Figure 5.26 shows that the saturation pressures obtained using the SRK and the PR equations of state match well with those obtained in the laboratory. However, since the design temperature of the air bath for the PVT Cell is 390°F, only saturation pressures for temperatures up to 390°F were measured. The trend obtained from the PVT experiments still compares very well with that from both equations of state. These results suggest that, given the accurate composition of the GTL and crude oil blends, the saturation pressures (in this case the bubble point pressures) can be modeled using either the PR or the SRK equations of state.

The range of TAPS operating conditions is shown in Figure 5.26 as a straight line, joining the pipeline inlet and outlet pressures and temperatures. This straight line is located far to the left of the two-phase envelope, and the line falls entirely in the single phase liquid region. Thus, it can be confidently stated that the GTL-crude oil blend of Figure 5.26 will remain as single phase liquid throughout the entire length of TAPS. Figures 5.27 through 5.34 show that the other GTL-crude oil blends will also remain as single phase liquids throughout the pipeline.

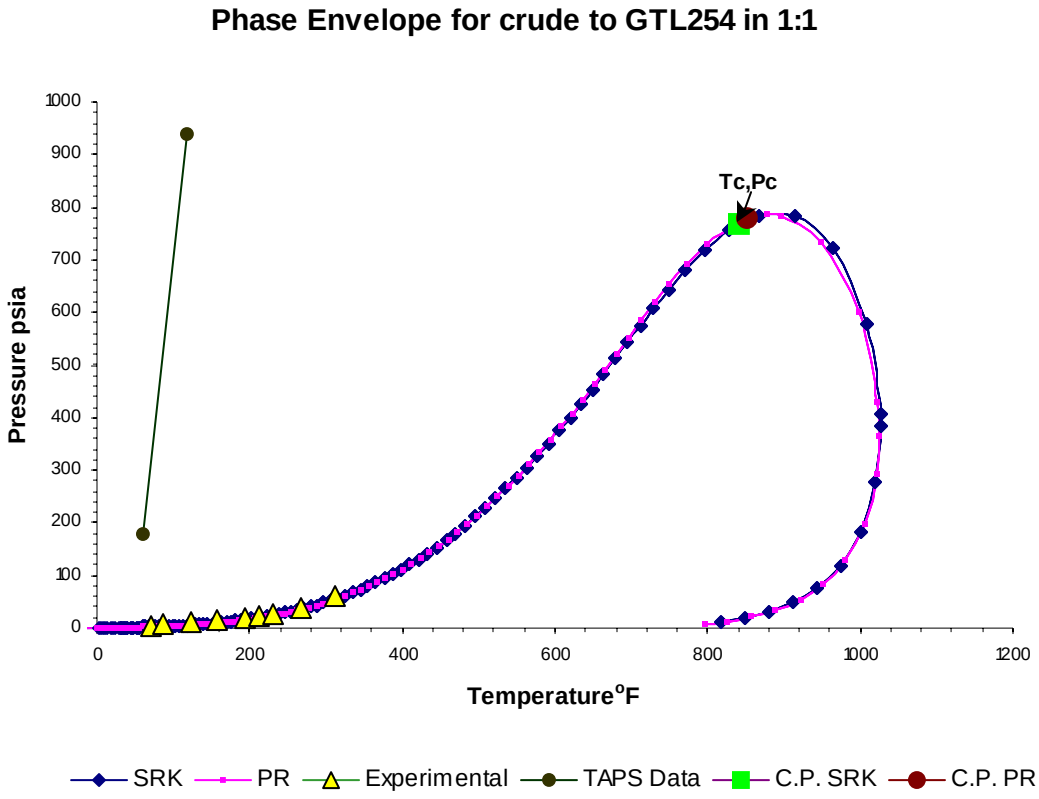

Figure 5.27. Phase envelope for TAPS crude/GTL 254 blend of 1:1.

Similar results were obtained for phase behavior modeling of TAPS crude oil in GTL 254, in ratios of 1:1 and 1:3 (shown in figures in 5.27 and 5.28, respectively). These results suggest that either an SRK or PR equation of state can be used for modeling the phase properties of GTL and crude oil blends under pipeline conditions. Moreover, the saturation pressures of these blends can also be predicted at other conditions, as well as similar fluid compositions of other GTL material, considering the excellent match obtained between the laboratory-measured values and EOS predicted values.

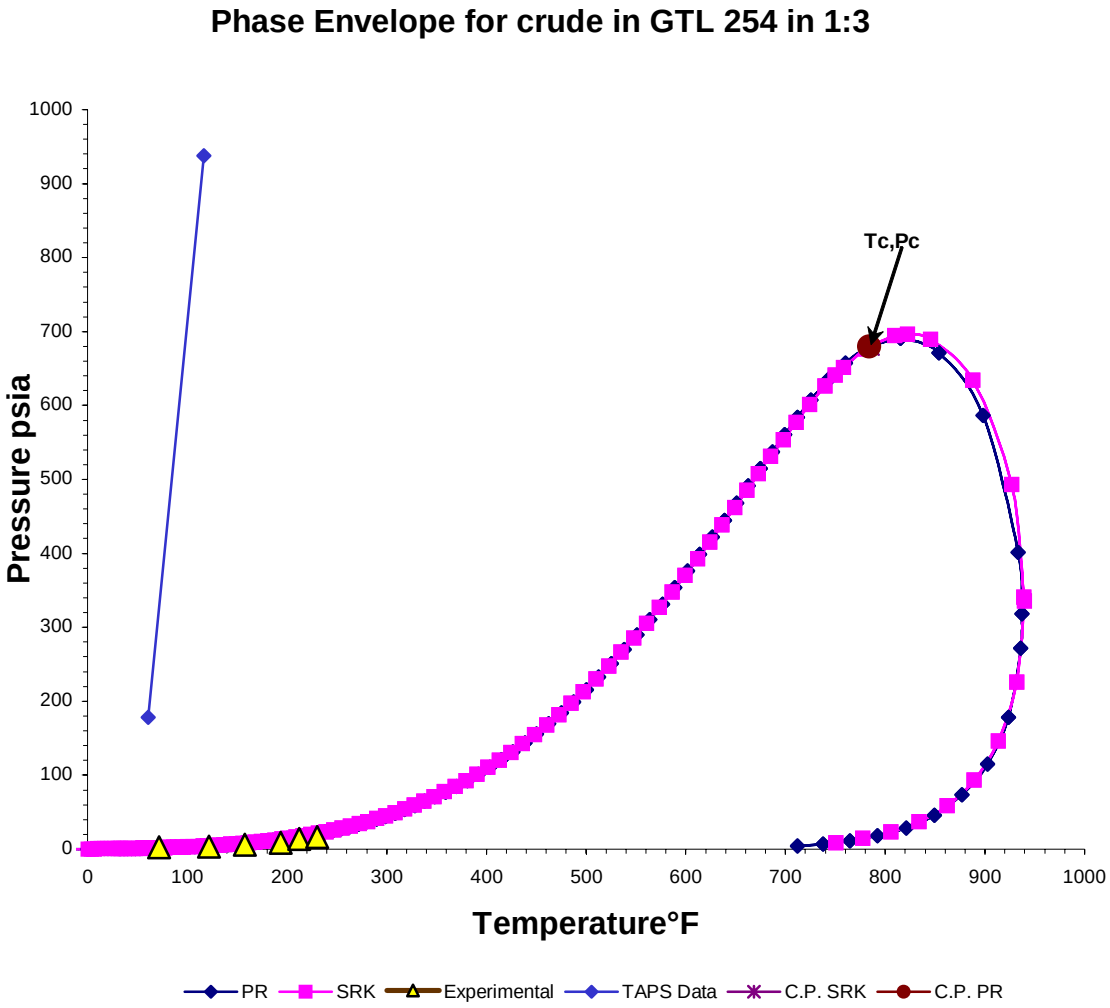

Figure 5.28. Phase envelope for TAPS crude/GTL 254 blend of 1:3.

Figures 5.29 through 5.31 show the saturation pressure for GTL 302 and TAPS crude oil blends. These figures demonstrate that the experimental results match well with those obtained from model predictions, and similar conclusions can be drawn for the blends of GTL 302 with crude oil. Both SRK and PR equations of state are equally good for predicting the phase behavior of GTL 302 and crude oil blends.

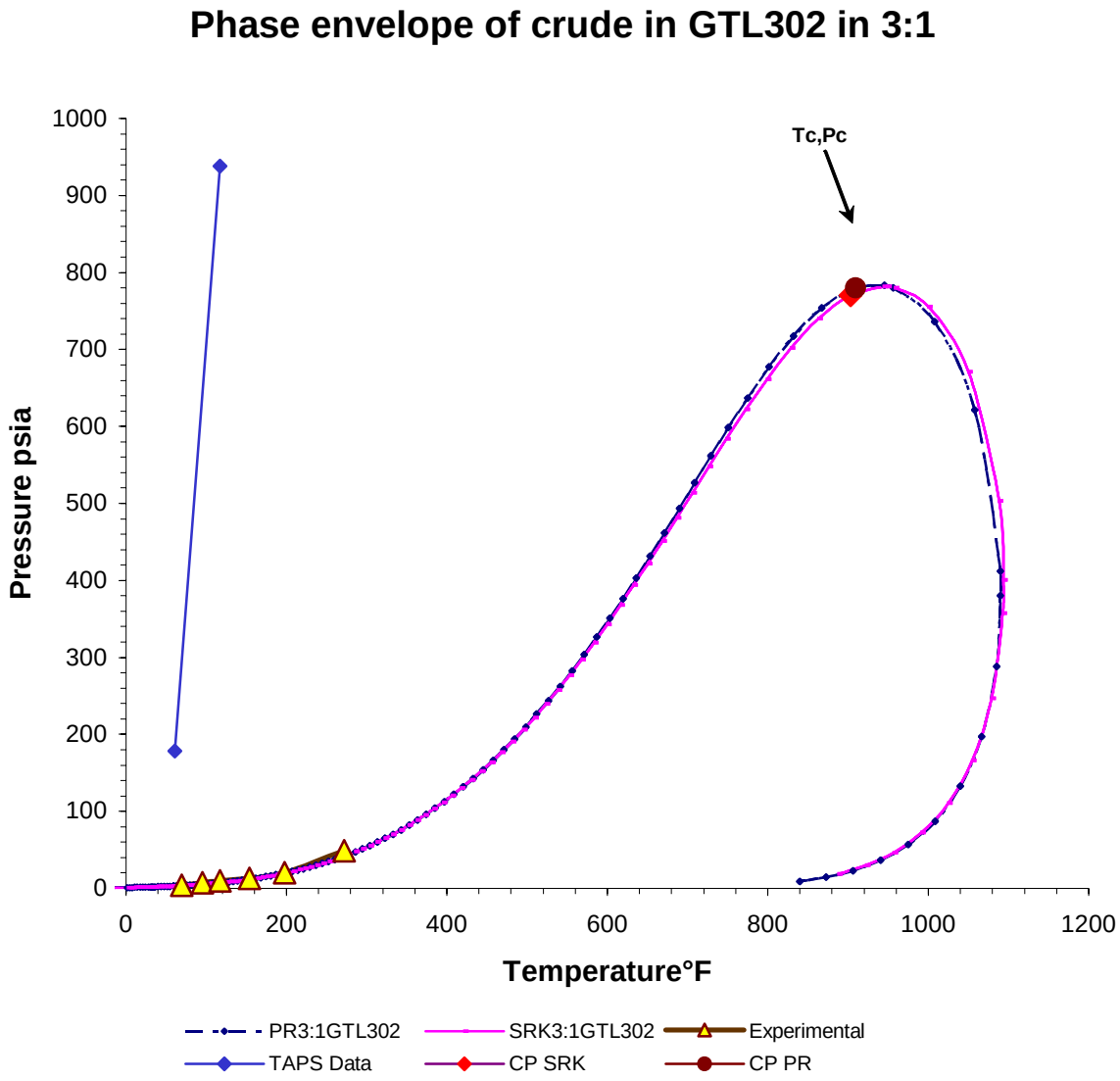

Figure 5.29. Phase envelope for TAPS crude/GTL 302 blend of 3:1.

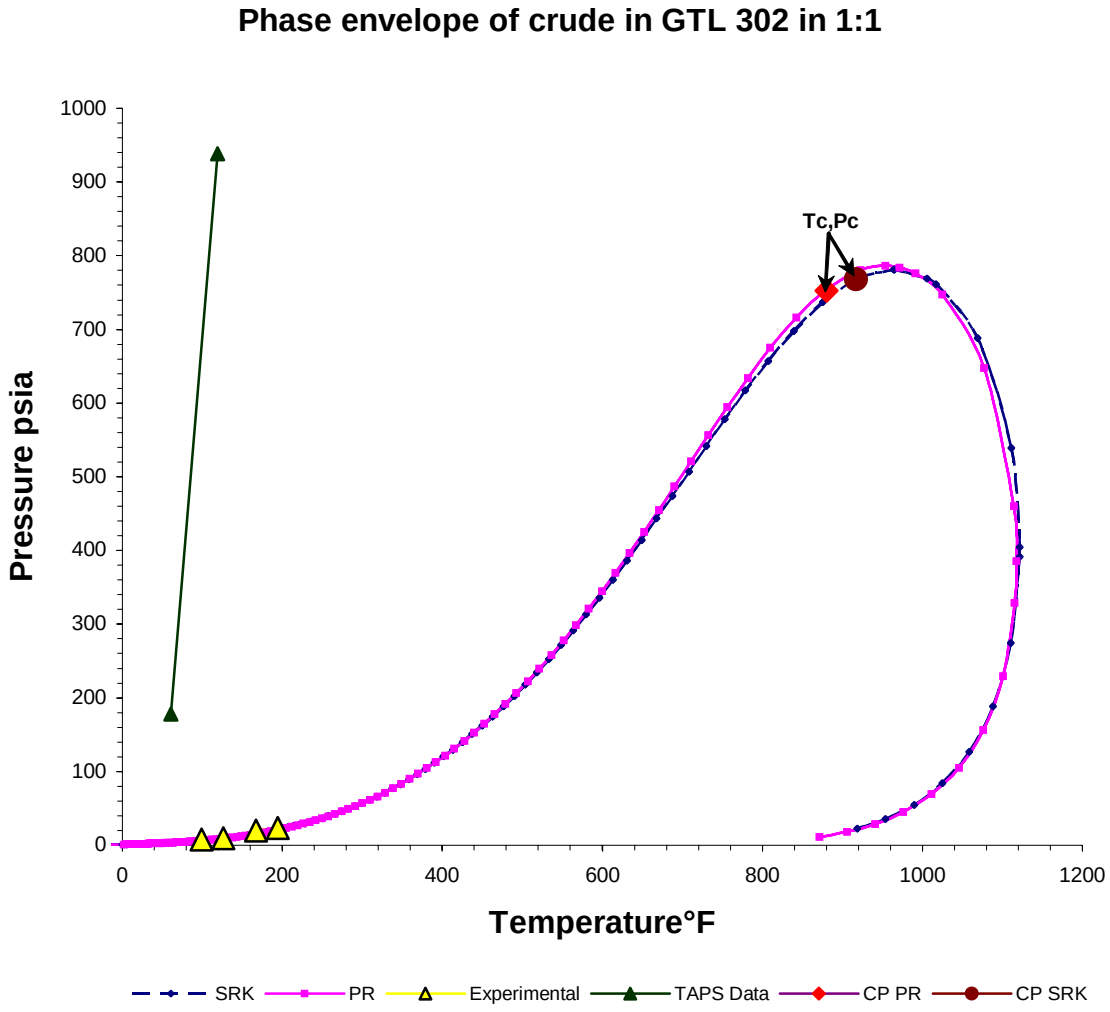

Figure 5.30. Phase envelope for TAPS crude/GTL 302 blend of 1:1.

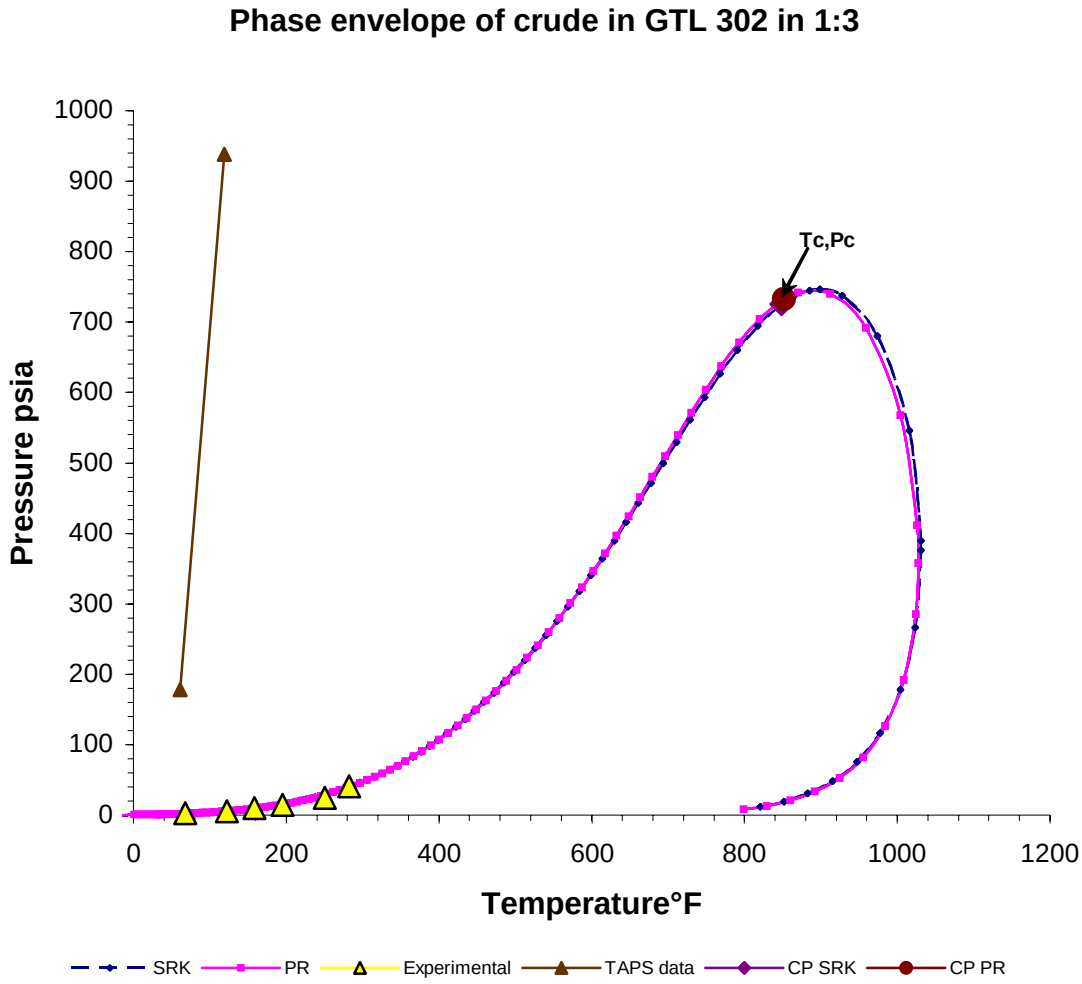

Figure 5.31. Phase envelope for TAPS crude/GTL 302 blend of 1:3.

Figure 5.32 demonstrates a very close EOS match with that of the experimental results for the GTL 344 blend. Figures 5.33 and 5.34 show the saturation pressures obtained for GTL 344 using various methods. Both the SRK and PR equations of state applications matched the measurements obtained in the laboratory and hence can be used for predicting the phase behavior of GTL 344 and crude oil blends.

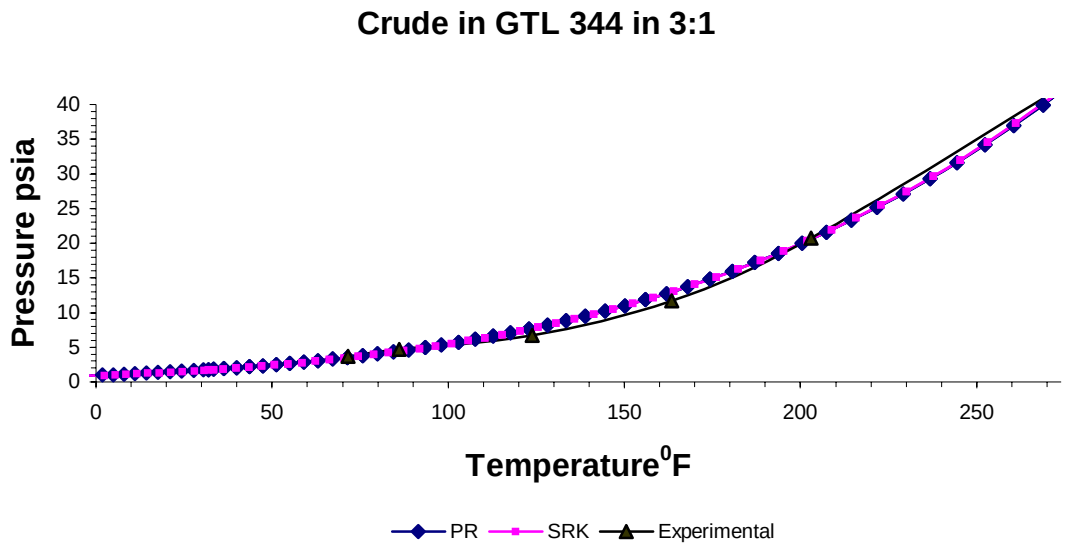

Figure 5.32. Bubble point for TAPS crude/GTL 344 blend of 3:1.

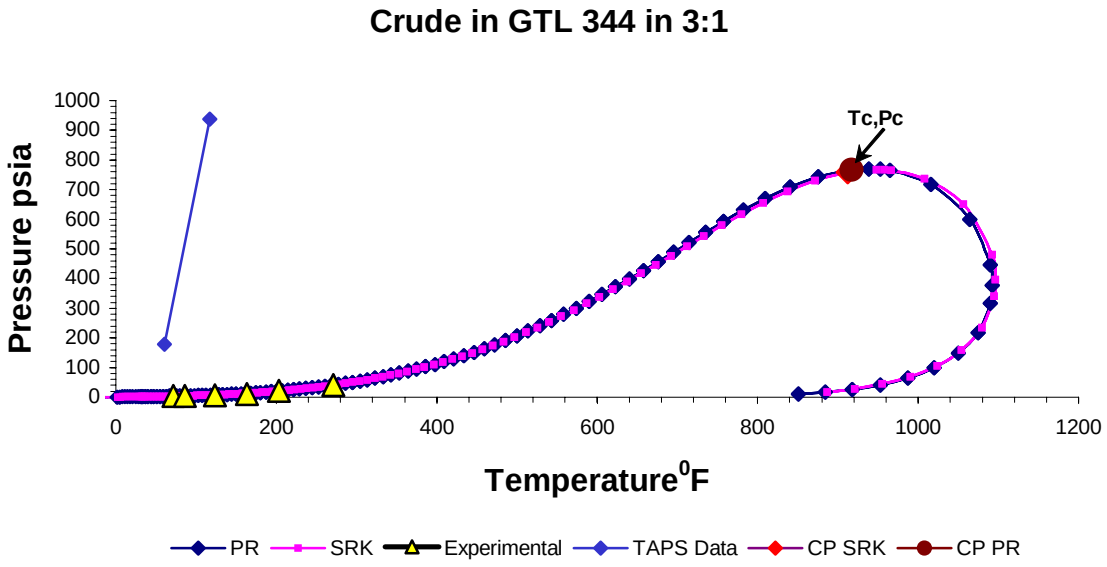

Figure 5.33. Phase envelope for TAPS crude/GTL 344 blend of 3:1.

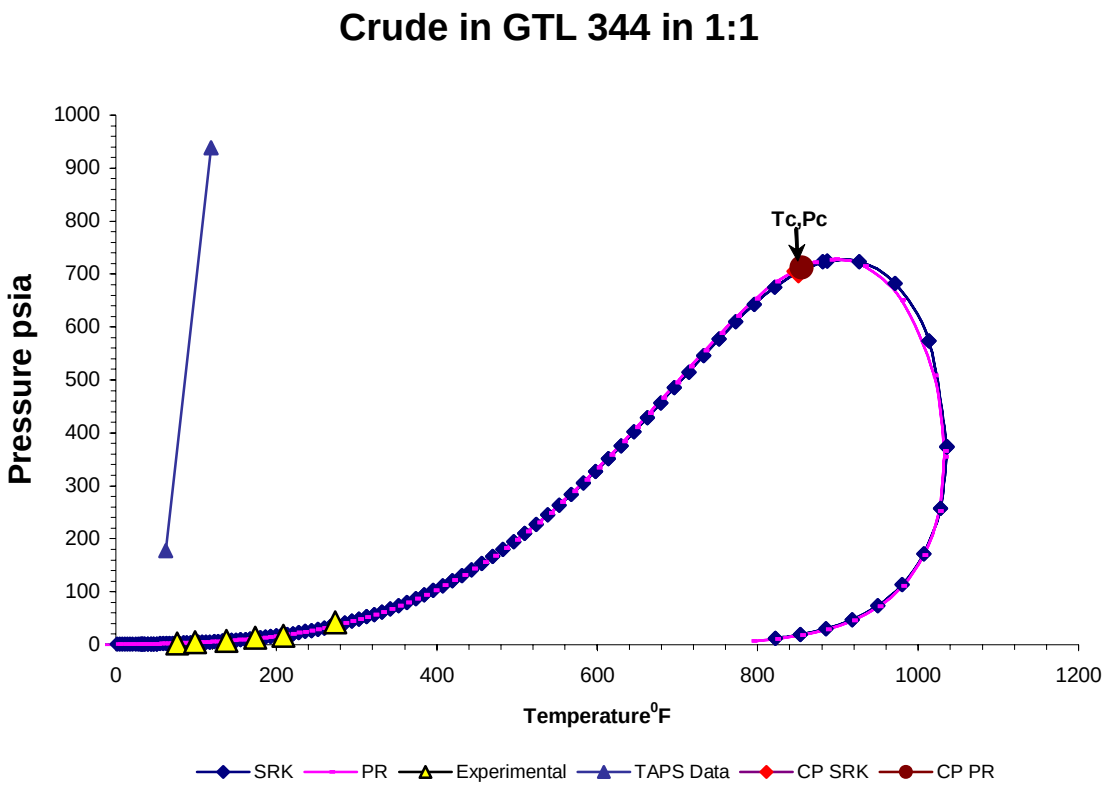

Figure 5.34: Phase envelope for TAPS crude/GTL 344 blend of 1:3.

Results of experimental work and prediction models suggest that either of the two most widely used equations of state can be used for modeling the phase behavior of GTL cuts and their blends with TAPS crude oil. The most important and positive result from the experimental and modeling work is that no two-phase flow problems while transporting GTL with TAPS crude oil to the markets are indicated.

Reference(s)

1. Chukwu, F.: Alyeska Pipeline Service Company, Fairbanks, Alaska, June 2003.

CHAPTER 6
REID VAPOR PRESSURE (RVP) EFFECTS

6.1 Overview of Vapor Pressure

Reid Vapor Pressure (RVP) measurements provided vapor pressure data, which, in conjunction with gel strength, helped to determine the range of GTL and crude oil blends that can be transported via TAPS. Reid Vapor Pressure, a technique (ASTM method D-323) used to measure vapor pressure, is converted to True Vapor Pressure (TVP) using the API nomograph or an equivalent mathematical equation, given in API publication 2517. RVP measurements are taken at 100°F. True Vapor Pressure is an industry standard, mandated by regulatory agencies such as EPA, and can be determined with commonly available technology. The API conversion to TVP corrects for temperature effect on vapor pressure and for partial vaporization of the sample in the Reid's apparatus. The practice provides the basis for correlating the hydrocarbon content of tank vapors and vapor emissions.

The vapor pressure of a liquid at a particular temperature is the pressure exerted on the liquid by its own vapor at that temperature. If the Net Positive Suction Head (NPSH) of a pump is less than or equal to the vapor pressure of the liquid it is pumping, then the liquid will boil as it enters the pump. The bubbles developed collapse on the pump impeller, resulting in cavitation damage to the impeller. As a result, keeping the vapor pressure of the blend of ANS crude oil and GTL transported through the TAPS below the pipeline's operating pressures at all operating temperatures will reduce unnecessary equipment failure.

Reid Vapor Pressure (RVP), the stabilized pressure exerted by a volume of liquid at 100°F, is related to the True Vapor Pressure (TVP) of the liquid as follows:

$$TVP = RVP \times Exp.(A) \tag{6.1}$$

Where,

$$A = C_o(IRTEMP - ITEMP) \tag{6.2}$$

C_0 is a proportionality constant, the value of which depends on the value of RVP as shown in Table 6.1 below.

$$ITEMP = (555.69^o R)^{-1} \quad 6.3$$

$$IRTEMP = (T_s + 459.69^o R)^{-1} \quad 6.4$$

T_s = The fluid temperature (°F)

Table 6.1. Values of C_o.

RVP	C_o	RVP	C_o	RVP	C_o
0 < RVP < 2	-6622.5	RVP = 5	-6186.5	RVP = 8	-6367.9
2 < RVP < 3	-6439.2	5 < RVP < 6	-6220.4	8 < RVP < 9	-6477.5
RVP = 3	-6255.9	RVP = 6	-6254.3	RVP = 9	-6587.9
3 < RVP < 4	-6212.1	6 < RVP < 7	-6182.1	9 < RVP < 10	-6910.5
4 = RVP	-6169.2	RVP = 7	-6109.8	RVP = 10	-7234.0
4 < RVP < 5	-6177.9	7 < RVP < 8	-6238.9	10 < RVP 15	-8178.0

More accurate values of TVP are obtained by applying the following correction procedure:

$$TVP_{Corrected} = TVP_{Calculated} + C_F \quad 6.5$$

Where the correction factor, C_F is given as follows:

If RVP < 3, then $C_F = 0.04 \times RVP + 0.1$ 6.6

If RVP > 3, then $C_F = Exp(2.3452061 \times Log(RVP) - 4.132622]$ 6.7

Amadi [1] measured the vapor pressures of ANS crude oil, cuts of the Laporte Light GTL sample, and their blends. He concluded that vapor formation during fluid transport through TAPS is not possible, since their vapor pressures are well below the minimum TAPS operating pressure. Thus, the fluids will successfully flow through the TAPS as single-phase (compressed) liquids. Part of this work is aimed at determining if vapor formation is possible during transport of the blends of AKGTL and ANS crude oil through the TAPS.

6.2 Effect of Vapor Pressure on Fluid Transportation

Vapor pressure is a thermodynamic property of a liquid, which, in conjunction with other thermodynamic properties, determines the liquid's emission rate and volatility. The consistency of a liquid's volume and composition is a function of its vapor pressure.

Solid deposition is, to some extent, also dependent on a liquid's vapor pressure. More solids tend to precipitate when a liquid is below its vapor pressure, as a result of changes in the liquid volume and composition.

The limiting factor in pumping liquids with a jet pump is the vapor pressure of the liquid involved; the pressure must be at a level that avoids potential vapor locking of pumps due to cavitation.

6.2.1 Pump Cavitation

Pump cavitation is the dynamic process of gas cavity growth and implosion in a pump. It occurs when there is inadequate Net Positive Suction Head Available (NPSHA); that is, when the total energy in the fluid, expressed as equivalent pressure, is equal to or less than the vapor pressure of the fluid. Cavitation takes place when a fluid in liquid phase vaporizes as it passes through a pump, then quickly returns to liquid state. Bubbles form at the position of lowest pressure at the pump inlet, which is just prior to the fluid being acted upon by the impeller vanes. Once the vapor pockets enter the impeller, the process begins to reverse itself. As the vapor reaches the discharge side of the pump, it is subjected to a high positive pressure, which condenses the vapor back to liquid. The collapse of the vapor bubbles creates destructive micro-jets of liquid strong enough to damage the pump. The compression of the vapor bubbles produces a small shock wave that impacts the impeller surface and pits the metal, creating over time large eroded areas and subsequent failure.

6.2.2 Effects of Cavitation

1. ***Reduction in Pump Capacity***

   Bubble formation decreases the space available for the liquid and thus diminishes pumping capacity. If the bubbles are big enough, the pump "chokes"; that is, the pump

loses all suction, resulting in a total reduction in flow. The unequal and uneven formation and collapse of bubbles causes fluctuations in the flow, and the pumping of liquid occurs in spurts [2].

2. Reduction in the Energy Head

Bubbles are far more compressible than a liquid. The head developed diminishes drastically because of the energy used to increase the velocity of the liquid used to fill up the cavities, as the bubbles collapse.

3. Abnormal Sound and Vibrations

Bubble movement with very high velocities from a low-pressure area to a high-pressure area and the subsequent collapse creates shockwaves, producing abnormal sounds and vibrations.

4. Erosion or Pitting of Pump Parts

Bubble collapse during cavitation takes place at a sonic speed, ejecting destructive micro-jets of extremely high velocity (as high as 1000 m/s) liquid, strong enough to cause extreme erosion of the pump parts, particularly the impellers.

5. Mechanical Deformation

Longer duration of cavitation conditions result in unbalancing (as a result of unequal distribution in bubble formation and collapse) of radial and axial thrusts on the impeller. This unbalancing leads to the following mechanical problems:

a. Bending and deflection of shafts
b. Bearing damage and rubs from radial vibration
c. Damage to thrust bearing
d. Breaking of impeller check-nuts
e. Damage to seals

6. Corrosion

Bubble collapse destroys existing protective layers, making the metal surface vulnerable to chemical attack (corrosion). Thus, even slight cavitation may lead to considerable material damage.

6.3 Reid Vapor Pressure Results

The fluid vapor pressure must be below the pipeline's line pressure to avoid forming vapors in the pipeline and the associated cavitation of centrifugal pumps. The RVP of the ANS crude oil, AKGTL and their blends were measured by Alyeska Pipeline Service Company at their Valdez Analytical Laboratory. The test temperature was 100°F. The RVP values were then converted to true vapor pressures using Equation 6.5 (above). The results are shown in Table 6.2, Figure 6.1 and Figure 6.2.

Table 6.2. Vapor pressure results.

Sample	RVP (psi)	TVP (psi)
ANS Crude Oil	4.63	5.09
25% AKGTL	5.13	5.64
50% AKGTL	5.45	5.99
75% AKGTL	6.03	6.63
AKGTL	7.87	8.66

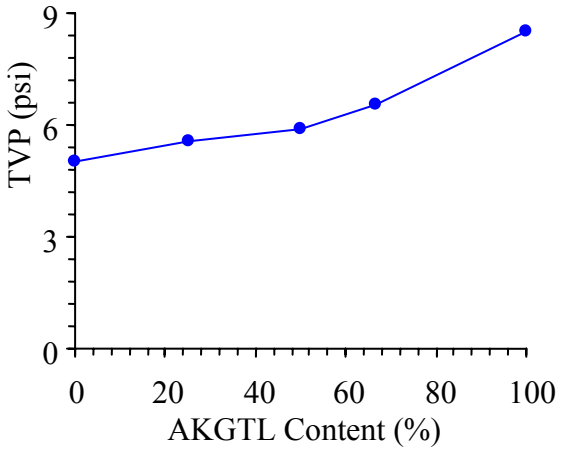

Figure 6.1. Plot of true vapor pressure results.

AKGTL has a vapor pressure of 8.66 psi, as measured in this work. However, its MSDS states that it has a vapor pressure of 5.53 psi (38.1 KPa) -- a difference of about 19.27% between the two results. The vapor pressures of the ANS crude oil and all the blends are less than the vapor pressure of the AKGTL. Thus, all the fluids would flow through the TAPS from inception to discharge as single-phase (compressed) liquids, since the average minimum TAPS operating pressure (Jan. – Oct. 2004) is 175.75 psi. The possibility of vapor formation in the pipeline, and the associated cavitation of centrifugal pumps, is unlikely.

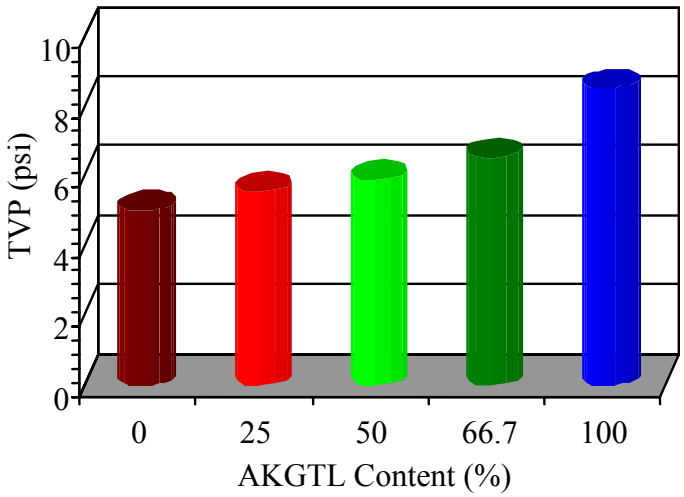

Figure 6.2. A 3-D plot of true vapor pressure results.

Amadi [1] also determined the vapor pressures of the different cuts of the Laporte Light GTL sample (GTL 254, 302 and 344) he used for his work and their blends with ANS crude oil. The results of his study showed that the vapor pressures were well below the minimum TAPS operating pressure. Thus, he also concluded that there is no possibility of vapor formation during the transportation of the blends through the TAPS.

References

1. Amadi, S.: "Experimental Study of Solid Deposition and Vapor Pressure in Gas-to-Liquid and Crude Oil Mixtures for Transportation through the Trans Alaska Pipeline System"; M.S. Thesis, University of Alaska Fairbanks, May, 2003.

2. Sahdev, M.: "Centrifugal Pumps: Basics Concepts of Operation, Maintenance, and Troubleshooting, Part II", The Chemical Engineers' Resource Page, 2003 www.cheresources.com.

CHAPTER 7
SOLIDS DEPOSITION EFFECTS

7.1 Solid Deposition

Solid deposits of wax and/or asphaltene can pose major problems in reservoirs, pipelines and separators, hampering TAPS efficiency and GTL transport economics. This project also examined severity of solids deposition of crude oil/GTL blend mixtures of operations conditions. High Temperature Gas Chromatograph (HTGC) and ASTM distillation apparatus were used for compositional analysis of pipeline wax. Asphaltene particles are known to provide sites for wax crystal buildup, which leads to increased wax deposition. Co-precipitation of asphaltenes and associated resins with wax could result in excessive solids buildup with significantly different properties (hardness); these could in turn adversely affect pipeline operation. Static asphaltene precipitation tests and total wax precipitation tests at varying temperatures were conducted to study the effect of asphaltene on wax deposition. Total precipitated solids (wax and asphaltene) were determined by low temperature centrifuge. Additionally, GTL presence was expected to alter the wax deposition characteristics of the crude oil in TAPS. Wax appearance temperatures for GTL and GTL-crude oil blends at atmospheric and typical TAPS operating pressures were determined under static conditions. The instability of the crude oil for asphaltene deposition was determined using flocculation onset titration on crude oil and its blends using n-heptane as a precipitant. In addition, some flocculation onset titration tests were conducted on crude oil using GTL as a precipitant.

Pressure, temperature, fluid composition, flow characteristics (turbulent or laminar) and geometry of the flow conduit are the key factors that affect solid deposition. Solid deposition causes reduction in effective pipe diameter, which means reduction in the line fill of the pipeline. It also causes increased pressure losses in the pipeline, malfunction of pipeline instrumentation, and contamination of the transported fluid. Waxes and asphaltenes are the solid deposition problems associated with transporting blends of ANS crude oil and GTL through the TAPS.

Asphaltenes

Asphaltenes are a class of compounds in crude oil defined as being insoluble in n-heptane but soluble in aromatic solvents such as toluene [1]. They are large molecules consisting of

polyaromatic and heterocyclic aromatic rings. Asphaltenes carry the bulk of the inorganic components of crude oil, including sulfur and nitrogen, and metals such as nickel and vanadium. These are also the components of crude oil that cause its characteristic black color [1].

Every crude oil contains a certain amount of asphaltene [1]. In crude oil, the asphaltenes tend to attract each other to form agglomerates. The literature reports that naturally occurring resins stabilize asphaltene particles in crude oils by forming repulsive layers around the asphaltene particles [2]. If the resin concentration is insufficient to cover the surface of the asphaltene particles, perhaps due to a decrease in temperature, pressure or pH, then the asphaltenes will precipitate out of the solution.

Changes in the composition of the crude oil, such as addition of solvents, partially dissolve the resin molecules that cover the surface of the asphaltenes and disrupt the resin-asphaltene system, leading to the flocculation of asphaltenes.

A study by Hirschberg et al.[2] showed that pressure affects asphaltene flocculation. The study further concluded that asphaltene solubility in a crude oil is minimal at the oil's bubble point pressure. That is, the maximum amount of asphaltenes is deposited at the bubble point pressure of the crude oil. Thawer et al.[3] attributed this phenomenon to the differences in the compressibilities of the lighter ends and the heavier components of the crude oil. As crude oil approaches its bubble point pressure, the relative volume fraction of the lighter ends within the oil increases. This phenomenon is similar to adding a light hydrocarbon to the crude oil. The result is asphaltene depeptization. Above the bubble point, the low-molecular-weight alkanes are released from the liquid into the gas phase. The tendency for asphaltene depeptization in the crude oil is therefore reduced. Asphaltene stability/instability is illustrated in Figure 7.1.

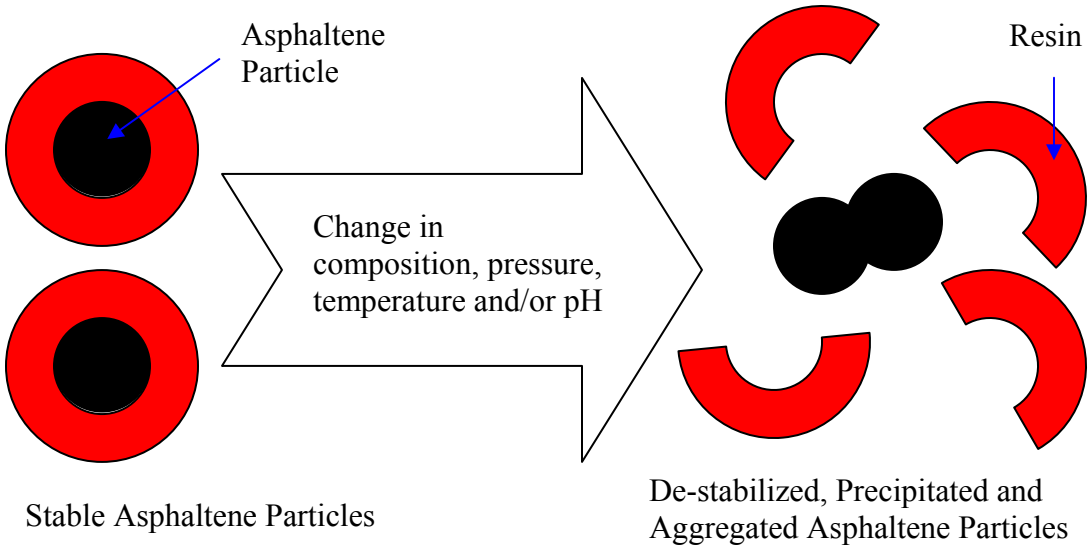

Figure 7.1. Graphical illustration of asphaltene stability/instability.

Rogel et al.[4] have shown that the amount of non-solvent (such as n-heptane) required for the onset of asphaltene flocculation in a crude oil is a measure of the stability of the asphaltenes in the oil . The more stable the asphaltenes, the higher the amount of solvent required for flocculation onset. Similarly, the amount of asphaltenes precipitated from a particular crude oil depends on how stable the asphaltenes are in that oil, as well as the type and amount of precipitating agent added. According to Amadi [5], asphaltenes are stable in pure ANS crude oil. However, all the cuts of Laporte Light GTL sample used in Amadi's studies (at atmospheric pressure) precipitated significant amounts of asphaltenes from the crude oil. As noted in Chapter 1, one objective of this study was to determine the amount of asphaltenes AKGTL will precipitate from the TAPS crude oil.

Asphaltenes dispersed in crude oil are electrically charged and have diameters of 30 – 40 Angstroms [6]. On the other hand, the mean size of asphaltene aggregates ranges from 4.5 to 291 μm [7]. The molecular structure of asphaltenes is not precisely known because they are not crystallized and cannot be separated into individual components or narrow fractions. However, chemists have proposed some possible structures for some crude oils. One of these is shown in Figure 7.2.

Little is currently known of the chemical properties of asphaltenes. Asphaltenes are lyophilic with respect to aromatics, in which they form highly scattered colloidal solutions. Also, asphaltenes of low molecular weight are lyophobic with respect to paraffins like pentanes and petroleum crude. There is a close relationship between asphaltenes, resins, and high molecular weight polycyclic hydrocarbons. Researchers theorize that in nature asphaltenes form as a result of oxidation of natural resins.

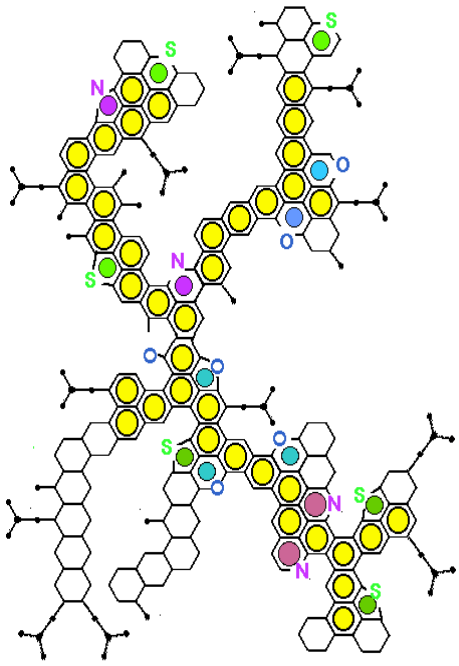

Figure 7.2. Molecular structure of asphaltene proposed for Maya crude (Mexico) (source: http://tigger.uic.edu/~mansoori/Asphaltene.Molecule_html).

In contrast, hydrogenation of asphaltic compound products containing neutral resins and asphaltene produces heavy hydrocarbon oils; that is, neutral resins and asphaltenes are hydrogenated into polycyclic aromatic or hydro-aromatic hydrocarbons. They differ, however, from polycyclic aromatic hydrocarbons by the presence of oxygen and sulfur in varied amounts.

On heating above 300 - 400^{o}C, asphaltenes do not melt, but decompose, forming carbon and volatile products. They react with sulfuric acid, forming sulfonic acids, as might be expected on the basis of the poly-aromatic structure of these components.

Wax

A wax is an organic, plastic substance solid below a certain temperature, called the Wax Appearance Temperature (WAT), and it becomes liquid when heated above the WAT. Waxes are thermoplastic, combustible and insoluble in water. The WAT is the temperature at which the first smallest amount of wax appears.

Although petroleum waxes are of three general categories - paraffin, microcrystalline and petrolatum, the major constituent is paraffin. Paraffin waxes contain predominantly straight-chain hydrocarbons with an average chain length of 20 to 30 carbon atoms. However, the presence of other hydrocarbon structures in paraffin waxes makes it a complex mixture. Generally, paraffin waxes are non-reactive, non-toxic, and colorless. Figure 7.3 shows structures of typical paraffin waxes.

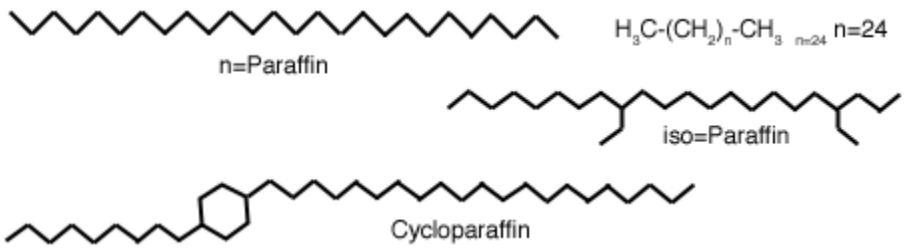

Figure 7.3. Typical structures of paraffin waxes.

Pressure has a significant effect on the temperature at which wax appears in crude oils. The works of Weingarten et al.,[8] and Brown et al.,[9] showed that the WAT decreases as pressure increases. However, using a thermodynamic model, Pan et al.,[10] inferred that a decrease in WAT is only pronounced at pressures below the bubble point pressure of the crude oil, and that above the bubble point pressure, WAT generally increases with pressure.

Wax in a petroleum pipeline adheres to the pipe walls and, as a result, reduces the pipe flow diameter. Some consequences are decreased flow rate, higher-pressure requirements, and general equipment malfunction. According to Amadi [5], wax formation during transport of blends of LaPorte GTL cuts and TAPS crude oil is not possible because the WAT for all the blends

reported in his study are well below TAPS minimum operating temperature. Part of this work is to determine the wax precipitation and WAT of TAPS crude oil, AKGTL and their blends under static condition. These results can offer some predictions regarding the possibility of wax formation during transport of the blends (of AKGTL and ANS crude oil) through the TAPS.

7.2 Procedure for Determining Asphaltene Stability in TAPS Crude Oil

A useful way to evaluate the relative stability of asphaltenes in a crude oil is to determine the asphaltenes' flocculation onset when adding a non-solvent to the oil [4]. Amadi [5] extensively discusses this test procedure. Brookfield Viscometer Standard Calibration Fluids 10 and 100 were used to calibrate the Cannon-Fenske viscometer before the actual tests were performed. The tests were performed at atmospheric pressure.

Blends of TAPS crude oil and toluene were used for this test. The procedure involved measuring the effluent time required for the sample to flow freely from mark "C" to mark "E" of the Cannon-Fennske viscometer (see Figure 2.9). For each test, 0.05 ml of n-heptane was titrated into the sample. After appropriate mixing, the efflux time was measured accurately.

At the end of the data acquisition, a plot of square of efflux time versus volume of n-heptane titrated was prepared for each blend (of TAPS crude oil and toluene). Initially, the efflux time decreased linearly with increase in the volume of n-heptane titrated. However, at the asphaltene flocculation point, the plot deviated from the straight line. To finally determine the stability (or otherwise) of the asphaltene in TAPS crude oil, the titrated volume of n-heptane at the onset of asphaltene flocculation was plotted against the concentration of toluene in the test fluid. A positive intercept of this plot on the ordinate indicates stability of asphaltenes in TAPS crude oil. Otherwise, the asphaltenes are reported unstable in this mixture.

7.3 Test Result of Stability of Asphaltenes in ANS Crude Oil

The aim of the performing an asphaltene stability test in ANS crude oil is to determine if asphaltenes are actually stable in the pure ANS crude oil. If the asphaltenes were stable in the pure ANS crude oil, then any instability after the addition of AKGTL would confirm that the AKGTL is a flocculant in ANS crude oil mixtures. Figures 7.4-7.6 are plots of viscosity for

toluene-diluted ANS crude oil against a titrated volume of n-heptane. As the n-heptane was gradually titrated into the solution, the viscosity (efflux time) decreased linearly. A deviation from this straight line appeared at the asphaltene flocculation onset point. Again, this deviation is a result of the presence of solids (flocculated asphaltenes) in the solution.

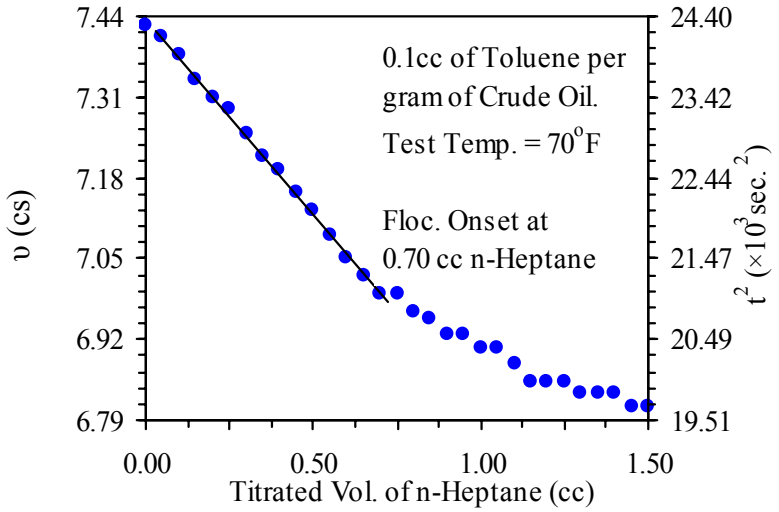

Figure 7.4. Asphaltene flocculation onset: 0.1 cc toluene per gram of ANS crude oil.

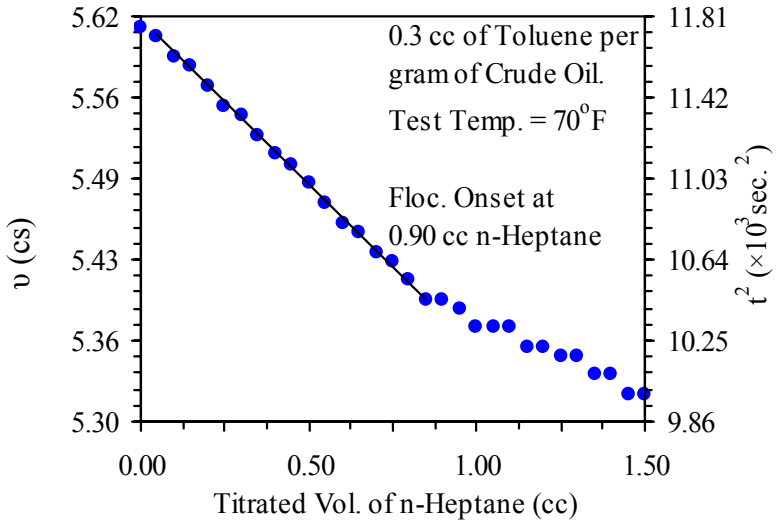

Figure 7.5. Asphaltene flocculation onset: 0.3 cc toluene per gram of ANS crude oil.

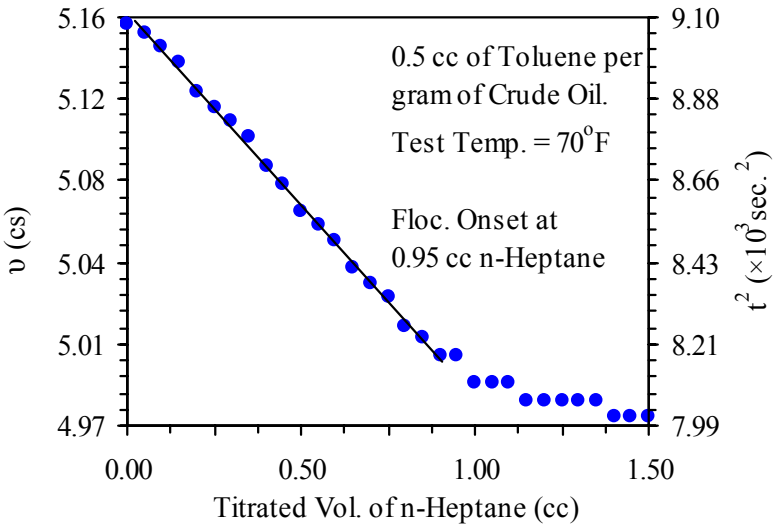

Figure 7.6. Asphaltene flocculation onset: 0.5 cc toluene per gram of ANS crude oil.

Stability test results are summarized in Table 7.1 and in Figure 7.7. Figure 7.7, a plot of titrated volume of n-heptane at asphaltene flocculation onset against volume of toluene per gram of crude oil in the solution, is linear with a positive intercept on the ordinate. What this means is that a certain amount of precipitant is required to initiate asphaltene flocculation in the pure undiluted ANS crude oil. Therefore, asphaltenes are stable in the pure ANS crude oil, implying that AKGTL was solely responsible for the flocculated 2.42kg of asphaltenes per barrel (1.522 g/ 100 ml) of ANS crude oil.

Table 7.1. Asphaltene stability test results.

cc toluene per gm of ANS crude oil	flocculation onset point (cc of n-heptane per gram of crude oil)
0.1	0.70
0.3	0.90
0.5	0.95

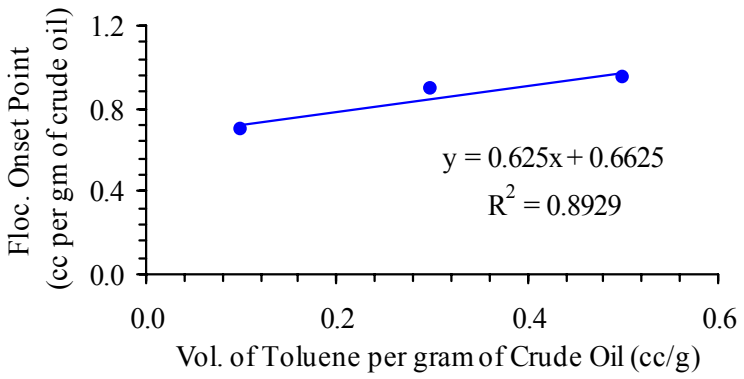

Figure 7.7. Plot of asphaltene stability in ANS crude oil.

Amadi [5] also investigated the stability of asphaltenes in pure ANS crude oil and concluded that the asphaltenes are stable in the crude oil.

7.4 Procedure for Asphaltene Flocculation Onset

The asphaltene flocculation onset and the asphaltene stability tests are based on the same principle: increase in fluid viscosity associated with the precipitation of solids in the fluid. However, since the aim of this test was to determine the minimum amount of precipitant that will initiate asphaltene flocculation in the crude oil, pure TAPS crude oil was used in the test, as opposed to the blends of TAPS crude oil and toluene used in the stability test.

The test was performed using the Brookfield LVDV-II+ viscometer. The sample holder was the Small Sample Adapter used for gel strength measurements while the spindle was the SC18 Spindle (see Figure 2.5). Test temperature and pressure were atmospheric. The spindle speed was set to give the maximum possible torque to avoid reducing the torque below 10% during the test. WinGather software was set to automatically record data every 75 seconds. During each of these intervals, 0.05 cc of the precipitant (AKGTL, n-pentane, or n-heptane) was added to the test fluid. After data acquisition, a plot of sample viscosity versus titrated volume of precipitant was prepared. Initially, the viscosity of the test fluid decreased linearly as the precipitant was added. However, at the asphaltene flocculation onset point, a deviation from this straight line appeared as a result of the presence of solids.

7.5 Test Result of Onset of Asphaltene Flocculation in ANS Crude Oil

Asphaltene flocculation onset is very important in identifying the best blend ratio of ANS crude oil and AKGTL to be pumped through the TAPS. Figure 7.8 is a typical graph used to obtain the onset of asphaltene flocculation in the ANS crude oil. The rest of the graphs are in Appendix C. As the precipitant was gradually added to the sample, its viscosity decreased linearly. However, deviation from this linear profile started at the onset of asphaltene flocculation. The change in the viscosity profile is a result of change in the rheological behavior of the fluid due to the presence of solids (asphaltenes).

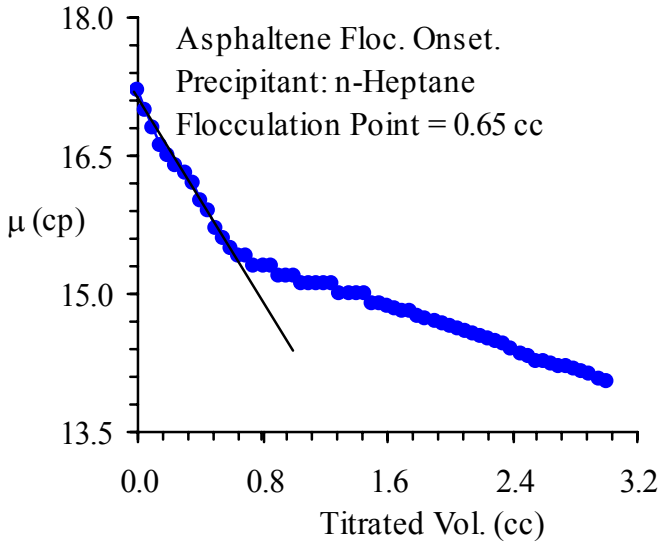

Figure 7.8. Typical asphaltene flocculation onset graph (test condition = atmospheric)

The asphaltene flocculation onset results are shown in Table 7.2 and Figure 7.9. Asphaltene flocculation started when 0.3 cc of AKGTL was added to 5 cc of ANS crude oil. This means that asphaltene flocculation will occur in a blend containing as little as 5.7% of AKGTL. Thus, the AKGTL is a very strong asphaltene precipitant. Asphaltene flocculation started when 0.40 and 0.65 cc, respectively, of n-pentane and n-heptane were titrated. Toluene is a solvent for asphaltenes and, as expected, did not precipitate any asphaltenes from the crude oil.

Table 7.2 Asphaltene flocculation onset results

Flocculation	Flocculation Point (cc)
Toluene	Nil.
AKGTL	0.30
n-Pentane	0.40
n-Heptane	0.65

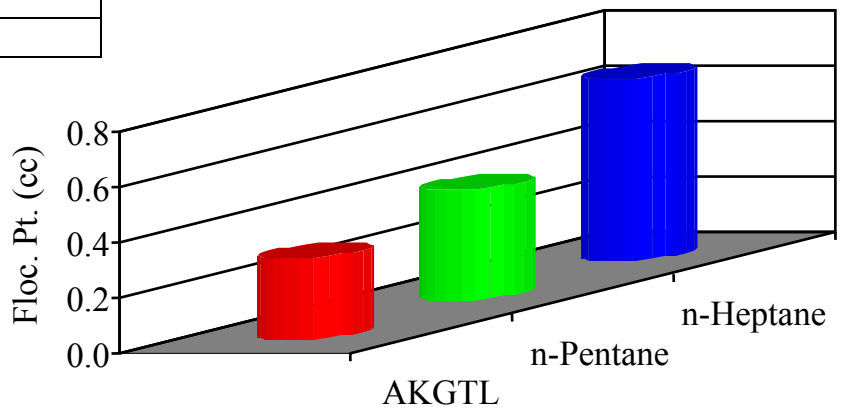

Figure 7.9. Asphaltene flocculation onset results (test condition = atmospheric).

7.6 Result of Static Asphaltene Deposition Test on AKGTL

Three precipitants (AKGTL, n-heptane and n-pentane) were used in the static asphaltene deposition tests. The results are shown in Table 7.3 and in Figure 7.10. Figure 7.11 is a picture of dried asphaltenes deposited on a 0.22 micron filter paper.

Table 7.3. Static asphaltene deposition results.

Precipitant	Amount of Precipitated Asphaltenes (g/100ml)
n-Heptane	0.988
n-Pentane	1.4165
AKGTL	1.522

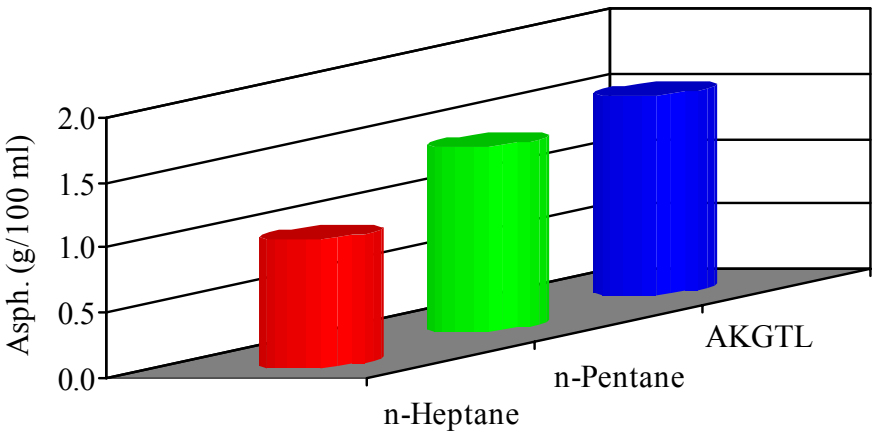

Figure 7.10. Static asphaltene deposition results.

Figure 7.11. Dried asphaltenes on a filter paper.

Based on the findings summarized in Table 7.3, the amount of asphaltenes precipitated by AKGTL is more than that precipitated by n-pentane, which in turn is more than that precipitated by n-heptane. This suggests that the AKGTL has more n-alkanes, which have shorter carbon chains than the other two precipitants, because the amount of precipitated asphaltenes decreases as the carbon number of the n-alkane precipitant increases. Actually, 1.522 gm of precipitated asphaltenes per 100 ml (that is 2.42 kg/ bbl) of ANS crude oil is very significant.

7.7 Static Wax Appearance Temperature (WAT) Test

Two techniques were employed in this test. The Arrhenius principle for the viscosity-temperature relationship of Newtonian fluids is the basis of the first method, which was performed with the Brookfield cone/plate viscometer. The second method, ASTM D3117, the standard ASTM method for determining WAT, is based on visual identification of the smallest visible wax in the sample and was performed with the Koehler apparatus (see Figure 2.14).

The Arrhenius principle states that the viscosity of a Newtonian fluid is an exponential function of temperature [11]. The equation is given by:

$$\mu = A \times Exp\left(\frac{B}{T}\right) \tag{7.1}$$

Where,

$$B = \frac{E_a}{R} \tag{7.2}$$

μ = viscosity (mPa × Sec.); A = Materials constant (mPas × Sec.);
R = Gas constant (J/mol × Kelvin); T = Absolute temperature (Kelvin)

In linear form, the equation is written as:

$$\log \mu = \log A + B\left(\frac{1}{T}\right) \tag{7.3}$$

Equation 7.3, shows that a logarithm plot of a Newtonian fluid's viscosity against the reciprocal of its absolute temperature is a straight line. A deviation from this straight line signifies that the fluid has become non-Newtonian. Therefore, for a Newtonian and waxy fluid that is cooled gradually, wax precipitation at the WAT would cause the fluid to become non-Newtonian and thus cause a deviation from the Arrhenius straight line. Note that the rheological behavior of a fluid with solid suspensions, such as suspensions of wax or asphaltenes, is generally non-Newtonian.

The viscosity-based procedure for determining WAT was adequately described by Amadi [5]. For each sample, a plot of log of viscosity and reciprocal of absolute temperature was prepared and the WAT appropriately identified on the plot.

The Koehler apparatus for determining WAT by the ASTM D3117 technique appears in Figure 2.14 and is described in Section 2.10. Since the method is based on visual identification of the smallest visible wax in the sample, only the AKGTL sample was used for this test, because all the other samples are opaque. Amadi [5] described this test in greater detail.

7.7.1 Result of Static WAT Test

Wax is an inevitable occurrence in TAPS operation; temperatures typical of an arctic environment are conducive to wax formation. Wax crystals change the flow behavior of crude oil from Newtonian to non-Newtonian, thus increasing the viscosity [12]. Viscosity changes are due to the formation of crystals in suspension, and a non-Newtonian behavior with decreasing temperature is observed based on the Arrhenius principle [13] for obtaining WAT under static conditions. The WAT is indicated by a deviation from linearity on a plot of Log of Viscosity ($\ln \eta$) versus the inverse of temperature in degrees Kelvin ($1/T$). This method was verified using the TAPS crude mix (Figure 7.12) as a bench mark. The WAT was observed to occur at a temperature of 21.7°C, which is consistent with the WAT results for TAPS crude mix as determined by Alyeska Pipeline Service Company (Table 7.4). Also, Roehner [14] observed a similar plot (Figure 7.13).

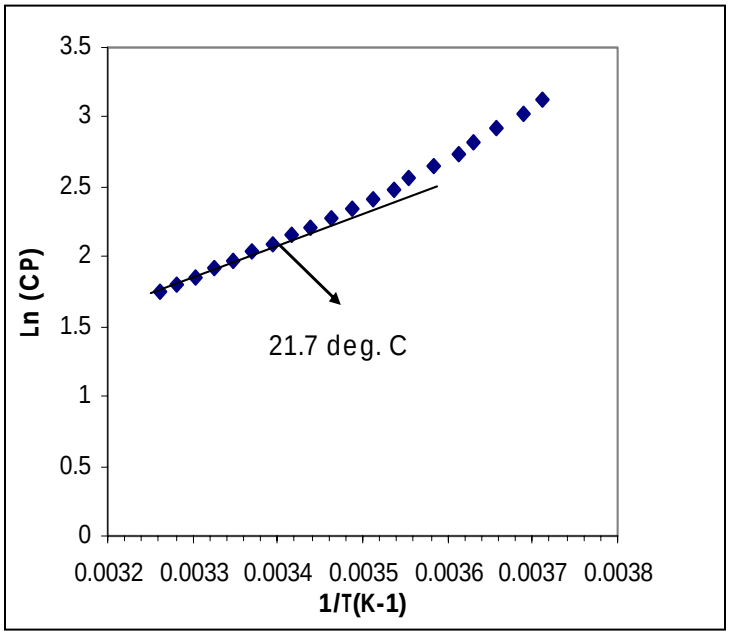

Figure 7.12. WAT for 100% TAPS crude oil.

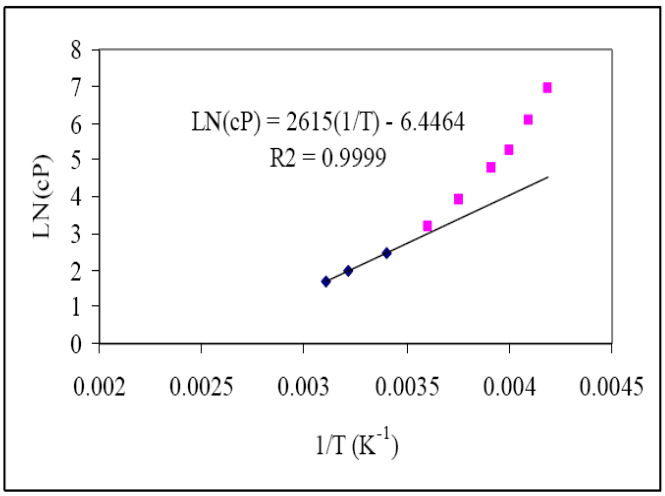

Figure 7.13. TAPS crude oil mix -Arrhenius fit of viscosity and temperature data [14].

Table 7.4. WAT results From Alyeska Pipeline Service Company [15].

Year	**2003**	**2004**	**2005**
WAT (^{o}C)	22.22	21.73	19.53

However, the WAT trend observed for both binary and ternary samples (Figure 7.14) implies that the fluid composition significantly influences WAT. GTL products can be classified as saturates (long chain paraffins) that promote wax appearance [15]; in addition, the paraffin content of a hydrocarbon determines that fluid's wax-forming tendency (www.hw.ac.uk). These results suggest that for all tested samples, a higher concentration of GTL products in the ternary blends increased the WAT (Figure 7.14), and the highest WAT values were observed in very high concentrations of SynWestSak crude (100% SynWestSak and SynWestSak/TAPS mix blend 4:1, supplied by the Alyeska Pipeline Service Company). This suggests that AKGTL has a strong affinity for wax, which will encourage wax deposition when mixed with another fluid of known properties.

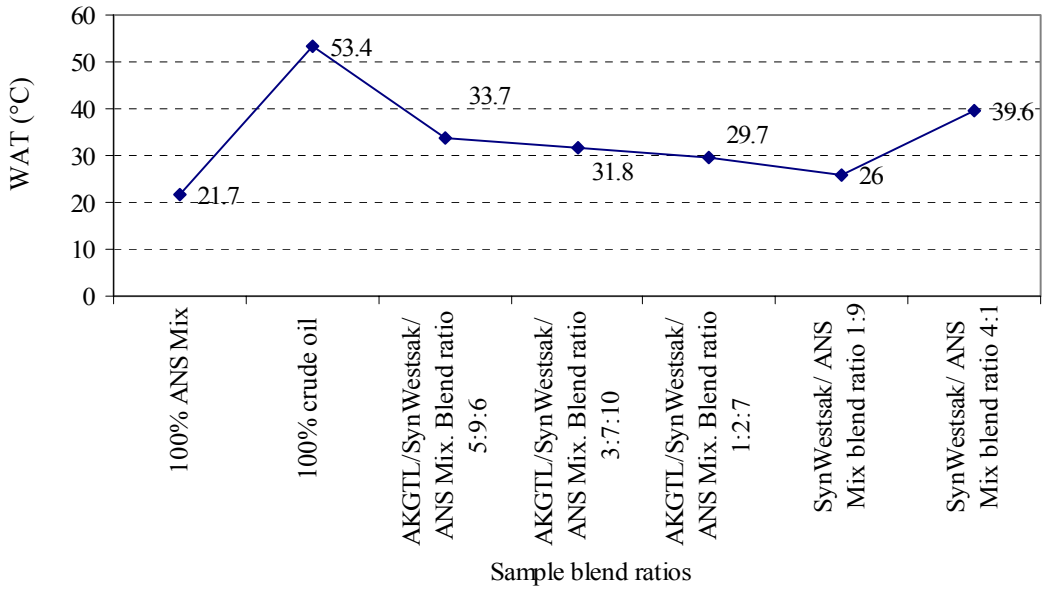

Figure 7.14. Composite plot of WAT for various blend ratios.

References

1. Lorimer, S. E. and Ellison, B. T.: "Design Guidelines for Subsea Oil Systems"; Facilities 2000: Facilities Engineering into the Next Millennium; Shell Deepwater Development Inc.; 2000.

2. Hirschberg, A.; deJong, L. N. J.; Schipper, B. A.; and Meijer, J. G.: "Influence of Temperature and Pressure on Asphaltene Flocculation"; SPE Paper Number 11202 Presented at the 1982 SPE Annual Technical Conference and Exhibition, New Orleans; Sept. 26 - 29, 1984.

3. Thawer, R.; Nicoll, D. C. A.; and Dick, G.: "Asphaltene Deposition in Production Facilities"; SPE Paper Number 18473 Presented at the 1989 SPE International Symposium on Oilfield Chemistry; Houston, 8 – 10 February, 1990.

4. Rogel, E.; Leon, O.; Espidel, Y.; and Gonzalez, Y.: "Asphaltene Stability in Crude Oils"; SPE Paper No. 53998 (Revised in SPE Paper No. 72050) Presented at the 1999 SPE Latin America and Caribbean Petroleum Engineering Conference, Caracas: 21 – 23 April, 1999.

5. Amadi, S.: "Experimental Study of Solid Deposition and Vapor Pressure in Gas-to-Liquid and Crude Oil Mixtures for Transportation through the Trans Alaska Pipeline System"; M.S. Thesis, University of Alaska Fairbanks, May, 2003.

6. Escobedo, J. and Mansoori, G. A.: "Asphaltene and Other Heavy-Organic Deposition during Transfer and Production Operations"; SPE Paper No. 30672 Presented at the 1995 SPE Annual Technical Conference and Exhibition, Dallas; 22 – 25 Oct., 1995.

7. Ferworn, K. A.; Mehrotra, A. K.; and Svrcek, W. Y: "Measurement of Asphaltene Particle Size Distributions in Crude Oils Diluted with n-Heptane"; Industrial and Engineering Chemistry Research, Vol. 32, No. 5, pp 955 – 959; May 1993.

8. Weingarten, J. S., and Euchner, J.A.: "Method for Predicting Wax Precipitation and Deposition"; SPE Paper Number 15654 Presented at the 1986 (Oct. 5 – 8) SPE Annual Technical Conference and Exhibition, New Orleans; Feb. 1988.

9. Brown, T. S.; Niesen, V. G.; and Erickson, D. D.: "The Effects of Light Ends and High Pressure on Paraffin Formation"; SPE Paper Number 28505 Presented at the SPE 69th Technical Conference and Exhibition; New Orleans, Louisiana; 25 – 28 September, 1994.

10. Pan, H.; Firoozabadi, A.; and Fotland, P.: "Pressure and Composition Effect on Wax Precipitation: Experimental Data and Model Results"; SPE Paper Number 36740 Presented at the 1996 SPE Technical Conference and Exhibition, Denver; 6 – 9 Oct., 1996.

11. Hamouda, A. A. and Viken, B. K.: "Wax Deposition Mechanism under High-Pressure and in Presence of Light Hydrocarbons"; SPE Paper Number 25189 Presented at the International Symposium on Oil Field Chemistry, New Orleans; 2 – 5 March, 1993

12. Leonataritis, Kosta, John D Leontritis.; "Cloud Point and Wax Determinantion measurement Techniques," SPE 80267 presented at SPE Houston Texas, USA. 5-7 February, 2003

13. Coutinho, Joao A.P. Jean-Luc Daridon. "The Limitation of Cloud Point Measurement Techniques and the Influence of Oil Composition on it's deposition"

14. Roehner, Richard. "Impact of Radial Temperature Profilrd on the initial Flow Restart in Pipelines transporting Intermediate and Parrafinic Type Crude Oils". A power point presentation, University of Utah. 2002.

15. Chukwu, Felicia. Integrity Management Engineering, Alyeska Pipeline Service Company. 2006.

CHAPTER 8
CONCLUSIONS AND RECOMMENDATIONS

8.1 Conclusions

Based on the experimental and simulation study conducted in this project, the following main conclusions are drawn.

Gel strengths are reduced as the percentage of GTL in the crude oil-GTL mixture increases, even at a low temperature of -20°F. This therefore is favorable to pipeline re-start conditions after an extended shut down at temperatures down to -20°F (cold re-start conditions).

The addition of AKGTL to ANS crude oil significantly affected the properties of the resulting fluid, causing reductions in density and viscosity.

The trend of both density (see Figure 4.1) as well as viscosity reduction (see tables 4.4- 4.7) as a function of increasing temperature is clearly evident for all tested sample blends.

From the rheological analysis conducted in this study;

i. AKGTL shows pseudoplastic behavior at all temperatures in the given temperature range (50°C to -20°C).
ii. Crude Oil shows Newtonian behavior at temperatures 20°C and above, and shows Bingham plastic behavior below 20°C.
iii. Blends of AKGTL and crude oil show pseudoplastic behavior at higher temperatures (above room temperature), Newtonian at intermediate temperatures (around room temperature) and Bingham plastic behavior at lower temperatures (near 0° and below) in the given temperature range.

This Bingham plastic flow characteristic indicates that high pumping power requirements are necessary to re-start the pipeline after extended shut down at low temperatures.

The vapor pressure increased with addition of AKGTL, but the values are below the minimum TAPS operating pressure, ensuring a liquid-only flow of the blends. Also, the bubble point

pressure results showed that the blends would flow through the TAPS as compressed liquids from inception to discharge. Therefore, vapor formation in the pipeline as the blends are transported is not likely.

From the phase behavior studies conducted in this work, it is clear that the addition of GTL (AKGTL and cuts of LaPorte GTL) to ANS crude oil under current TAPS operating conditions does not pose a problem related to multi-phase flow. Considering the low TAPS operating temperature and high flow pressure, this study suggests that if GTL were to flow through TAPS in either batch mode or as a commingled mixture, under current TAPS operating conditions, the fluid will always exist as a single phase liquid throughout the pipeline.

It is possible that the composition of the GTL samples (AKGTL and LaPorte GTL samples) used in this work may not be the same as the representative GTL that will be ultimately transported through TAPS; however the prediction model evaluated under this study could be used for determining the properties of another type of GTL that would flow through the TAPS.

Experiment results were used to model the equation of state for predicting the phase properties of the GTL and crude oil blends. Comparative results indicate that the Soave-Redlich-Kwong or The Peng-Robinson equations of state should be used for predicting phase properties.

Currently, asphaltene flocculation and deposition is a major problem in transporting blends through the TAPS. Asphaltenes are stable in pure TAPS crude oil, but adding AKGTL disrupts this stability, causing significant amounts of asphaltene precipitation from the crude oil. Asphaltene flocculation occurred in a blend containing as little as 5.7% by volume of AKGTL. Mitigation of solids deposition remains the primary challenge before a commingled mode of transportation can be used.

Wax deposition is inherent based on the wax appearance temperature (WAT) results obtained from analyzing various TAPS crude oil/AKGTL blend ratios. The WAT increased (higher temperature) with increasing concentrations of AKGTL in ANS crude oil (see Figure 7.14).

Blending TAPS crude oil with AKGTL or with cuts of the Laporte Light GTL sample offered the same trend of results (reduction in density, viscosity, gel strength, bubble point pressure, and WAT). Both options also led to significant amounts of asphaltene precipitation from the crude oil. Again, a method for mitigating solids deposition remains the primary challenge of using a commingled mode of transportation.

8.2 Recommendations for Future Work

The AKGTL is a very strong asphaltene precipitant and asphaltenes are very undesirable. Since asphaltene precipitation is not a confirmed reversible process, it is highly recommended that a study of asphaltene stabilizers, such as dodecylbenzene sulphonic acid (DBSA), be performed. Such stabilizers, added at pre-determined points along the TAPS during the transportation of blends through the pipeline may act in a similar way to the resins, peptizing the asphaltenes and keeping them in solution.

A study of solid deposition of GTL/ANS crude oil mixtures under dynamic conditions should be performed. A study of the rate of deposition of these solids in the fluid main stream and along the walls of the pipeline will help to understand the true behavior of such mixtures for practical considerations.

The detailed chemical compositions of the blends need to be established through qualitative chemical analyses. The chemical compositions of the blends would be input for a proper evaluation of the effect of composition on the effectiveness of different commercial asphaltene inhibitors on the blends. This will enhance adequate selection of asphaltene inhibitors.

While GTL technology may be an available means of recovering and transporting Alaska's heavy oil resources, a feasibilty study and flow characterization of blends of AKGTL and ANS heavy oil through the TAPS is crucial, and its results can be further evaluated for economic viability compared to other technologies in place.

REFERENCES

1995 Assessment of United States Oil and Gas Resources," US Geological Survey, Circular No. 1118, (1995).

Akwukwaegbu, C.F. "Evaluation of the Modes of Transporting GTL Products Through the Trans Alaska Pipeline System (TAPS)", M.S. Thesis, University of Alaska Fairbanks, May 2001.

Amadi, S. "Experimental Study of Solid Deposition and Vapor Pressure in Gas-to-Liquid and Crude Oil Mixtures for Transportation through the Trans Alaska Pipeline System"; M.S. Thesis, University of Alaska Fairbanks, May, 2003.

Brown, T. S.; Niesen, V. G.; and Erickson, D. D.: "The Effects of Light Ends and High Pressure on Paraffin Formation"; SPE Paper Number 28505 Presented at the SPE 69th Technical Conference and Exhibition; New Orleans, Louisiana; 25 – 28 September, 1994.

Chukwu, Felicia. Integrity Management Engineering, Alyeska Pipeline Service Company. 2006.

Coutinho, Joao A.P. Jean-Luc Daridon. "The Limitation of Cloud Point Measurement Techniques and the Influence of Oil Composition on its deposition". In *Petroleum Science and Technology,* Volume 23, Number 9-10/2005: 1113-1128. Published by Taylor & Francis (ISSN1091-6466) DOI10.1081/LFT-200035541.

Escobedo, J. and Mansoori, G. A.: "Asphaltene and Other Heavy-Organic Deposition during Transfer and Production Operations"; SPE Paper No. 30672 Presented at the 1995 SPE Annual Technical Conference and Exhibition, Dallas; 22 – 25 Oct., 1995.

Ferworn, K. A.; Mehrotra, A. K.; and Svrcek, W. Y: "Measurement of Asphaltene Particle Size Distributions in Crude Oils Diluted with n-Heptane"; Industrial and Engineering Chemistry Research, Vol. 32, No. 5, pp 955 – 959; May 1993.

Hamouda, A. A. and Viken, B. K.: "Wax Deposition Mechanism under High-Pressure and in Presence of Light Hydrocarbons"; SPE Paper Number 25189 Presented at the International Symposium on Oil Field Chemistry, New Orleans; 2 – 5 March, 1993.

Hirschberg, A.; deJong, L. N. J.; Schipper, B. A.; and Meijer, J. G.: "Influence of Temperature and Pressure on Asphaltene Flocculation"; SPE Paper Number 11202 Presented at the 1982 SPE Annual Technical Conference and Exhibition, New Orleans; Sept. 26 - 29, 1984.

Leonataritis, Kosta, John D Leontritis.; "Cloud Point and Wax Determinantion Measurement Techniques," SPE 80267 presented at SPE Houston Texas, USA. 5-7 February, 2003.

Lorimer, S. E. and Ellison, B. T.: "Design Guidelines for Subsea Oil Systems"; Facilities 2000: Facilities Engineering into the Next Millennium; Shell Deepwater Development Inc.; 2000.

"Natural Gas 1994: Issues and Trends," prepared under the direction of Diane W. Lique by multiple authors. DOE/EIA-0560(94) (July 1994).

Pan, H.; Firoozabadi, A.; and Fotland, P.: "Pressure and Composition Effect on Wax Precipitation: Experimental Data and Model Results"; SPE Paper Number 36740 Presented at the 1996 SPE Technical Conference and Exhibition, Denver; 6 – 9 Oct., 1996.

Perkins, T. K. and Turner, J. B.: "Starting Behavior of Gathering Lines and Pipeline Filled with Gelled Prudhoe Bay Oil"; SPE Paper No. 2997 Presented at the SPE 45th Annual Fall Meeting, Houston; 4 – 7 October 1971.

Ramakrishnan, H. “Experimental and Economic Evaluation of GTL Fluid Flow Properties and Effect on TAPS”, M.S. Thesis, University of Alaska Fairbanks, December 2000.

Robertson, E.P., Thomas, C.P., and Avellanet, R.A. “Economics of Alaska North Slope Gas Utilization Options,” A paper presented at the SPE Western regional Meeting, Anchorage AK, (May 1996).

Rogel, E.; Leon, O.; Espidel, Y.; and Gonzalez, Y.: “Asphaltene Stability in Crude Oils”; SPE Paper No. 53998 (Revised in SPE Paper No. 72050). Presented at the 1999 SPE Latin America and Caribbean Petroleum Engineering Conference, Caracas: 21 – 23 April, 1999.

Roehner, Richard. “Impact of Radial Temperature Profilrd on the initial Flow Restart in Pipelines transporting Intermediate and Parrafinic Type Crude Oils”. A power point presentation, University of Utah. 2002.

Sharma, A. “Phase Behavior Analysis of Gas-To-Liquid (GTL) Products for Transportation through the Trans Alaska Pipeline System”; M.S. Thesis, University of Alaska Fairbanks, August 2003.

Sahdev, M.: “Centrifugal Pumps: Basics Concepts of Operation, Maintenance, and Troubleshooting, Part II”, The Chemical Engineers’ Resource Page, 2003 www.cheresources.com.

Timmcke, M. D: “Rapid Evaluation of the Gel Strength of GTL Products during Prolonged Trans-Alaska Pipeline Shutdown”; M.S. Thesis, University of Alaska Fairbanks, December, 2002.

Thawer, R.; Nicoll, D. C. A.; and Dick, G.: “Asphaltene Deposition in Production Facilities”; SPE Paper Number 18473 Presented at the 1989 SPE International Symposium on Oilfield Chemistry; Houston, 8 – 10 February, 1990.

Weingarten, J. S., and Euchner, J.A.: “Method for Predicting Wax Precipitation and Deposition”;SPE Paper Number 15654 Presented at the 1986 (Oct. 5 – 8) SPE Annual Technical Conference and Exhibition, New Orleans; Feb. 1988.

APPENDIX A

GEL STRENGTH PLOTS

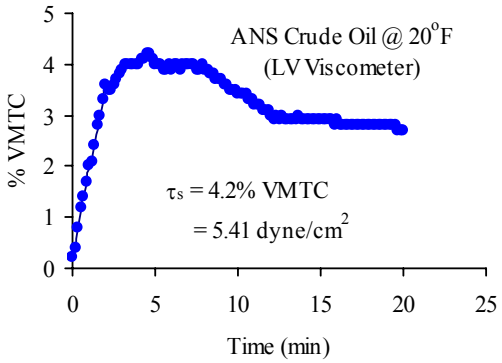

Figure A1. Gel strength curve for ANS crude oil at 20°F.

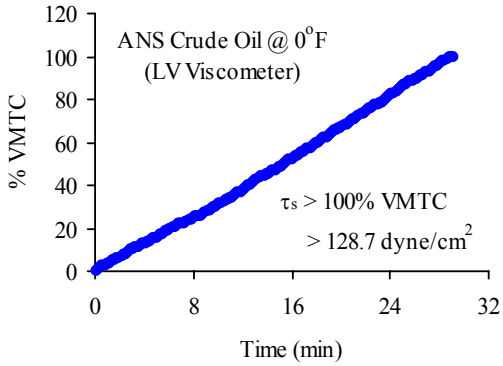

Figure A2. Gel strength curve for ANS crude oil at 0°F.

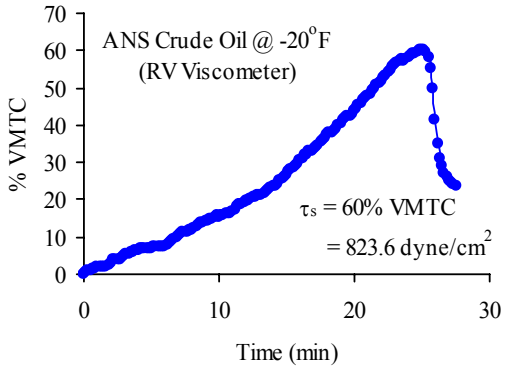

Figure A3. Gel strength curve for TAPS crude oil at -20°F.

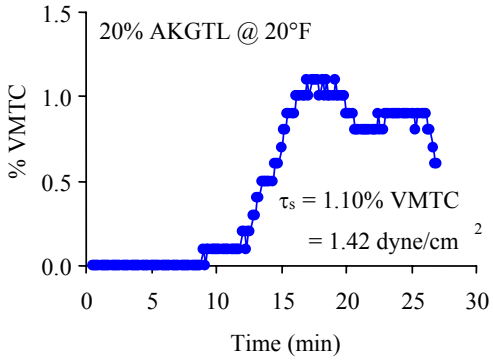

Figure A4. Gel strength curve for 20% AKGTL at 20°F.

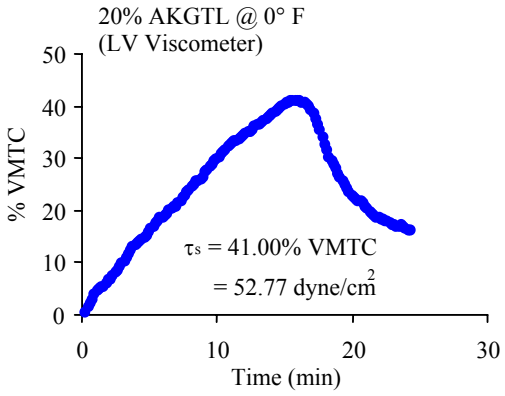

Figure A5. Gel strength curve for 20% AKGTL at 0°F.

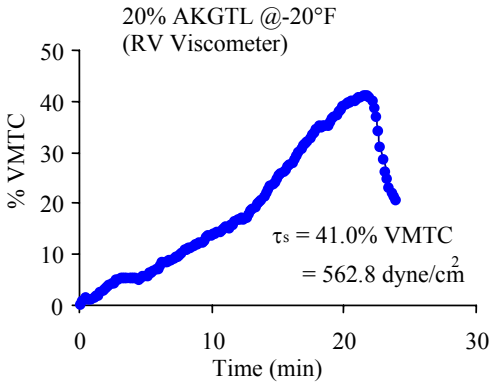

Figure A6. Gel strength curve for 20% AKGTL at -20°F.

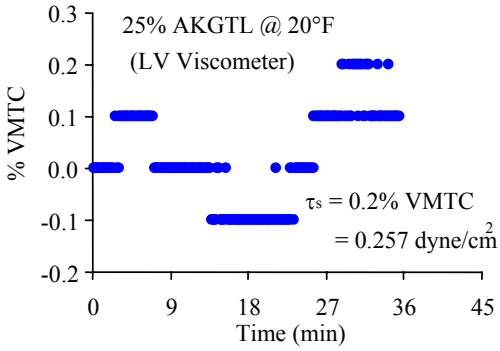

Figure A7. Gel strength curve for 25% AKGTL at 20°F.

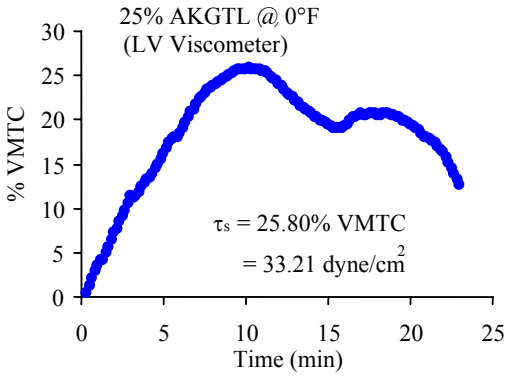

Figure A8. Gel strength curve for 25% AKGTL at 0°F.

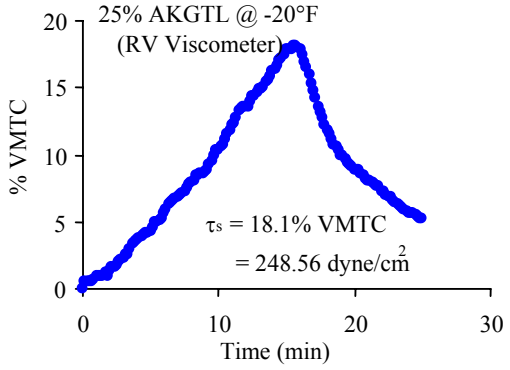

Figure A9. Gel strength curve for 25% AKGTL at -20°F.

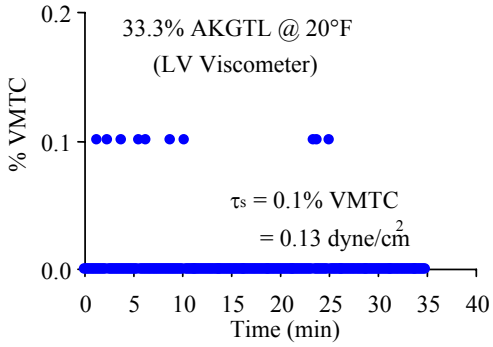

Figure A10. Gel strength curve for 33.3% AKGTL at 20°F.

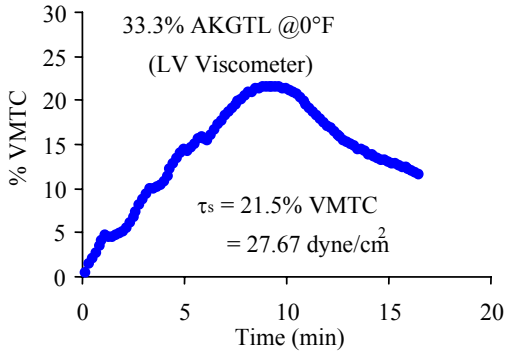

Figure A11. Gel strength curve for 33.3% AKGTL at 0°F.

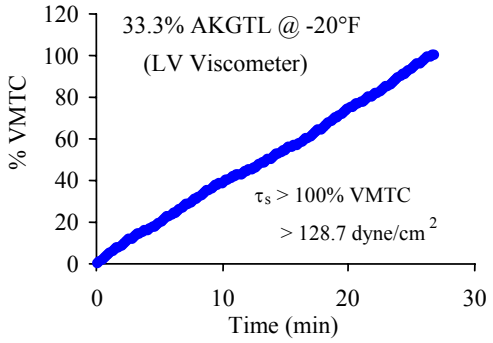

Figure A12. Gel strength curve for 33.3% AKGTL at -20°F.

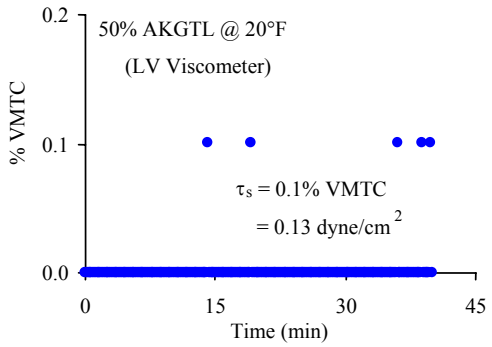

Figure A13. Gel strength curve for 50% AKGTL at 20°F.

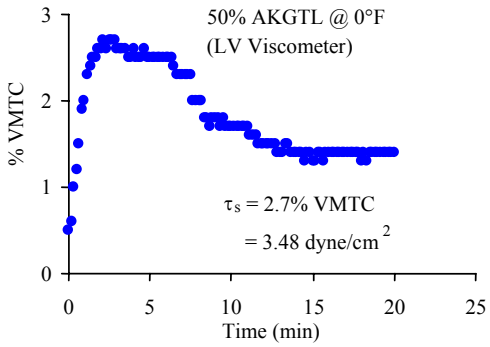

Figure A14. Gel strength curve for 50% AKGTL at 0°F.

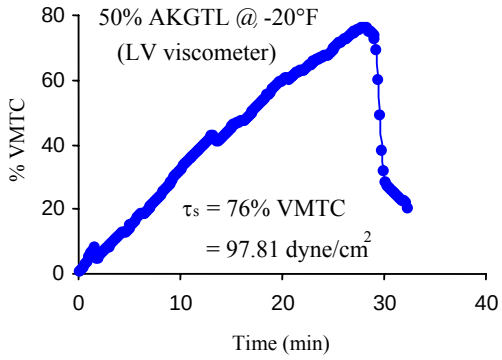

Figure A15. Gel strength curve for 50% AKGTL at -20°F.

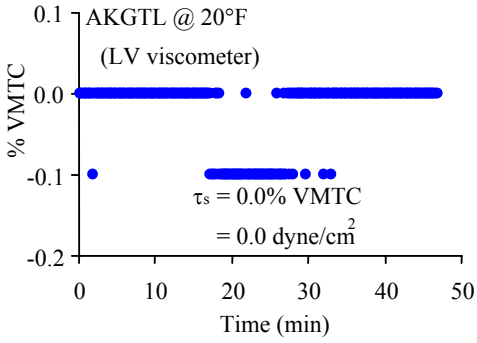

Figure A16. Gel strength curve for AKGTL at 20°F.

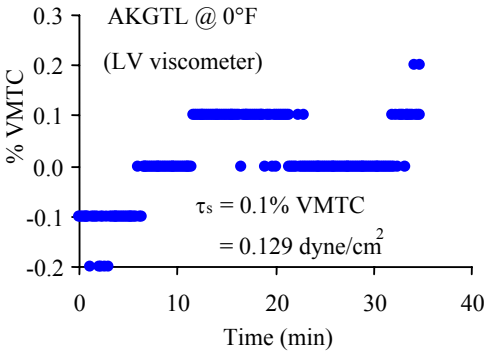

Figure A17. Gel strength curve for AKGTL at 0°F.

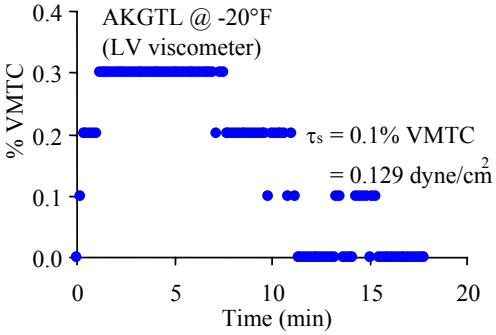

Figure A18. Gel strength curve for AKGTL at -20°F.

APPENDIX B

PV AND PT DIAGRAMS

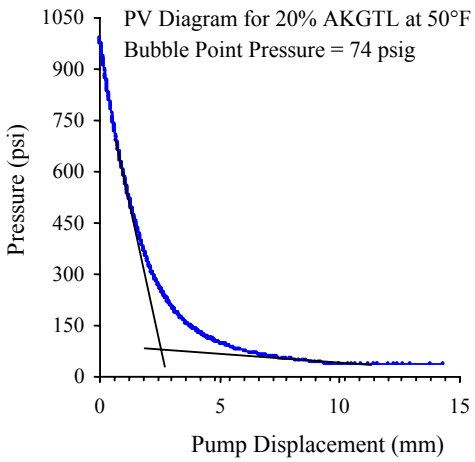

Figure B1. PV diagram for 20% AKGTL at 50°F.

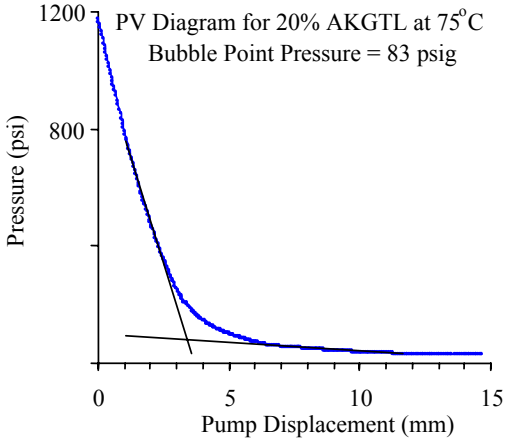

Figure B2. PV diagram for 20% AKGTL at 75°F.

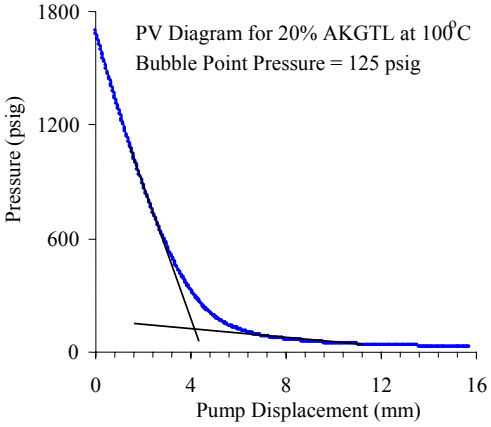

Figure B3. PV diagram for 20% AKGTL at 100°F.

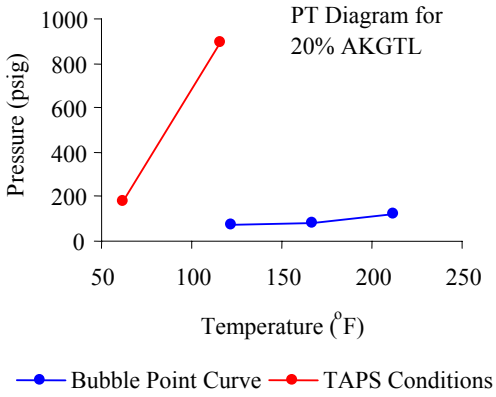

Figure B4. P-T diagram for 20% AKGTL.

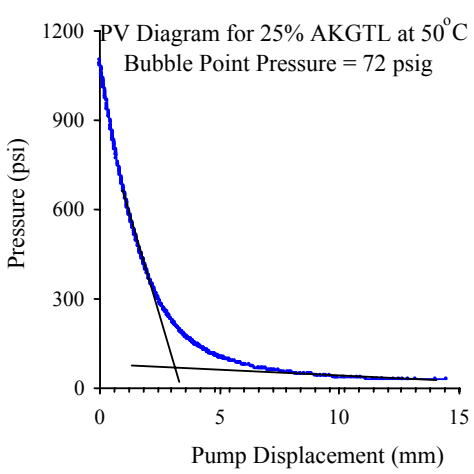

Figure B5. PV diagram for 25% AKGTL at 50°F.

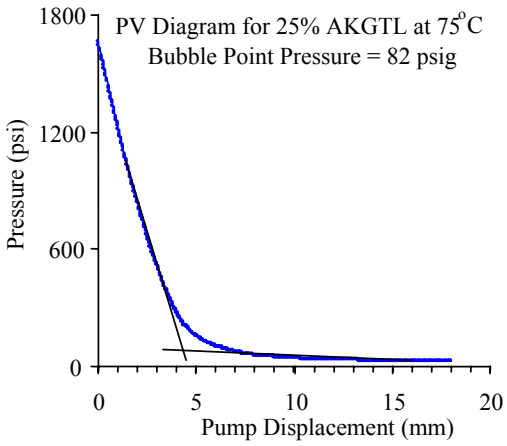

Figure B6. PV diagram for 25% AKGTL at 75°F.

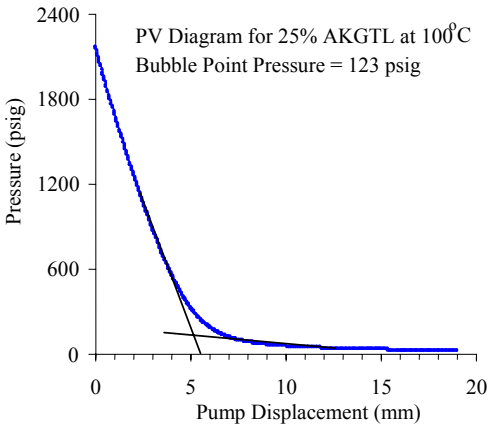

Figure B7. PV diagram for 25% AKGTL at 100°F.

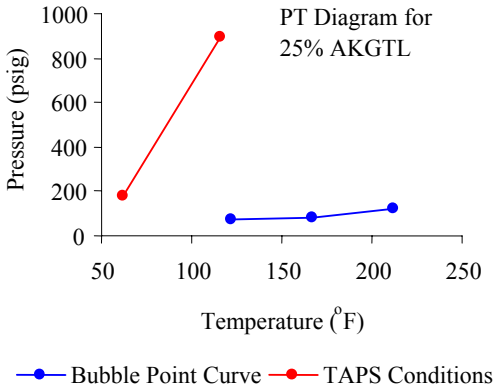

Figure B8. P-T diagram for 25% AKGTL.

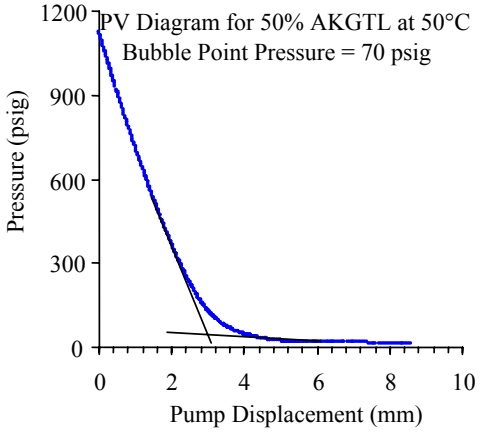

Figure B9. PV Diagram for 50% AKGTL at 50°F.

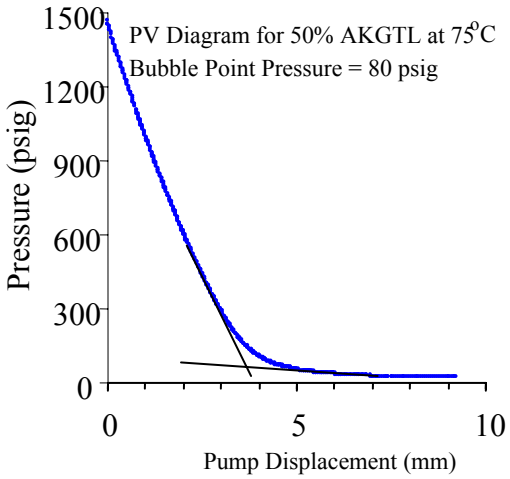

Figure B10. PV Diagram for 75% AKGTL at 50°F.

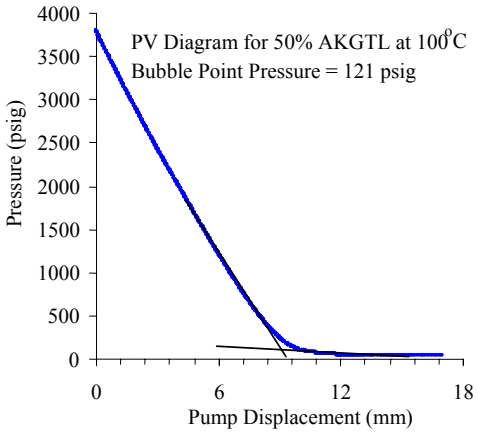

Figure B11. PV diagramfor 50% AKGTL at 100°F.

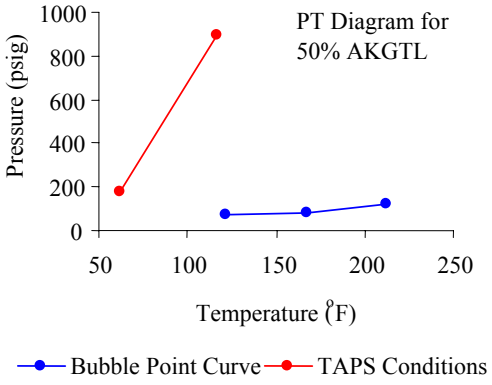

Figure B12. P-T diagram for 50% AKGTL.

APPENDIX C

GRAPHS FOR ONSET OF ASPHALTENE FLOCCULATION

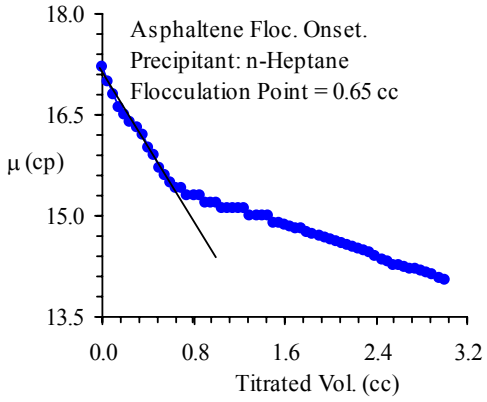

Figure C1. Asphaltene flocculation onset precipitant: n-Heptane.

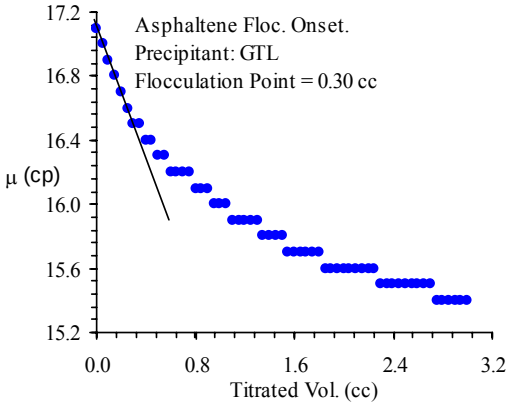

Figure C2. Asphaltene flocculation onset precipitant: GTL.

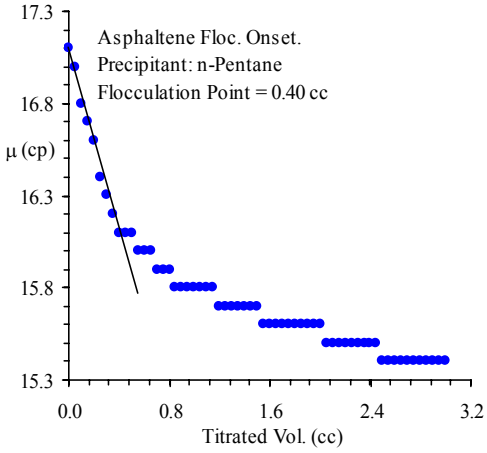

Figure C3. Asphaltene flocculation onset precipitant: n-Pentane.

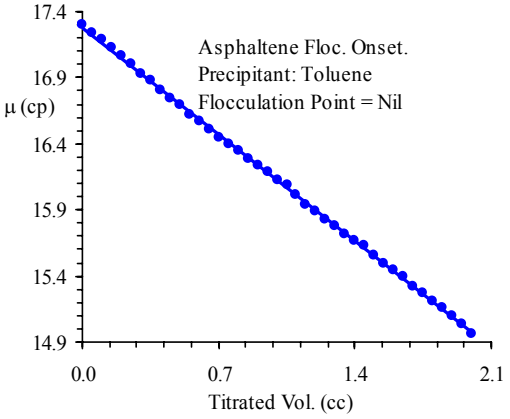

Figure C4. Asphaltene flocculation onset precipitant: Toluene.